This is to certify that the

dissertation entitled

SYNTHESIS AND CHARACTERIZATION OF POLYMANDELIDE AND LACTIDE/METHACRYLATE BLOCK COPOLYMERS

presented by

Tianqi Liu

has been accepted towards fulfillment
of the requirements for

Ph.D. degree in Chemistry

Major professor

Date 2/21/02

SYNTHESIS AND CHARACTERIZATION OF POLYMANDELIDE AND LACTIDE/METHACRYLATE BLOCK COPOLYMERS

By

Tianqi Liu

A DISSERTATION

Submitted to
Michigan State University
in partial fulfillment of the requirements
for the degree of

DOCTOR OF PHILOSOPHY

Department of Chemistry

2002

ABSTRACT

SYNTHESIS AND CHARACTERIZATION OF POLYMANDELIDE AND LACTIDE/METHACRYLATE BLOCK COPOLYMERS

By

Tianqi Liu

Polymers derived from lactic acid are attractive alternatives to traditional petroleum-based polymers due to their degradability and biocompatibility. Once used exclusively in biomedical applications, polylactide is now being developed as a high volume commodity polymer for packaging and coatings. The task of replacing the non-degradable polymeric materials used in these fields with polylactides requires that a broad spectrum of physical properties be available from polylactides. This objective can be achieved, in part, by the synthesis of new derivatives and block copolymers of polylactide.

Polymandelide is a derivative of polylactide where the methyl group has been replaced by a benzene ring. We synthesized high molecular weight polymandelide via ring opening polymerization of mandelide, the cyclic dimer of mandelic acid, and characterized its properties. Polymandelide is a clear amorphous material with physical properties that resemble polystyrene. In particular, polymandelide has a glass transition temperature of ~ 100 °C, higher than any known polylactide, and similar to that of polystyrene (109 °C). At pH 7.4 and 55 °C, polymandelide samples degrade at ~ 1/120 the rate of amorphous

polylactide run under the same degradation conditions, and polymandelide's degradation profile matches that for heterogeneous hydrolytic degradation. Copolymerizations of mandelide with racemic lactide resulted in homogeneous materials with glass transition temperatures that range from 60 – 95 °C. Copolymerizations using L-lactide and <12 mol% mandelide yielded semi-crystalline materials, but higher levels of mandelide inhibited crystallization of the L-lactide segments and gave amorphous materials.

Block copolymers of lactide and two methacrylates, methyl methacrylate and methoxy-capped oligo(ethylene glycol) methacrylate (OEGMA), were synthesized via a combination of ring opening polymerization and atom transfer radical polymerization. Poly(lactide)-*block*-poly(methyl methacrylate) synthesized via an end group transformation approach exhibited much higher thermal stability than a comparable polymer prepared from a difunctional initiator. The block copolymers prepared from racemic lactide were homogeneous and exhibited a single glass transition temperature that increased with the mole fraction of poly(methyl methacrylate) in the copolymer. The effect of poly(methyl methacrylate) on the crystallization of the poly(L-lactide) block was also studied. Longer poly(methyl methacrylate) blocks led to a decreased crystallization rate for the poly(L-lactide) block.

Block copolymers of racemic and L-lactide with OEGMA were synthesized using a difunctional initiator. Miscibility of the two blocks increased with decreases in the length of the OEGMA. Block copolymers of L-lactide and OEGMA were used to prepare nanoparticles via dialysis.

To my family

ACKNOWLEDGMENTS

First, I would like to thank my advisor, Professor Gregory L. Baker, for his guidance all through the years. During my stay at "Baker Lab", I was given the freedom not only to make mistakes (thanks for the tears we shed together!) but also learn from them. His encouragement and patience have led me through this learning process and will also affect my future life.

I would like to thank my committee members: Professors Ned Jackson, Milton Smith and David Weliky for their suggestions and comments. I would also like to thank past and current members of the Baker group: Yiyan, Gao, Mao, Tara, Chun, Cory, Wenxi, Micah, JB, Kirk, Erin, Fadi, Zhiyi, Xuwei, Leslie, Ping, Feng and Ying, for their assistance and support.

Thanks also go to Dr. Andre Lee and Dr. Haiping Geng for their assistance with polymer characterization. I also must acknowledge the NMR and X-ray staff: Long Le, Kermit Johnson, Art Bates and Rui H. Huang, for their help on the instruments. Thanks also go to Lisa Dillingham in the Graduate Office, for going out of her way to make my life in this department so much easier.

Special thanks also go to Kunxiu for his constant support and friendship.

Finally, I would like to thank my Mom, Dad, sister and brother-in-law for their love and encouragement.

TABLE OF CONTENTS

List of Figures

List of Schemes

List of Tables

List of Abbreviations

AFM	Atomic force microscopy
ATRP	Atom transfer radical polymerization
BBA	*t*-Butyl benzyl alcohol
bpy	2,2'-bipyridine
DSC	Differential scanning calorimetry
DTC	2,2-Dimethyl-trimethylene carbonate
DTG	Differential thermogravimetry
EDTA	(Ethylenedinitrilo)tetraacetic acid disodium salt dihydrate
ESEM	Environmental scanning electron microscopy
GC/MS	Gas chromatography/mass spectroscopy
GPC	Gel permeation chromatography
^{c}HTC	2,2-[2-Pentene-1,5-diyl]-trimethylene carbonate
MALDI-TOF	Matrix assisted laser desorption/ionization – time of flight
Me_6TREN	Tris[2-(dimethylamino)ethyl]amine
MMA	Methyl methacrylate
M_n	Number average molecular weight
MS	Mass spectroscopy
Oct	2-ethylhexanoate
OEGMA	Oligo(ethylene glycol) methacrylate
PDI	Polydispersity index
PDMS	Poly(dimethyl siloxane)
PE	Poly(ethylene)

PEO	Poly(ethylene oxide)
PETE	Poly(ethylene terephthalate)
PMMA	Poly(methyl methacrylate)
POEGMA	Poly[oligo(ethylene glycol) methacrylate)]
PS	Poly(styrene)
PTFE	Poly(tetrafluroethylene)
PVC	Poly(vinyl chloride)
PLA	Polylactide or poly(lactic acid)
PLLA	Poly(L-lactide)
Pmdl	Polymandelide
ROP	Ring opening polymerization
$Sn(Oct)_2$	Tin(II) 2-ethylhexanoate or tin octoate
T_g	Glass transition temperature
TGA	Thermal gravimetric analysis
TMC	Trimethylene carbonate

Chapter 1 Introduction

Many synthetic polymers are produced and utilized because they are cheap, versatile and durable. Nearly all of today's synthetic polymers are derived from oil and natural gas, which are finite resources that are diminishing in supply. Because of their durability and resistance to chemical and physical degradation, polymers tend to accumulate in what is today's most popular disposal system, the landfill. According to a study by the U.S. Environmental Protection Agency, polymers account for 21% (by volume) of the 200 million tons of municipal waste produced each year in the US. Possible solutions such as recycling and incineration have proved either uneconomical or environmentally unfriendly. A better solution would be to tailor polymers from renewable resources to provide the necessary properties during use, and then have the polymers undergo degradation to non-toxic products leaving no hazardous impact on the environment. These environmentally friendly polymers could replace traditional polymers in single-use applications such as resins for packaging.

Degradable polymers, especially biodegradable polymers, are well-suited for such applications. Biodegradable polymers are materials that are quantitatively converted either to CO_2 and H_2O or to CH_4 and H_2O by microorganisms under aerobic or anaerobic conditions, respectively. Biodegradable polymers can be either natural (e.g. starch, cellulose, hemp) or synthetic materials. Generally speaking, synthetic polymers offer advantages over natural polymers in that they can be easily tailored to display a wide range

of properties. Polylactide, poly(ε-caprolactone), poly(β-hydroxybutyrate) and poly(vinyl alcohol) are examples of synthetic biodegradable polymers.

1.1. History of polylactide

Polylactide is not a new polymer. In 1932, Carothers synthesized a low molecular weight polylactide sample by heating lactic acid under vacuum. Historically, scientist have tried to make polymers resistant to environmental factors such as H_2O, O_2 and UV, and since polymers made from glycolic acid and other α-hydroxy acids were unstable toward hydrolysis, research on this class of polymers was discontinued in the first half of the 20th century. But this "instability" eventually found multiple applications in the medical field, beginning with the first biodegradable surgical sutures in the 1960s. Since the early 1980s, there have been three generations of biodegradable polymers. The first two generations were starch-based polymer systems, and were only partially degradable or failed to provide the desired mechanical properties. Third generation biodegradable polymers are based on polylactide and polyhydroxybutyrate which combine reasonable biodegradability with good mechanical properties.

1.2. Applications of polylactide and other biodegradable polymers

1.2.1. Polylactide as a commodity polymer

In many aspects, the basic properties of polylactide polymers lie between those of crystalline polystyrene and PETE. Some noteworthy properties include:

- A flexural modulus > polystyrene
- A resistance to fatty foods and dairy products equivalent to PETE
- Excellent flavor and aroma barriers
- Good heat sealability
- A high surface energy allowing easy printability

These properties, in addition to its inherent biodegradability have made polylactide a promising candidate as a commodity polymer intended for single-use or limited use applications. **Table 1.1** lists some of the applications of polylactide with its associated processing techniques.

1) Fibers for apparel

Polylactide can be readily converted into various fiber forms using conventional melt-spinning processes. Compared to PETE/cotton, polylactide/cotton offers the following advantages:

- An all-natural high performance fabric
- physiological comfort due to improved thermal insulation and water vapor transport
- Lower density
- UV stability
- Lower flammability and smoke generation

Table 1.1. Applications of polylactide as commodity polymers[2]

Process	End-Products
Fibers	Clothing (active wear, sportswear, intimate apparel), carpet tiles
Non-woven fibers	Personal hygiene, protective clothing, filtration
Oriented films	Container labels, tape
Extrusion coating	Dinnerware, food packaging, mulch film
Flexible film	Food wrap, trash bags, shrink wrap
Cast sheet	Deli trays
Injection molding	Rigid containers, daily containers
Foam	Clam shells, meat trays

2) Personal hygiene and medicare

Single use products based on biodegradable polymers have important applications in personal hygiene and medical care. Single-use degradable products such as baby diapers, surgical masks, blouses and compresses can limit contamination and secondary skin reactions.

3) Agriculture and horticulture

The use of non-woven cloth allows natural cultivation of seeds without pesticides or herbicides. The cloth easily allows air and rain to reach plants while preventing insects from penetrating. If made of polylactide, it degrades easily by hydrolysis and the degradation product - lactic acid oligomers, were observed to promote seed germination.[1]

4) Paper coatings

Paper is coated with either wax or polymeric coatings for various reasons including better water resistance and enhancement of gloss. A problem with the recycling of coated paper is the disposal of the coatings liberated during the repulping process. Since current coatings are mostly made from polyethylene, they typically do not break down during the repulping process and cannot be recycled.

Polylactide polymers have a high surface energy and easily form coherent, smooth and glossy surfaces with satisfactory printability. The low melt viscosity and high polarity of polylactide is superior to polyethylene in terms of

adhesion to the paper and compatibility with low temperature extrusion. During repulping, polylactide can hydrolyze to water soluble, non-toxic products and pose no problem in waste water treatment.

1.2.2. Medical applications of polylactide and other biodegradable polymers

Due to the current high cost of polylactide-based polymers, applications for these materials have been largely limited to biomedical fields. **Table 1.2** shows the major companies involved in producing polylactide or polylactide based-products. Examples of such products include sutures, implants and drug delivery matrices. The major advantage of using biodegradable implants over traditional synthetic polymers, metals, or ceramics is that the device can degrade *in situ* and a second operation is not necessary to retrieve the device. Biodegradable polymers offer other important features. For example, fractured bones fixated with a rigid, non-degradable stainless steel implant tend to re-fracture upon removal of the implant since the regenerated bone tissue often does not carry an appreciable load during the healing process. In contrast, a carefully tailored degradable implant that degrades at an appropriate rate will slowly transfer load to the damaged area, affording stronger bone tissue.

Sutures were the first commercial product from biodegradable polymers and still account for 95% of all sales. The other 5% is attributed to orthopedic devices in various forms such as pins, rods, tacks, staples and dental applications. Several end products include Dexon®, Vicry® and Maxon® sutures,

Lactomer® and Absolok® clips and staples; Biofix® and Phusiline® plates and screws and Capronor® drug delivery devices.

Table 1.2. Major companies involved in lactic acid and PLA biomedical fields[2]

Company	Country	Lactic acid	Lactide	Polylactide (co)polymers	End products
Galactic Laboratories	Belgium	X	X	X	
Bioscience	Finland				X
Phusis	France		X	X	X
Boehringer Ingelheim	Germany		X	X	
Purac	Netherlands	X	X	X	
ICI	U. Kingdom				X
BPI	USA				X
Davis & Geck	USA				X
Etnor	USA				X
Henley & Johnson	USA		X		
Johnson & Johnson	USA				X
Medisorb Technologies	USA			X	

1.3. Synthesis of polylactide

1.3.1. Synthesis of lactic acid

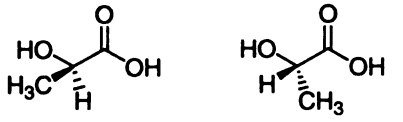

D-Lactic acid L-Lactic acid

Figure 1.1. Structure of D,L-lactic acid

Lactic acid is a chiral molecule that exists as two stereoisomers, L- and D-lactic acid (**Figure 1.1**). Lactic acid can be produced from petrochemical sources or by fermentation as shown in **Figure 1.2.**[3] In the petrochemical route (**Figure 1.2 A**), ethylene is oxidized to acetaldehyde, and following treatment with HCN, the cyanohydrin is hydrolyzed to give racemic lactic acid (*rac*-lactic acid). Presently, Musashino in Japan is the only producer of *rac*-lactic acid. The fermentation process (**Figure 1.2 B**) produces almost exclusively L-lactic acid. Most major companies involved in the production of lactic acid such as Purac, Cargill/Dow, Galactic and ADM use fermentation processes to produce lactic acid.

1.3.2. Manufacture of polylactide

1) Direct condensation

Lactic acid is a difunctional molecule and can self-condense by intermolecular esterification to form polylactide (**Scheme 1.1 A**). One drawback

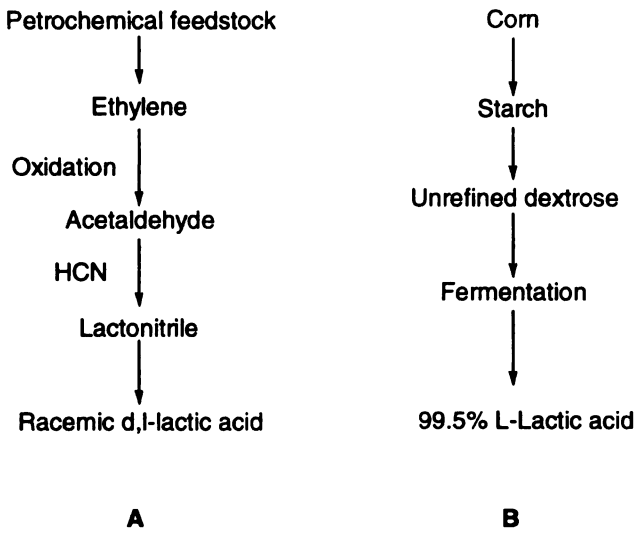

Figure 1.2. Petrochemical (A) and fermentation (B) routes for the synthesis of lactic acid

of this approach is the long reaction time, which is related to the equilibrium between the starting α-hydroxy acid, and the polyester product and water. High molecular weight polylactide cannot be obtained unless water is efficiently removed from the reaction system to drive the reaction to completion. Besides using high vacuum, researchers have used azeotropic distillation with a high boiling point solvent to remove water continuously. The effect of catalysts on direct condensation of lactic acid was also investigated. Protonic acids and tin compounds are effective at producing high molecular weight polymers at relatively low temperatures. Currently, Mitsui Toatsu[4] utilizes a high boiling solvent to produce high molecular weight polylactide. Another option is to react the end groups of low molecular weight polylactide with coupling agents such as

diisocyanates to yield high molecular weight polymer (**Scheme 1.1 B**). A drawback of this approach is the potential formation of branched or crosslinked molecular structures.[5]

2) Ring opening polymerization of lactide

Ring Opening Polymerization (ROP) of lactide is the dominant route to polylactide with molecular weights ranging from several thousand to several hundred thousand g/mol. Cargill/Dow adopted this route to synthesize polylactide on a large scale. In the ROP route shown in **Scheme 1.1 C**, lactic acid is polymerized to afford a low molecular weight polylactide, which is then depolymerized to give lactide, the cyclic dimer of lactic acid. Lactide can be further purified by distillation under vacuum. Polymerization of lactide by ROP yields polylactides, whose molecular weight can be easily controlled by varying the monomer to initiator ratio. The continuous process developed by Cargill/Dow is shown in **Figure 1.3**.[3]

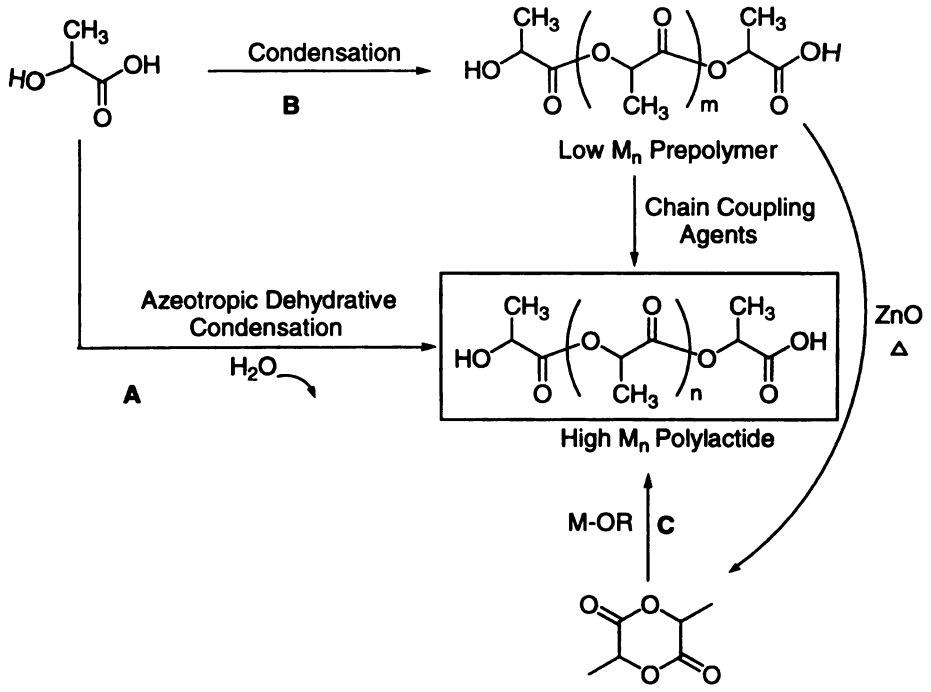

Scheme 1.1. Three routes for polylactide syntheses: **A**, azeotropic condensation; **B**, condensation followed by chain coupling; **C**, ring opening polymerization

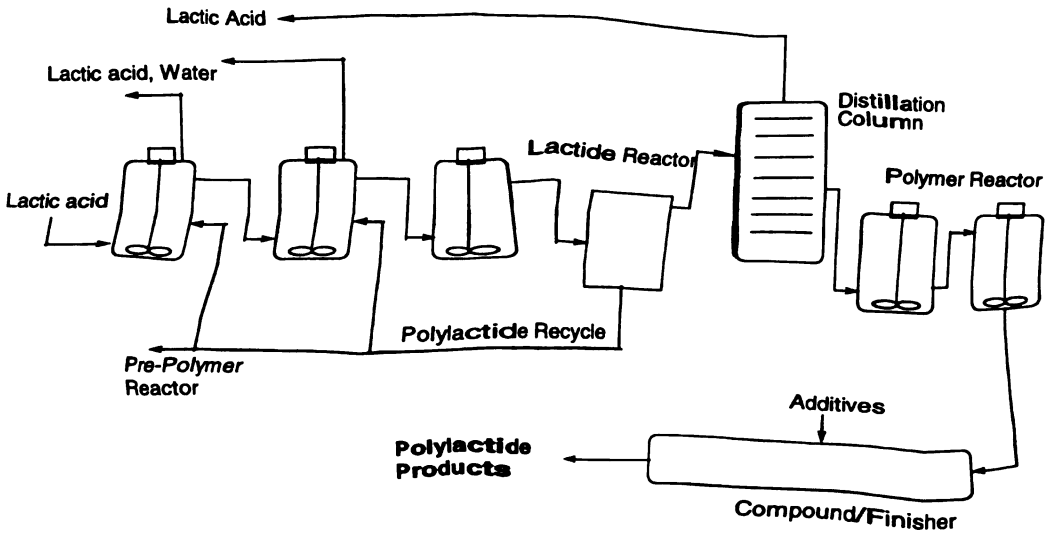

Figure 1.3. The Cargill/Dow continuous process for the synthesis of polylactide.

1.4. Catalysts and mechanism of ring opening polymerization

1.4.1. Metal catalysts

Many metal complexes have been proposed as lactide *polymerization* catalysts. In the US, the FDA has approved the use of $Sn(Oct)_2$ (Oct = 2-ethylhexanoate) for the synthesis of materials for surgical and pharmacological applications and zinc catalysts have been used industrially in France. Most catalysts fall into two categories: metal alkoxides and metal carboxylates.

Aluminum alkoxides ($Al(OR)_3$) belong to the first category. Ring opening *polymerization of lactide initiated* by aluminum alkoxides is believed to proceed through a "*coordination-insertion*" mechanism.[6] Coordination of the carbonyl oxygen of lactide to aluminum to followed by selective acyl-oxygen cleavage leads to the formation of linear polyesters. The alkoxide transferred from aluminum ends up as an ester group at one end of the polyester chain. The use of functional aluminum alkoxides as initiators places the functional group at the end of the chain, and enables macromolecular engineering of *polylactides as* illustrated by the well-controlled synthesis of macromonomers and *block* copolymers.[7-9]

In recent years, alkoxy aluminum Schiff's base complexes *have been* developed for stereoselective polymerizations.[9] Spassky[10] and Coates[11] reported the stereoselective synthesis of isotactic and syndiotactic polylactide from *rac*-lactide and *meso*-lactide respectively. Radano[12] showed the first example of producing the polylactide stereocomplex from *rac*-lactide using racemic catalyst (**Figure 1.4 A**). As shown by Cameron,[13] adding electron-

withdrawing chlorine to the Schiff-base ligand increases the reactivity of aluminum Schiff-base initiators (Figure 1.4 B), making controlled ambient temperature polymerizations of lactide more practical.

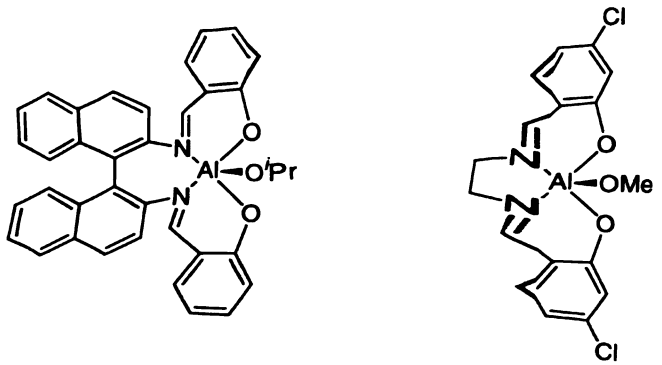

A B

Figure 1.4. Aluminum Schiff-base initiator systems

$Sn(Oct)_2$ is one of the most widely used metal carboxylates for the ring opening polymerization of lactide and other cyclic esters. H_2O and alcohol, either deliberately added or present as impurities, serve as the true initiating species. It is assumed that a fast equilibrium is established between $Sn(Oct)_2$ and the alcohol or water to generate a tin alkoxide species, which then polymerizes lactide via the "coordination-insertion" mechanism illustrated in **Scheme 2**.[14] The alkoxy or hydroxy group forms an ester or acid at the terminus of the polylactide chain. Theoretical studies also support the generation of a tin alkoxide species

prior to the ring opening polymerization of lactide by a "coordination-insertion" mechanism.[15]

Despite the wide use of aluminum and tin-based catalysts, Al^{3+} is under suspicion as a potential player in Alzheimer's disease and the use of tin derivatives in the biomedical field has been questioned despite the lack of any related acute problems in clinical applications. In response, some research groups have focused on developing magnesium,[16,17] zinc,[18-20] and iron[21,22] based catalysts, since the ions of these metal participate in the normal metabolism of the human body and exhibit low toxicity.

The development of lanthanide alkoxide catalysts has been limited by the toxicity of the heavy metals[23-31]although these catalysts are extremely active toward ring opening polymerization of lactide and other cyclic esters even at ambient temperatures.

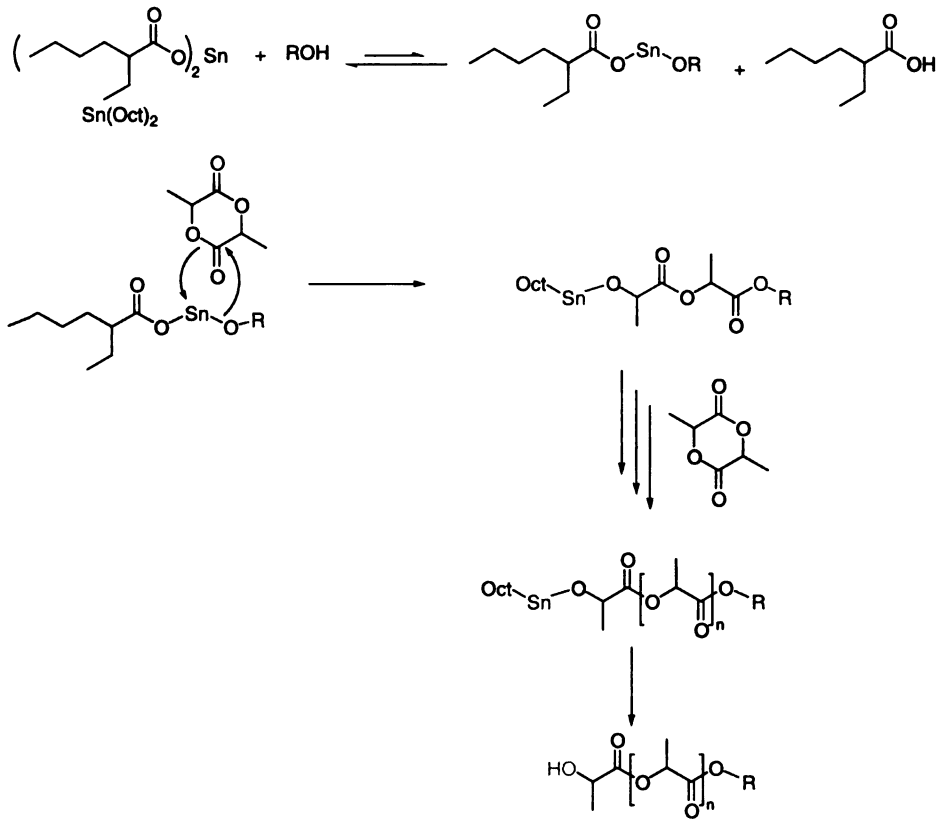

Scheme 1.2. Mechanism of ring opening polymerization of lactide catalyzed by $Sn(Oct)_2$

1.4.2. Transesterification

Besides polymerization of monomers, metal catalysts can also catalyze side reactions such as inter- or intramolecular transesterification reactions (**Scheme 1.3**). Transesterification reactions can be identified by GPC, ^{13}C NMR and MALDI-TOF analysis.[24,32,33] Intramolecular transesterification, often termed "back-biting", leads to cyclic structures and a decrease in the number average molecular weight. Intermolecular transesterification can cause redistribution of polymer chain lengths and an increase in the polydispersity index. MALDI-TOF spectra are particularly useful for detecting both cyclic and linear oligomers, since they allow the direct identification of mass-resolved polymer chains. Because certain stereosequences in the polymerization of *rac*- or *meso*-lactide can only be obtained by transesterification, ^{13}C NMR spectroscopy can detect transesterification reactions.

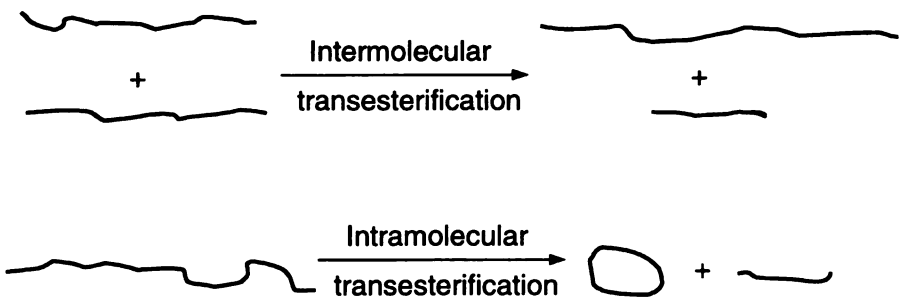

Scheme 1.3. Intramolecular and intermolecular transesterification

1.5 - Thermal degradation and stability

Polylactide belongs to a family of polymers with poor thermal stability. It can undergo slow thermal degradation at temperatures lower than the melting point of the polymer, but the degradation rate increases rapidly above its melting point.[34] Thermal instability is a major limitation for some applications. For example, polylactide implants used in orthopedic surgery are supposed to provide adequate strength, ductility, modulus, wear and fatigue resistance for internal fixation of bone fractures, and are expected to last until the new tissues are generated. However, if polylactide degrades during melt-processing (compression, extrusion and injection-molding) or sterilization, the degradation profile and mechanical properties of the polylactide implants can be quite different from what is expected because the mechanical properties and *in vivo* degradation rates are largely dependent upon the molecular weight of the device.

Polylactide samples from commercial suppliers are quite susceptible to extensive degradation after injection molding.[35] For molding temperatures between 130 °C and 215 °C and mold residence time of 12-16 seconds, the peak in the molecular weight distribution declined by 50-88% and the polydispersity increased.

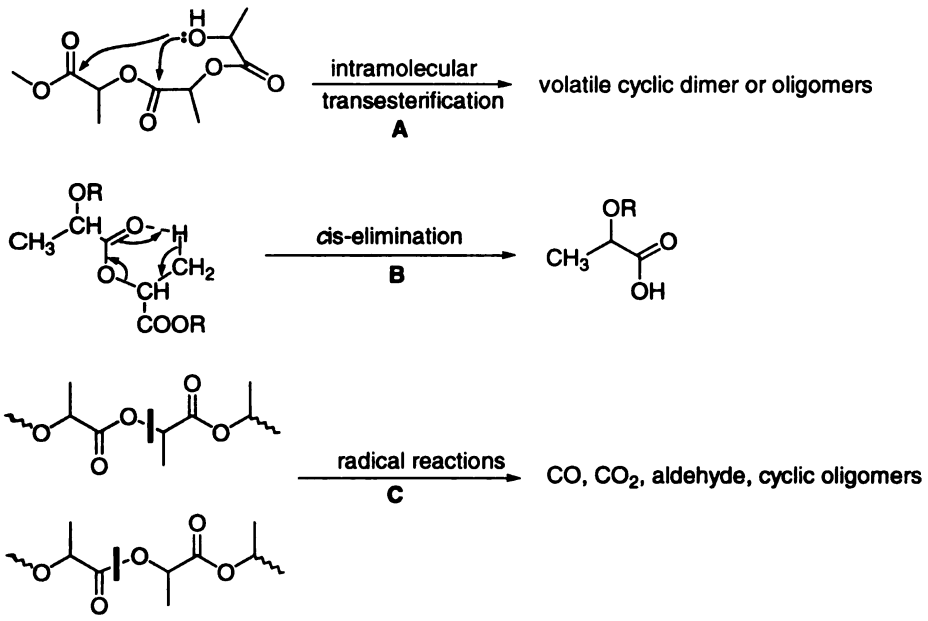

Scheme 1.4. Thermal degradation pathways for polylactide

1.5.1. Thermal degradation pathways

As shown in **Scheme 1.4**, there are three principal pathways for the ermal degradation of polylactide. Path **A** illustrates thermal degradation by ramolecular transesterification, also known as "back-biting", which generates latile cyclic dimer or oligomers. Path **B** describes degradation by a *cis*-mination mechanism via the formation of a six-membered ring transition state. ath **C** shows degradation by radical pathways and the generation of volatile all molecules.

Cis-elimination is a concerted, un-catalyzed reaction. It can be the minant pathway for esters with activated C-H bonds such as the poly(hydroxy tyrate)s which contain methylene hydrogens activated by an adjacent carbonyl oup.[36] However, although it possesses three β-C-H bonds available for *cis*-mination, the methyl C-H bonds of polylactide are not activated and as a result, e contribution of the *cis*-elimination pathway to the total thermal degradation of olylactide is trivial.[36]

Intramolecular transesterification[34] is the dominant pathway for the thermal egradation of polylactide. Often catalyzed by residual metal catalyst, it is itiated from free hydroxy groups at the ends of the polymer chain. The cyclic mer, lactide, is the major degradation product from this pathway.

The third pathway, radical reactions, is significant only at temperatures 200 °C.[37] Homolytic cleavage of alkyl-oxygen bond or acyl-oxygen bond to rm macroradicals leads to the formation of volatile cyclic oligomers, CO, CO_2 nd other small molecules.

The thermal degradation pathways and degradation products were investigated using several thermal analysis techniques including Thermogravimetric Analysis (TGA, DTG), Differential Scanning Calorimetry (DSC), time and temperature resolved pyrolysis-MS and pyrolysis-GC/MS. Two distinct peaks (at 275 °C and 337 °C) were observed from DTG experiments indicating two dominant degradation mechanisms. GC/MS identified the low temperature peak as almost exclusively lactide, while the high temperature peak consisted of cyclic oligomers including lactide and other volatile small molecules.[38] The products were consistent with the low temperature degradation dominated by depolymerization, while the high temperature degradation resulted from radical reactions.

Lactide was produced in both low and high temperature degradation steps, but it was formed by different mechanisms.[38] In low temperature degradation, it was produced as a result of depolymerization. In high temperature degradation, lactide as well as cyclic trimers up to pentamers were produced by a radical mechanism.

1.5.2. Factors affecting thermal degradation of polylactide

1) Effect of polymer molecular weight

Polylactide samples with different molecular weights show differences in thermal stability. Tests on highly purified samples (precipitation followed by washing with dilute acid, and extensive drying) showed that the degradation temperature initially increased sharply, and approached 353 °C as the viscosity

molecular weight rose to 100,000.[39] This effect is related to the concentration of terminal hydroxy groups in the polymer sample, which decreases as the molecular weight increases. Since the terminal hydroxy groups initiate intramolecular transesterification, decreases in their concentration shift the onset for thermal degradation to higher temperatures. When the molecular weight of the polymer was high enough, the number of terminal hydroxy groups became negligible and any further reduction in their concentration leads to only small increases in the thermal degradation temperature.

2) Effect of residue metal catalysts on thermal degradation

Polylactide samples that have not been scrupulously purified are usually contaminated with >100 ppm of metal catalyst residues. These metals can lower the polymer degradation temperature by coordinating with the carbonyl oxygen of esters and facilitate intramolecular transesterification. Several different organometallic compounds of Sn, Al were studied,[40-42] and in general, Sn(II) compounds were more active transesterification catalysts than Al compounds. The Sn(II) compounds are thought to interact more strongly with polylactide ester groups than Al(III) compounds due to their larger ionic radius.

3) Effect of residual unreacted lactide or lactic acid on thermal degradation

Residual lactide and lactic acid in polylactide samples can cause a weight loss at lower temperatures.[39] However, the thermal degradation temperature of

polylactide samples is unaffected once lactide or lactic acid is removed by low temperature isothermal treatment.

4) Effect of additives

Various additives have been used to enhance the thermal stability of polylactide. For example, peroxides were added to stabilize polylactide melts.[43,44] It was proposed that peroxides could deactivate residual metal catalysts and introduce branches on polymer chains to counteract chain scission. When mixed with crude polylactide prior to processing, tropolone (2-hydroxy-2,4,6-cycloheptatrienone), stabilized polylactide during melt processing by forming chelating complexes with tin.[45]

1.6. Hydrolytic degradation

The most attractive feature of polylactide is its degradability. It contains a high density of ester groups in the main chain and degrades through their hydrolysis. The hydrolytic degradation of polylactide has attracted much attention during the past two decades because of the polymer's potential as degradable medical and consumer products as well as the existence of many factors which can influence the degradation process. Despite some important advances, some controversies still exist in the literature.

The hydrolytic degradation time for polylactide samples varies from a couple of weeks to several years depending on the polymer molecular weight, crystallinity, chemical composition, purity, size, additives (incorporated drugs), medium pH, and temperature.

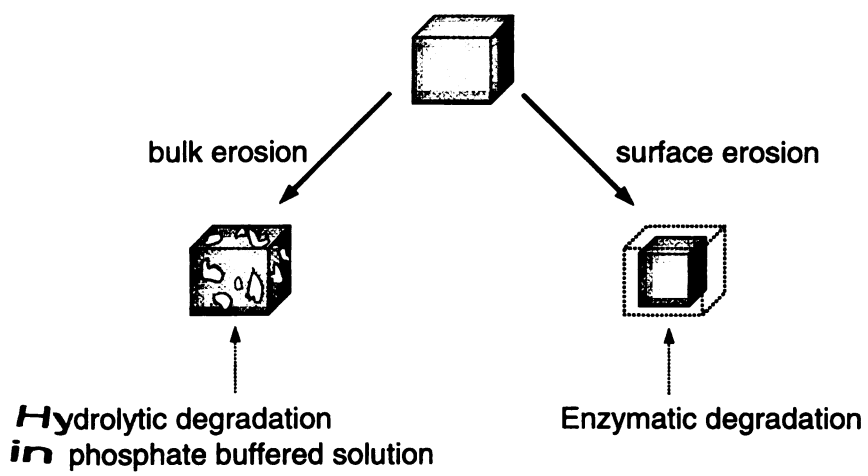

Figure 1.5. Bulk erosion and surface erosion in biodegradable polymers

1.6.1. Degradation mechanisms

There are two types of degradation processes: bulk erosion and surface erosion (**Figure 1.5**). Surface erosion is observed when the rate of water diffusion into the polymer matrix is lower than the rate of converting the polymer into water soluble oligomers. Polyanhydrides and polyorthoesters, which contain chemical bonds highly sensitive to hydrolysis, are examples of materials that exhibit surface erosion.[46,47] The hydrolytic degradation of polylactide follows a different mechanism - bulk erosion. Polylactide degrades through the hydrolysis of ester bonds generating one carboxylic acid and one hydroxyl group for each ester hydrolyzed. The carboxyl groups thus formed catalyze the hydrolysis of other ester bonds and increase the degradation rate, a phenomenon known as autocatalysis. A feature of bulk erosion is that the molecular weight of the sample decreases from the beginning of the degradation process, but weight loss can only be observed after extensive cleavage of ester bonds and the formation of water soluble oligomers.

Small-sized polylactide particles and devices such as thin films and macro/nanospheres are thought to degrade homogenously, however, much faster degradation rates have been reported for the interior of large amorphous polylactide samples.[48] The surface-interior differentiation was obvious due to the formation of a hollow structure. GPC data also revealed a bimodal molecular weight distribution. This degradation phenomenon is termed heterogeneous degradation and can be explained by a reaction-diffusion mechanism. Before degradation the polymer sample is homogeneous in terms of molecular weight

and molecular weight distribution. Once placed in a degradation medium, water penetrates into the polymer sample resulting in homogeneous hydrolytic cleavage of ester bonds throughout the sample. This macroscopically homogeneous hydrolytic degradation continues until water-soluble oligomers are generated. Those oligomers generated on or near the surface can escape from the matrix, dissolve in surrounding medium and are neutralized by the buffer. However, the oligomers generated inside the matrix cannot diffuse out of the sample, especially when the degradation temperature is lower than the glass transition temperature of the polymer. As degradation proceeds, acid-terminated oligomers accumulate at the core of the polymer leading to enhanced autocatalysis. Thus, the core of the polymer specimen degrades at a much faster rate than the shell, resulting in surface-interior differentiation. The bimodal molecular weight distribution reflects the existence of two polymer populations that degrade at different rates.

1.6.2. Factors affecting the hydrolytic degradation of polylactide

1) Monomer

The effect of a small amount of monomer remaining in polymer samples on hydrolytic degradation was investigated by Ikada.[49] Accelerated hydrolysis of as-polymerized amorphous samples was observed compared to purified ones even if the monomer content was as low as 5 wt%. During degradation experiments, residual monomers can be extracted from a matrix or hydrolyze to give a hydroxy acid. The hydrophilicity of the hydroxy acid not only enhances the

diffusion of water into the polymer matrix, but also catalyzes the hydrolysis of other ester groups. Reproducible degradation results require monomer-free samples.

2) Crystallinity

In crystalline poly(L-lactide), hydrolytic degradation was found to occur preferentially in amorphous regions. For samples of the same molecular weight in phosphate-buffered solution, samples with higher degrees of crystallinity showed faster declines in molecular weight, and the crystallinity of all films increased monotonically with hydrolysis.[50] Due to looser chain packing, the diffusion coefficient of water is higher in the amorphous regions of a semi-crystalline polymer than in the crystalline phase. There are two types of amorphous regions, the amorphous region between the lamellae of spherulites, and free amorphous regions. Hydrolytic degradation occurs preferentially in the amorphous region near the surface of lamellae because of a high concentration of terminal carboxyl and hydroxyl groups, which are excluded from the crystalline region during crystallization. A higher initial crystallinity can introduce more defects in the amorphous region, thus leading to easier water penetration and faster degradation.[50]

3) Additives

When drug delivery systems are considered, the effect of loaded compounds on the hydrolytic degradation of the polymer matrix is particularly

interesting. If an acidic compound is incorporated, it accelerates the degradation of the polymer matrix. However, a basic compound can act as either a catalyst or an acid neutralizer. Its effect on the degradation of the polymer depends on the relative importance of the two effects. For example, when coral was incorporated in polylactide for bony tissue regeneration, it mainly neutralized carboxyl end groups and slowed the degradation rate by eliminating the autocatalytic effect.[51] However, when the base was caffeine, its effect on the degradation strongly depended on the loading concentration.[52]

4) Effect of copolymers

Copolymers of polylactide, such as poly(lactide-*co*-glycolide) were synthesized to tailor the rates of degradation. A copolymer of 50% *rac*-lactide and 50% glycolide degraded faster than both homopolymers and copolymers with other compositions. Surprisingly, there was no linear relationship between the copolymer composition and the degradation rates. This effect may be related to crystallinity in the polymer since the homopolymers have a higher degree of crystallinity than the copolymers.

1.6.3. Degradation models

Random chain scission and autocatalysis models have been constructed for the molecular weight and sample weight change during hydrolytic degradation. The random chain scission model[53] is based on two assumptions: each ester link has equal probability of being attacked by water, and *dn/dt*, the rate of breaking links is proportional to *n*, the number of links present in the system.

$$dn/dt = kn$$

The degree of degradation, *a*, is defined as the number of broken links per chain divided by P_0, the original degree of polymerization the chains.

$$a = (M_n(0)/M_n(t)-1)/(P_0-1)/$$

$M_n(0)$ is the initial number average molecular weight and $M_n(t)$ is the number average molecular weight at degradation time *t*. Thus, at any time during the degradation process,

$$n = n_0 - an_0 = n_0(1-a)$$

and

$$- d[n_0(1-a)]/dt = kn_0(1-a)$$

Integrating and using the approximation $-ln(1-a) \approx - a$ gives

$$a = kt$$

and when $P_0 >> 1$

$$M_n(0)/M_n(t) - 1 = kP_0t \qquad \textbf{eq. 1.1}$$

In the autocatalysis model, the cleavage of ester links is catalyzed by carboxylic acid end groups in the system at a rate proportional to the concentration of acidic end groups (**eq. 1.2**).[54,55]

$$d[COOH]/dt = k''[H_2O][ester][COOH] \qquad \textbf{eq. 1.2}$$

where *[COOH]*, *[ester]* and *[H_2O]* are the concentration of the terminal carboxyl groups, ester groups and water in the system repectively. k" and the following k' and k are rate constants.

When the number of chain scissions is small, both [H_2O] and [ester] can be considered to be constants and combined with k".

So, $d[COOH]/dt = k'[COOH]$

Since $[COOH] \propto 1/M_n$

$$\ln[M_n(0)/M_n(t)] = kt$$

The Prout-Tompkins equation (**eq. 1.3**) was applied by Ramtoola to evaluate mass loss from poly(lactide-*co*-glycolide) particles.[56] The original model was based on auto-catalytic thermal decomposition of potassium permanganate.

The expression is as follows:

$$\ln[x/(1-x)] = kt + m \qquad m = -kt_{max} \qquad \textbf{eq. 1.3}$$

Where x is the fractional mass remaining at time t; k is the rate constant weight loss and t_{max} is the time to achieve 50% weight loss.

1.6.4. Enzymatic degradation

The enzymatic degradation of polylactide follows a surface erosion mechanism because the size of an enzyme prevents it from diffusing into the polymer matrix. Enzymes that degrade polylactide include pronase, proteinase-K and bromelain. Proteinase K preferentially degrades L-lactyl units, and the hydrolysis rate decreases for high concentrations of D-lactyl units, and when the distribution of the D and L monomer units becomes more random.[57,58] For crystalline poly(L-lactide), enzymes selectively attack amorphous regions rather than crystalline regions,[59] and as the degree of crystallinity increases, the enzymatic degradation rate decreases. The degree of crystallinity of poly(L-lactide) samples also increases upon degradation due to preferential degradation and partial crystallization of the amorphous region. Due to the specificity of enzymes, a two-component blend, composed of poly(L-lactide) and poly(ε-caprolactone), can be selectively degraded to yield porous biodegradable polyester materials.[60]

1.6.5. Biodegradable polymers as drug carriers

Drug release from biodegradable polymers is a complicated process, which occurs by several, often simultaneous, mechanisms such as diffusion through intact polymers, diffusion through water-swollen polymers and surface layers, or bulk erosion of polymers. The importance of each individual mechanism in drug release depends on the composition and molecular weight of

the polymer matrix, particle size, the nature and content of incorporated drugs as well as fabrication methods.

The three general cases are diffusion control (polymer erosion slower than the diffusion processes), erosion control (polymer erosion is the fastest process), and control by swelling (diffusion of water into the polymer is faster than polymer erosion, but slower than polymer relaxation). In some studies,[61,62] biodegradable polymer erosion was not observed during the period when drug release took place, and the only advantage in these systems would be the eventual disappearance of drug carriers though degradation.

Nanoparticles are defined as solid particles ranging from 1-1000 nm in size. Polymeric nanoparticles can be prepared by polymerization of reactive monomers in a dispersed phase or from preformed polymers. Drawbacks of the first strategy include the use of large volumes of organic solvents and the presence of residual monomers, catalysts, and solvents. The second strategy offers a more promising approach especially when biodegradable and biocompatible polymers such as polylactide and its copolymers are used as the polymer matrices.

Various methods have been used to prepare nanoparticles from preformed polymers including emulsion-evaporation, solvent displacement (nano precipation), emulsification, solvent diffusion, and dialysis. These methods are similar in that they all require an organic solution containing the nanoparticle components and an aqueous solution with or without stabilizers. At present, emulsion-evaporation is the most widely used method, but it poses problems

such as removal of solvent and surfactant residues due to their toxicities. In addition, a homogeneous emulsion is required to produce nano-sized particles. The conventional procedure, ultrasonication, can sometimes induce chemical reactions or polymer degradation.

Recently, a dialysis method using amphiphilic materials was developed for the preparation of nanoparticles with narrow size distributions.[63-65] It also proved to be a simple and effective preparation method for poly(lactide-*co*-glycolide) nanoparticles.[66]

1.7. Random copolymers of polylactide

Despite the attractive properties of polylactide, it is difficult for polylactide to fulfill all applications due to its high crystallinity, hydrophobility and a lack of functional groups. Copolymerization of lactide with other monomers has been intensively investigated to better control the degree of crystallinity as well as its degradation behavior.

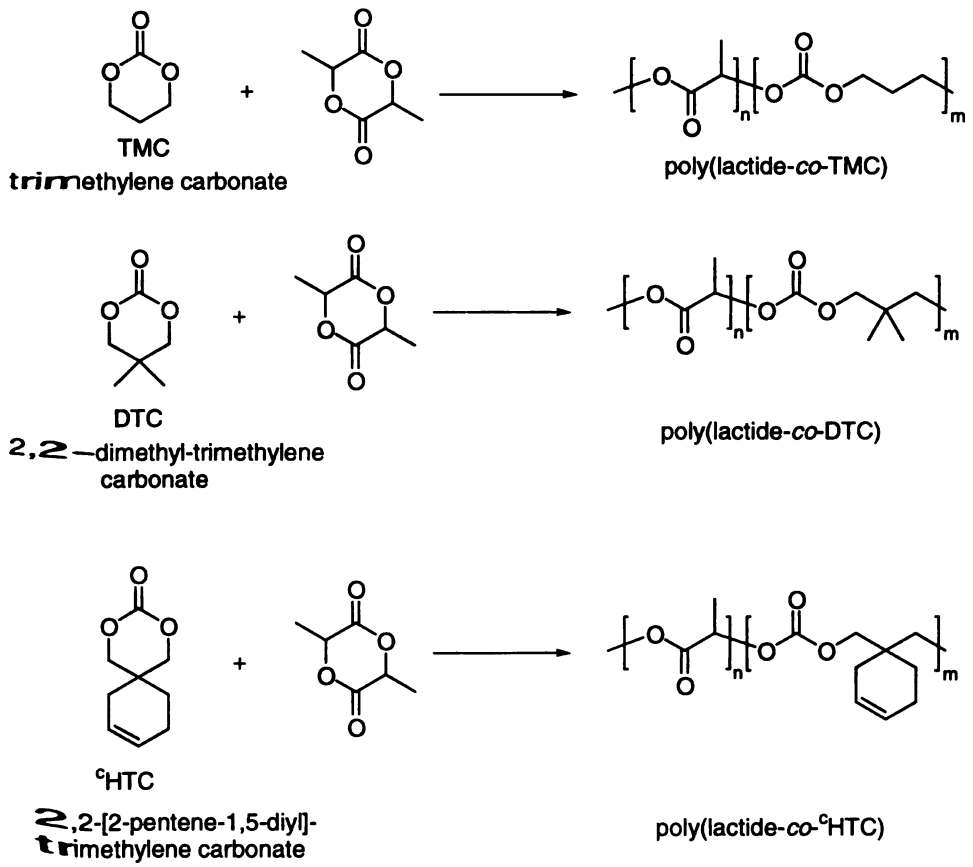

Scheme 1.5. Copolymers of lactide and carbonates

1.7.1 Copolymerization with carbonates

The carbonates that have been copolymerized with lactide include trimethylene carbonate (TMC), 2,2-dimethyl-trimethylene carbonate (DTC) and 2,2-[2-pentene-1,5-diyl]-trimethylene carbonate (^{c}HTC) (**Scheme 1.5**). The carbonate linkage is more hydrophobic than an ester, and copolymers of carbonates and lactide are expected to be more stable toward hydrolytic degradation than polylactide.

The homopolymer of TMC is an amorphous or poorly crystalline material with a glass transition temperature of ~ –18 °C. The melting temperature, crystallinity, and glass transition temperature of polylactide decreased with increasing TMC in the copolymers.[67-69] Copolymers with mechanical properties ranging from brittle and highly crystalline to rubbery and flexible, can be prepared by adjusting the monomer feed ratio. For example, polyglycolide, an analog of poly(L-lactide), is highly crystalline, stiff (melting point around 219 °C) and fails to meet the material requirements for surgical sutures. Copolymers containing TMC have been developed for flexible, strong and absorbable monofilament sutures. Although poly(lactide-*co*-TMC) was more stable toward *in vitro* hydrolytic degradation conditions, *in vivo* degradation revealed a much faster degradation due to an enzymatic degradation process. Thus, incorporation of TMC in polylactide leads to increased shelf life and faster *in vivo* degradation.

The DTC homopolymer is crystalline (mp ~108 °C) with a glass transition temperature of ~ 27 °C. Poly(L-lactide-*co*-DTC) copolymers containing 11-88 mol% DTC are amorphous despite the fact that both homopolymers are

crystalline.[70,71] When the DTC content in the copolymer is higher than 50 mol%, the glass transition temperature is below normal body temperature (37 °C). This may have important implications for biomedical applications, since both mechanical properties and degradation rates change dramatically at the glass transition temperature.

^{C}HTC, a cyclic carbonate containing a cyclohexene moiety, was copolymerized with L-lactide to introduce unsaturated C=C double bond groups in the copolymer and provide opportunities for further modifications such as epoxidation.[72,73] The incorporation of ^{C}HTC decreased the glass transition and the melting temperature of poly(L-lactide) as in the above cases.

1.7.2. Copolymerization with caprolactone and its derivatives

Poly(ε-caprolactone) is a semi-crystalline biocompatible and biodegradable polyester with low melting temperature (63 °C) and low glass transition temperature (-60 °C). It degrades with a half life of one year *in vivo* and possesses higher permeability than polylactide, which is hardly permeable to most drugs. Thus, a wide range of drug delivery matrices with adjustable properties can be achieved by combining the features of both polymers through copolymerization (**Scheme 1.6**).[74-76] Substituted caprolactone derivatives were also copolymerized with lactide.[77,78]

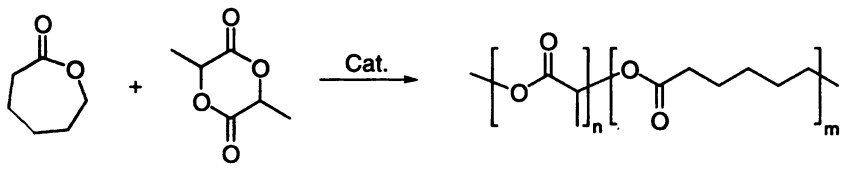

poly(lactide-*co*-caprolactone)

Scheme 1.6. Copolymerizations of lactide and caprolactone

1.7.3. Copolymerization with morpholine-2,5-dione derivatives

The hydrophobicity of polylactide and its lack of functional groups has made it unattractive as a carrier for water-soluble drugs such as peptides and proteins. One attempt to improve hydrophilicity and provide functional groups is the synthesis of polyesteramides from morpholine-2,5-dione derivatives that have amino, carboxylic and hydroxy side chain functional groups. α-Amino acids such as lysine,[79,80] glutamic acid[81] and aspartic acid[82] have been copolymerized with lactide by an indirect method. After protecting their side chain functional groups, the amino acids were condensed with 2-bromopropionyl bromide to give morpholine-2,5-dione derivatives (**Figure 1.6**), which can be copolymerized with lactide and deprotected.

These morpholine-2,5-diones polymerize poorly, giving low polymerization rates and low molecular weights. Copolymers with lactide were synthesized to overcome this difficulty and take advantage of the desirable physical properties of polylactide. During homopolymerization and copolymerization, the ring opening of the morpholine derivatives proceeded exclusively by the cleavage of the ester bond.

The deprotected functional group can be further modified to improve polylactide-cell interactions. For example, Langer[79,80] reported the synthesis of poly(lactide-*co*-lysine) and attachment of a cell adhesion promoting peptide to the copolymer's primary amino group.

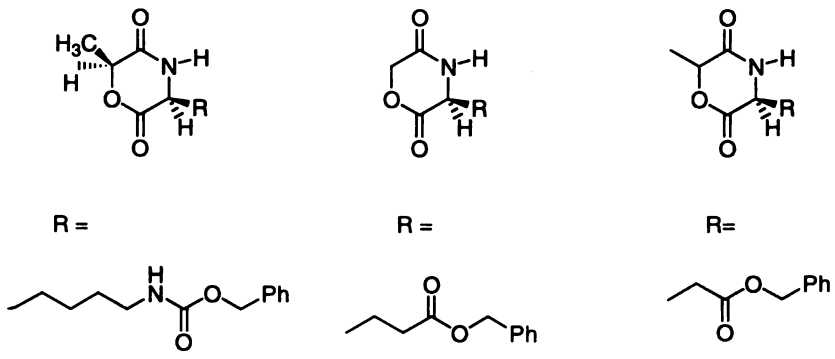

Figure 1.6. Various morpholine-2,5-dione derivatives copolymerized with lactide

1.7.4. Copolymerization with glycolide and other substituted glycolides

Polyglycolide is highly crystalline with a low solubility in most organic solvents. Copolymerization of glycolide with lactide provides a method for disrupting the crystallinity and tuning the degradation rate. The absence of methyl substituents on the glycolide ring makes the monomer more reactive toward ring opening polymerization due to reduced steric hindrance. Copolymers of lactide with substituted glycolides such as ethylglycolide and isopropylglycolide have been studied by Yin and Wang (**Scheme 1.7**).[83,84] Random copolymers with glass transition temperatures ranging from 15 – 66 °C were prepared by varying the feed ratio of lactide and ethylglycolide.

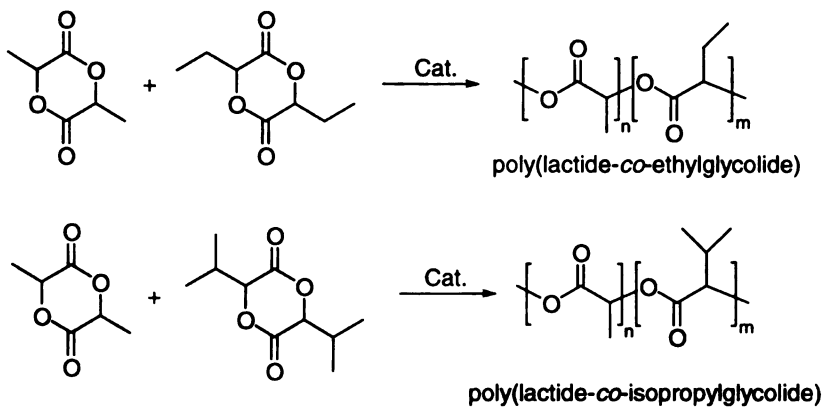

Scheme 1.7. Copolymerization of substituted glycolides with lactide

1.8. Block copolymers

1.8.1. General

Block copolymers are macromolecules comprised of blocks or homosequences that are joined at their ends. Different block copolymer architectures can be realized by using synthetic procedures that control the connectivity of the blocks. The most common block copolymer architectures are AB diblock, ABA(C) triblock, comb, star and multiblock copolymers.

Block copolymers are different from polymer blends in that the blocks are chemically linked. Besides displaying the properties of each block, block copolymers often microphase separate and give rise to interesting physical behavior. In a heterogeneous polymer blend, polymers phase separate at the macroscopic level which leads to domains >100 μm that can easily been seen under an optical microscope. Since the blocks of a block copolymer are chemically joined to each other, as they phase separate they must place the junction between the two blocks at the interface between the phases. Thus the domains must be small, on the order of several nanometers to several micrometers. This microphase separation can lead to new polymer morphologies and thus new properties. One of the most successful examples of microphase separated block polymers is thermoplastic elastomers derived from polystyrene-polybutadiene-polystyrene ABA block copolymers, where polystyrene forms spherical domains in a continuous matrix of polybutadiene. Polystyrene has a glass transition temperature above 80 °C and can act as physical crosslinkers for the polybutadiene softblock matrix. The block

copolymers are thus elastomers at room temperatures while still processible at temperatures higher than the glass transition temperatures of polystyrene because the polymers are not chemically crosslinked.

Microphase separation behavior also leads to important applications such as adhesives, compatiblizers. For instance, diblock copolymers can be used to decrease the size of phase separated domains, decrease the interfacial tension and improve the mechanical properties of immiscible blends.[85-88]

1.8.2. Phase separation and morphology

When two polymers are mixed, more often than not, they are immiscible and phase separate. The free energy of mixing ΔG_M is given in **eq. 1.4**:

$$\Delta G_M = \Delta H_M - T\Delta S_M \qquad \textbf{eq. 1.4}$$

where ΔH_M and ΔS_M are the enthalpy and entropy of mixing respectively and T is temperature. Usually polymers have very small values of ΔS_M due to their high molecular weight and ΔS_M decreases as molecular weight increases. Therefore, a slightly positive enthalpy due to endothermic mixing is sufficient to make ΔG_M positive, resulting in phase separation.

Microphase separation leads to different classes of structures depending on the block copolymer composition. For non-crystalizable AB clocks, both A and B blocks form random coils and segregate into separate phases. If the space requirement of the A blocks matches that of the B blocks, i.e., $N_A \approx N_B$, where N_A and N_B are the number of monomer units in blocks A and B respectively, then, lamellae with alternating A and B blocks will form (**Figure 1.7**

C). If $N_A << N_B$, packing in lamellae would either dissatisfy the requirement of a densest packing of segments, or lead to a large deviation from the unperturbed coil structure. Thus small A blocks will form spherical domains in the continuous matrix of B blocks (**Figure 1.7 A**). For larger N_A (still $N_A < N_B$), A blocks will assemble into cylindrical domains in a continuous matrix of B (**Figure 1.7 B**). In addition to the ordered spheres, cylinders and layers, a bicontinuous structure exist in a narrow range of N_A/ N_B, between the cylindrical ad lamellar phases.

Figure 1.7. Morphologies of AB block copolymers. White portions represent block A, while dark portions represent block B of the AB block copolymer

1.8.3. Block copolymers with poly(ε-carprolactone)

Block copolymers of lactide and caprolactone combine the good permeability of polycaprolactone with the relatively fast degradation rate of polylactide, providing controllable periods of biodegradation and drug release. They also act as blend compatiblizers for polylactide blends because polycaprolactone is known to be miscible with many commodity polymers such as poly(vinyl chloride) and polycarbonates.

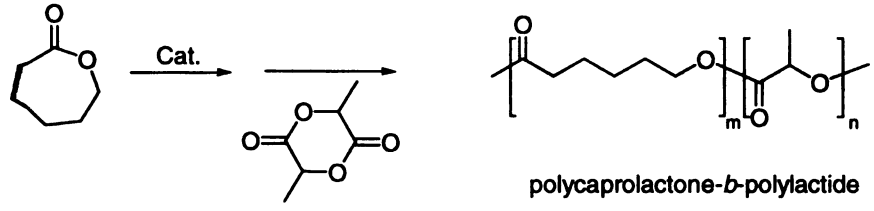

Scheme 1.8. Block copolymer of lactide and caprolactone

Lactide and caprolactone can be polymerized by common metal catalysts such as $Al(OR)_3$ and $Sn(Oct)_2$. The terminal hydroxy group of each homopolymer can be considered as the initiator for the next ring opening polymerization. In reality, block copolymers are obtained only when caprolactone is polymerized and then used to initiate lactide polymerization, as shown in **Scheme 1.8.**[89] When the order of polymerization was reversed, random copolymers of lactide and caprolactone were obtained under bulk polymerization conditions. The formation of random copolymers was attributed to transesterification reactions. The hydroxy chain end of polycaprolactone is more reactive than that of polylactide due to both electronic and steric factors. The polylactide hydroxy chain end is less nucleophilic because it is α to the electron

withdrawing carbonyl group. In addition, the α-methyl group of the lactyl end group sterically hinder nucleophilic attack by the hydroxy end group. Since the occurrence of transesterification largely depends on the reactivity of the hydroxy end groups in the polymerization system, growing the polycaprolactone after lactide favors transesterification.

To bypass the chain end reactivity issue and synthesize triblock copolymers with polylactide as the center block, Song[90] used a bimetallic catalyst to polymerize caprolactone followed by lactide. By extending the polylactide chain with ethylene oxide, they were able to obtain active initiating sites for ring opening polymerization of caprolactone (**Scheme 1.9**).

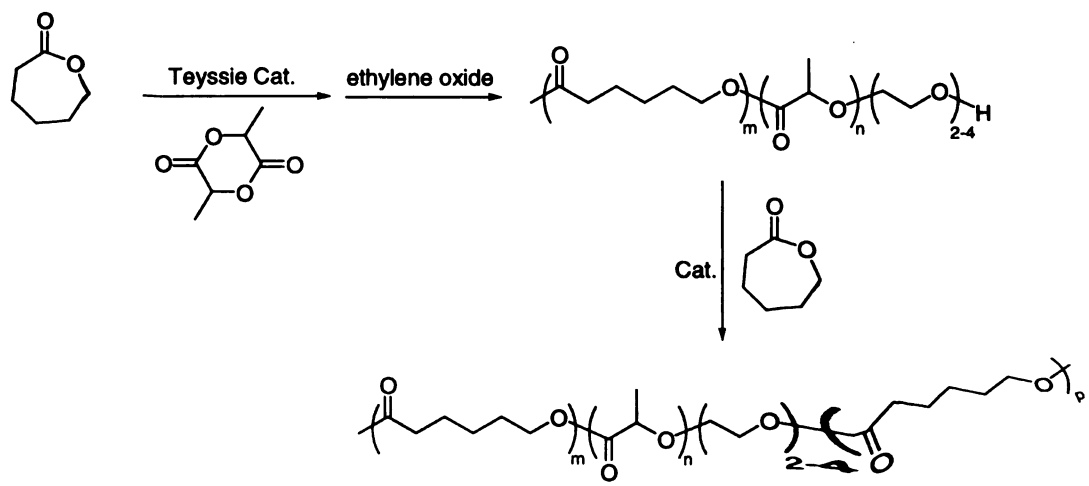

Scheme 1.9. Lactide and caprolactone triblock copolymers

1.8.4. Block copolymers with poly(ortho ester)s

The poly(ortho ester)s are a family of hydrophobic biodegradable polymers, which under certain conditions, undergo hydrolytic degradation by a surface erosion mechanism. Because the ortho ester linkages in the polymer are very susceptible to acidic conditions, acidic additives are usually physically incorporated into the polymer to accelerate the rate of degradation. This approach can be problematic because the additives can diffuse out of the

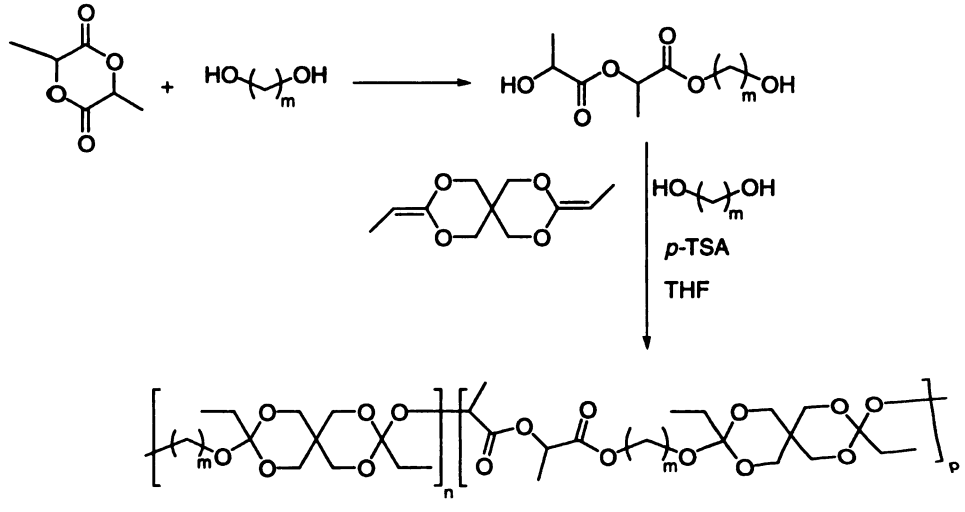

Scheme 1.10. Poly(ortho ester) containing short polylactide blocks

polymer matrix leading to a complicated drug release profile. To overcome this problem, self-catalyzed poly(ortho ester)s were synthesized[91-93] (**Scheme 1.10**) by linking the poly(ortho ester)s with short segments of lactic acid. Thus the degradation products from lactic acid segments catalyze the controlled degradation of poly(ortho ester)s and the surface erosion characteristics of poly(ortho ester)s are maintained.

1.8.5. Copolymers with rubbery blocks

The mechanical properties of polylactide, especially crystalline poly(L-lactide), need to be improved for certain applications. For example, orthopedic applications require an improvement in impact resistance and in polylactide's elongation at break. Copolymerization of polylactide with elastomers can address these problems and lead to materials with tuned mechanical properties.

Poly(dimethylsiloxane) (PDMS), a biocompatible material with a low glass transition temperature and high oxygen and water permeability, was used as the rubbery block for poly(L-lactide) copolymers.[94,95] The multiblock poly(L-lactide-*b*-PDMS) was prepared by polycondensation of bifunctional polylactide oligomers and PDMS oligomers (**Scheme 1.11**). Triblock copolymers with PDMS as the center block were synthesized by ring opening polymerization of L-lactide in the presence of dihydroxy terminated PDMS macroinitiator. These materials exhibited good elastomeric properties.

Diblock copolymers of lactide and butadiene,[96] isoprene[97] and ethylene[98] (**Scheme 1.12**) were synthesized by a combination of living anionic and ring opening polymerizations. Poly(ethylene-*b*-L-lactide) proved to be a good compatiblizer for poly(L-lactide)/polyethylene blends.

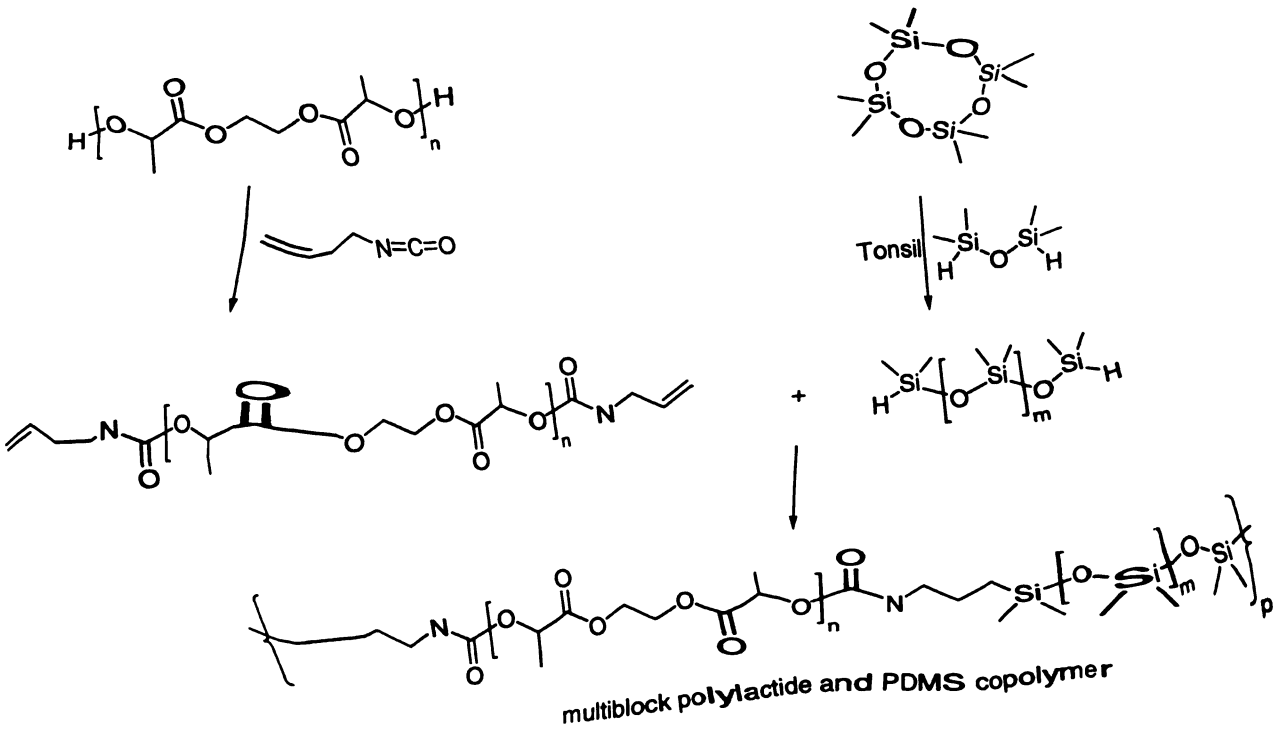

Scheme 1.11. Multiblock copolymer of lactide and dimethylsiloxane

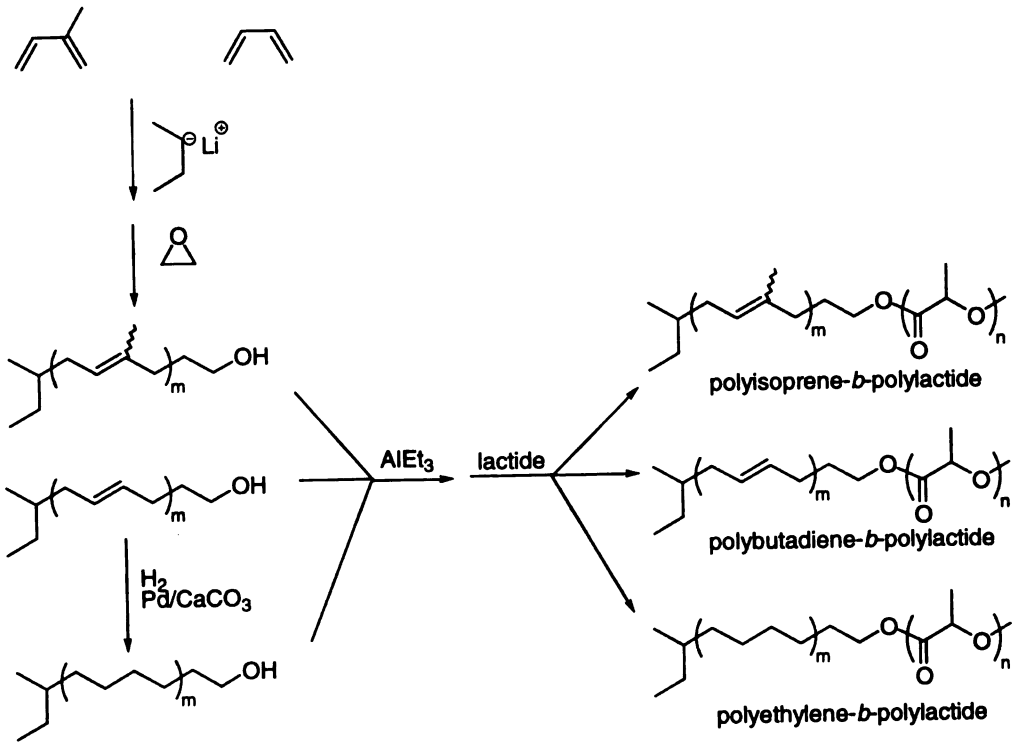

Scheme 1.12. Block copolymers of lactide with olefins

1.8.6. Block copolymers with poly(ethylene oxide)

Poly(ethylene oxide) (PEO) is a water soluble and biocompatible polyether, and has been approved by most countries as a food additive. Because PEO is highly flexible and provides no binding sites for proteins, polylactide-*b*-PEO copolymers show less protein and cell adhesion, which makes specific attachment possible by intentional immobilization of bioactive factors. Block copolymers of PEO and polylactide also represent a class of biodegradable/biocompatible polymers with balanced hydrophobicity and hydrophilicity.

Linear diblock or triblock copolymers with PEO as the central block have been made using hydroxy or dihydroxy terminated PEO as the macroinitiator (**Scheme 1.13**).[99-106] Triblock copolymers with polylactide as the central block were prepared by coupling two diblock copolymers with hexamethylene diisocyante (HMDI) (**Scheme 1.13**).

L-lactide and ethylene oxide multiblock copolymers were synthesized using an initiator generated *in-situ* from AlR_3 and H_2O (**Scheme 1.13**). Although the ring opening polymerization of both monomers was carried out in one pot, the copolymers apparently are blocky, since it contained two distinct crystalline phases.[107]

Graft copolymers were prepared to promote hydrolytic degradation of polylactide. During hydrolytic degradation, the oligomers generated would reach

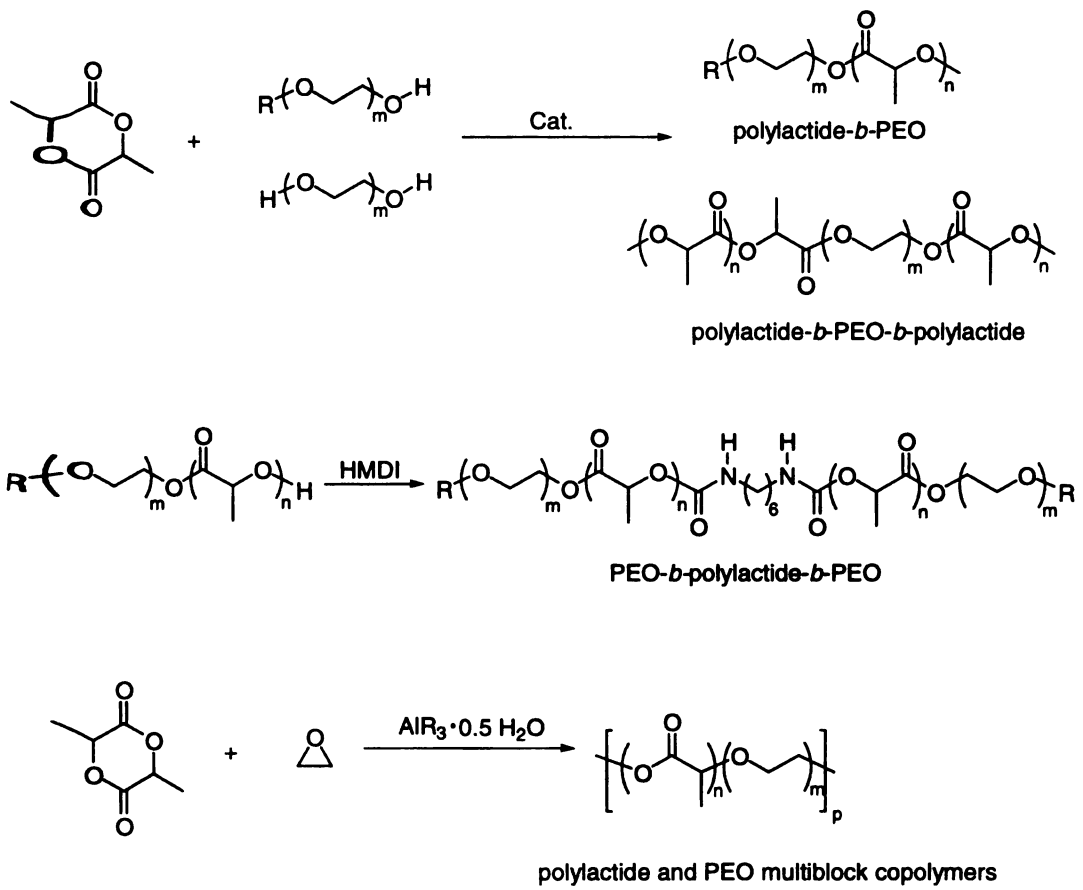

Scheme 1.13. Block copolymers of lactide and ethylene oxide

the threshold of water solubility much more rapidly because they are composed of both PEO and polylactide segments. In graft copolymers, both polylactide and PEO can serve as the backbone or teeth. Graft copolymers with PEO as the backbone and either polylactide or polyglycolide as the teeth were prepared by condensation of a PEO oligomer bearing an epoxy group at each end with a second PEO oligomer terminated with two carboxylic acids. Ring opening polymerization of lactide and glycolide was initiated from the pendent hydroxy groups to give a graft copolymer (**Scheme 1.14**).[108] Graft copolymers with polylactide as the backbone were prepared as shown in **Scheme 1.14**.[109]

One practical limitation in applications of poly(lactide-*b*-ethylene oxide) copolymers is the PEO block length. Although PEO is biocompatible, it is non-degradable, and due to its large hydrodynamic volume, PEO with molecular weights >10,000 g/mol cannot be filtered through human kidney membranes and eliminated from human bodies. To solve this problem, star-shaped copolymers were prepared[110,111] because their hydrodynamic volumes and solution viscosities are lower than for linear copolymers with the same composition and molecular weight. Thus larger blocks of PEO can be incorporated into star-shaped polymers to increase the hydrophilicity of the system without affecting the excretion of the degradation products.

Block copolymers of lactide and ethylene oxide with cross-linkable end groups were also synthesized to form core-polymerized stable nanospheres[112] and scaffolds for tissue engineering.

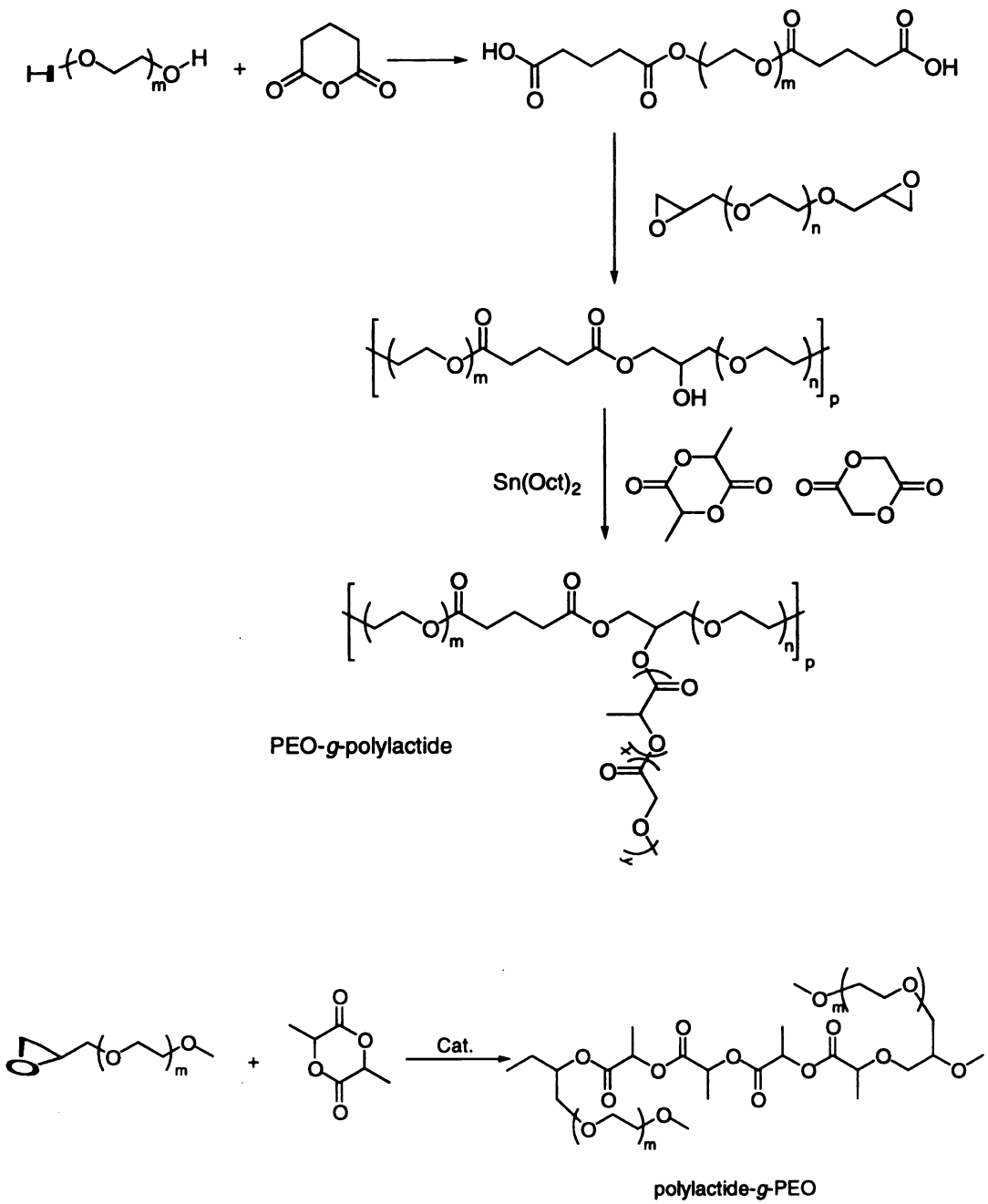

Scheme 1.14. Graft copolymers of lactide and ethylene oxide

One application of block copolymers of lactide and ethylene oxide in drug delivery systems has focused on developing systems that can form *in situ* drug delivery matrices in the body. Although microspheres with encapsulated drugs can be fabricated from these block copolymers and injected into the body, the fabrication process is usually complicated and requires the use of organic solvents, which sometimes cause denaturation of proteins incorporated in the microspheres.

The notion of forming an *in situ* drug delivery system is based on the fact that block copolymers of lactide and ethylene oxide can undergo reversible temperature-dependent sol-gel transitions in aqueous environments. The gellation temperature can be tuned by varying the composition of the block copolymer architecture as well as its concentration.[113,114] For example, the polymers can be dissolved into water to form a homogeneous solution (sol) at room temperature, and once the solution is injected into human bodies, it quickly gels *in situ* to form a drug delivery matrix as shown in **Figure 1.8**.

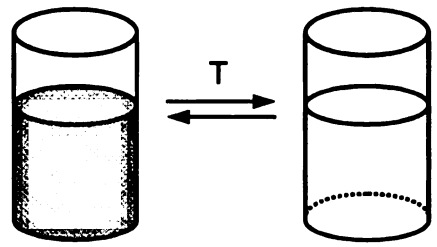

Figure 1.8. Sol-gel transition in lactide and ethylene oxide

1.9. Atom transfer radical polymerization (ATRP)

The past few years have witnessed the rapid development of transition metal catalyzed atom transfer radical polymerization (ATRP). ATRP has been widely used in the literature to prepare polymeric materials with novel functionalities, compositions and architectures.[115-117]

ATRP is one of the most versatile systems among the recently developed controlled radical polymerization methods.[118] It is based on establishing a rapid dynamic equilibration between a low concentration of active free radicals and a large concentration of dormant species. The well accepted mechanism for ATRP is shown in **Scheme 1.15**. In the initiation and propagation steps, the radicals or active polymer sites are generated by a reversible transition metal mediated redox process, where X and Y are (pseudo) halogens. The transition metal (Cu for example) undergoes a one-electron oxidation with abstraction of a (pseudo) halogen atom X from the dormant species. The process is reversible with the rate constant of activation being k_{act} and the rate constant of deactivation being k_{deact}. The active species can grow by addition of monomers or terminate by coupling or disproportionation with the rate constants of propagation and termination being k_p and k_t respectively. In well-controlled ATRPs, the position of the equilibrium between the dormant and active species favors the dormant species to ensure low radical concentrations and minimize bimolecular chain termination reactons.

ATRP is a multicomponent polymerization system. The effect of each component (monomer, initiator, catalyst/ligand, solvent and temperature) should be considered to ensure a well-controlled ATRP.

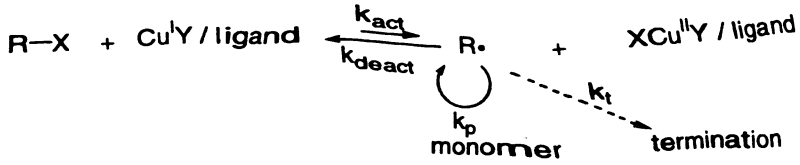

Scheme 1.15. Mechanism of copper-catalyzed ATRP

1) Monomers

A variety of monomers can be polymerized by ATRP. Typical monomers include methacrylates, acrylates, styrenes, acrylonitriles and (meth)acrylamides. The common feature of these monomers is that they all contain substituents that stabilize the propagating radicals.[116,117]

However, there are two major types of monomers that cannot be polymerized successfully by ATRP. One type includes halogenated alkenes, alkyl substituted olefins, and vinyl esters, all of which have intrinsically low reactivity in free radical polymerizations. The other type includes acidic monomers such as methacrylic acids, which poison transition metal catalysts through formation of metal carboxylates. In addition, acidic monomers can protonate transition metal catalysts that contain nitrogen ligands and interfere with their complexation ability. This problem can be overcome by using protected monomers. For example, by adjusting the pH, sodium methacylate was polymerized in aqueous phase by a PEO macroinitiator and CuBr/bpy.[119]

Alternatively, the acid can be protected with an easy to remove ester, allowing ATRP of protected methacrylic acids such as trimethylsilyl methacrylate and benzyl methacrylate.[120]

2) Initiators

Halogenated alkanes, benzylic halides, α-haloesters, α-haloketones, α-halonitriles and sulfonyl halides have been used as ATRP initiators. Not all initiators work well for all monomers. The basic requirement for a good initiator is that it should be at least as reactive as the subsequently formed growing chains. If the reactivity is too low, polymers with low polydispersities cannot be obtained because new chains can form at very late stages of the polymerization. If the reactivity is too high, too many radicals are generated at the beginning of the polymerization leading to the loss of initiating species by radical coupling. Typically, initiators whose structure is similar to the propagating species are chosen for a particular monomer. The most popular halogen atoms in initiators are Br and Cl. Since radical polymerizations can tolerate many functional groups, initiators with functional groups or macroinitiators can also be used to prepare functional polymers[121-123] or block copolymers.[119,124]

3) Transition metal catalysts and ligands

There are a few prerequisites for efficient ATRP catalysts. First, the metal catalyst must be able to switch between two oxidation states separated by one electron. Second, the catalyst should have suitable affinity toward halogen atoms. Third, the metal should be able to expand its coordination sphere to accommodate a (pseudo)halogen. Fourth, the ligand should complex the metal relatively strongly. A variety of metal catalysts based on nickel, ruthenium, iron and copper meet these requirements, but copper catalysts are favored by most researchers due to their versatility and low cost.

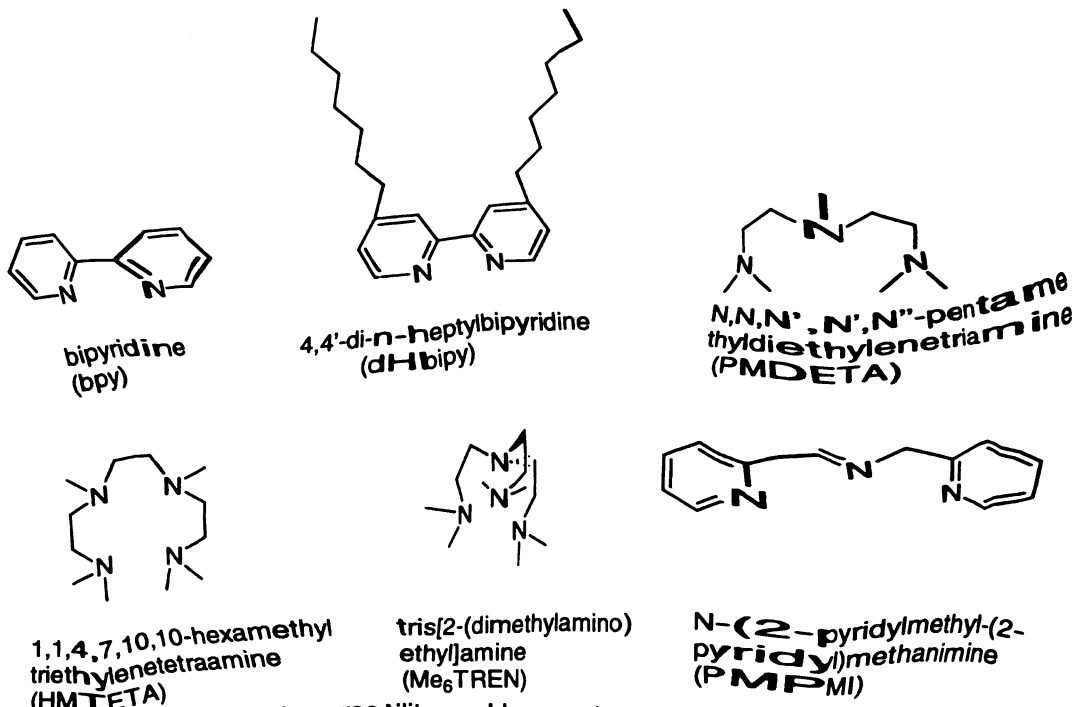

Figure 1.9. Examples of nitrogen-containing ligands used in ATRP

The catalyst activity is strongly dependent upon the ligand. Various bidentate and multidentate nitrogen-containing ligands were developed (**Figure 1.9**) to tune the activity of copper halide catalysts. Tetradentate ligands such as Me_6TREN form more active catalyst/ligand complexes and lead to well controlled ATRP even at room temperatures.[125] Ligands also help solubilize transition metal halides in monomers or solvents. Long chain alkyl groups on bipyridine rings can improve the solubility of copper catalysts and lead to homogenous polymerization conditions.

Ligands also play an important role in catalyst removal and recycling. Schiff base ligands were covalently bound to silica gel and cross-linked polystyrene beads for ease in catalyst separation and recycling.[126]

Upon abstraction of one halogen atom by a Cu(I) complex, the coordination number as well as the coordination structure changes. The determination of the active catalyst structures remains a challenge, and the exact structure of the active species in the Cu/bpy system is not yet completely clear. In the proposed **Scheme 1.16**, $Cu(I)(bpy)_2$ exists in a tetrahedral geometry, and upon halogen abstraction, the coordination sphere of copper expands to accommodate the extra halogen by adopting a trigonal bipyramidal geometry.

4) Solvents

ATRP can be carried out in bulk, in solution or in heterogeneous systems such as emulsions and suspensions. Generally, solvents are used for better heat transfer and minimization of viscosity problems. If the resulting polymer is

not soluble in its monomer, as in the case of polyacrylonitrile, a solvent is indispensable. The solvent should be chosen to minimize chain transfer and other solvent assisted reactions.

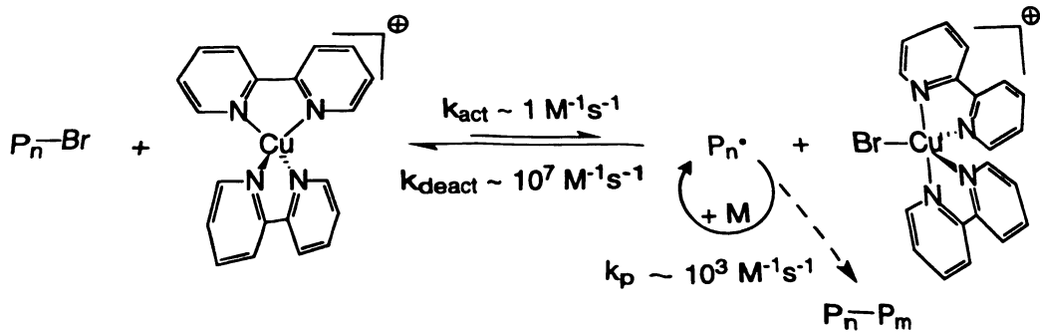

Scheme 1.16. Proposed Cu(I) and Cu(II) species using bpy as the ligand

1.10. Combination of ring opening polymerization and (controlled) radical polymerization

Ring opening polymerization and (controlled) radical polymerization are both widely used in polymer synthesis. A combination of both polymerization methods can lead to interesting polymer structures and properties. In general, four strategies, end group transformation, the use of difunctional initiators, difunctional monomers and functional macromonomers have been employed to combine these two polymerization methods.

1) End group transformation

End group transformation converts the propagating center from the first polymerization to the initiating species needed for the second polymerization. This technique has been used to prepare block copolymers[127] and dendrimers[128] using two or more mechanistically incompatible monomers. For example, ring opening polymerization of caprolactone by Al(O*i*-Pr)$_3$ placed an ester group on one end and a hydroxy end group on the other end of the polycaprolactone chain. The hydroxy chain end was transformed into an ATRP initiator moiety by reaction with 2-bromoisobutyrylbomide, and then used to initiate the ATRP of *t*-butylacrylate by a nickel or copper catalyst (**Scheme 1.17**).

2) Difunctional initiators

Difunctional initiators are molecules with two initiating sites. The use of difunctional initiators can avoid problems encountered in end group

transformation such as a low concentration of the active species and time-consuming separation and purification steps. The greatest advantage of such a strategy is that block copolymers can be prepared in a minimum of steps without intermediate functionalization reactions. In cases where the two polymer mechanisms are compatible, one-pot synthesis of block copolymers are possible.[129]

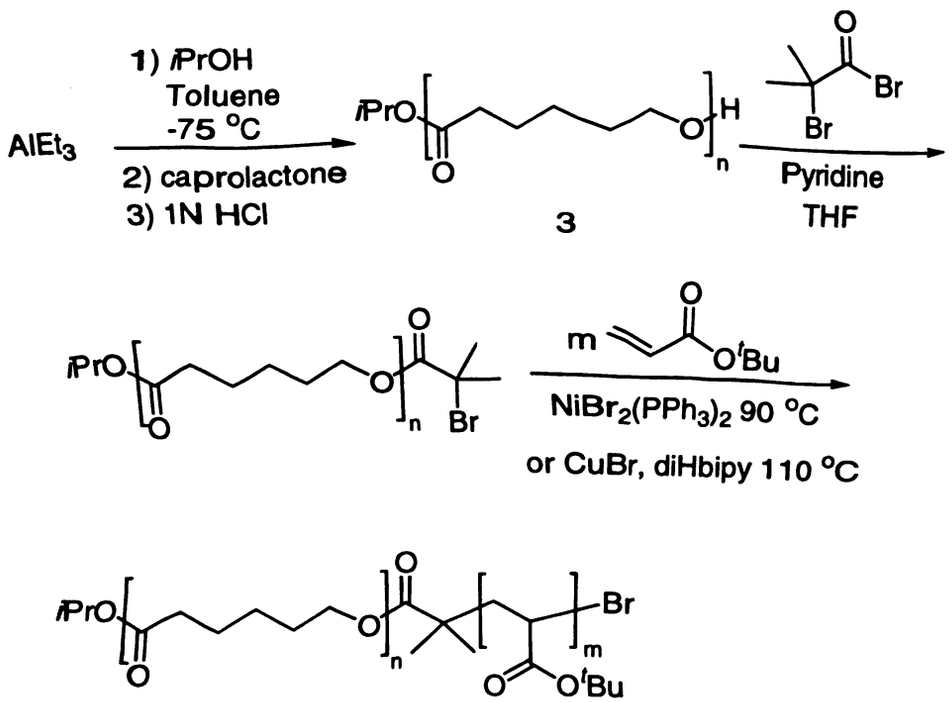

Scheme 1.17. Block copolymers synthesized by end group transformation

Several research groups have applied this strategy to dual radical and ring opening polymerizations. For example, the product of the alcohol exchange reaction between $Al(O\text{-}iPr)_3$ and benzopinacol can be used as a difunctional initiator since the substituted tetraphenylethane moiety in the initiator thermally

decomposes to initiate the radical polymerization of MMA and styrene, while the Al-alkoxide bond can initiate the ring opening polymerization of caprolactone.[130]

In a preparation of shell-cross-linked nanoparticles, Wooley *et al.* used another difunctional initiator, $Al(OCH_2CBr_3)_3$, to initiate the ring opening polymerization of caprolactone and the ATRP of *t*-butylacrylate.[127] Combined ring opening polymerization of caprolactone and nitroxide-mediated "living" radical polymerization of styrene were realized by employing a difunctional initiator bearing a primary alcohol group and a nitroxide moiety. **(Scheme 1.18)**

3) Difunctional monomers

Difunctional monomers provide a new way to manipulate the structures and properties of polymers through controlled block or graft polymerizations. Hedrick *et al.* reported the synthesis of graft hyperbranched and crosslinked polymer systems using functional monomers via a combination of ring opening polymerization and controlled radical polymerizations.

The ring opening copolymerization of monomer **A** in **Figure 1.10** with lactide yielded an aliphatic polyester containing pendent acrylate groups. UV or radical initiated polymerization of the resulting polymer gave a crosslinked system.[78] Functional monomer **B** in **Figure 1.10** was copolymerized sequentially with caprolactone and MMA in a one reaction. It acted as both a monomer and an initiator for ring opening polymerization and ATRP respectively.[131]

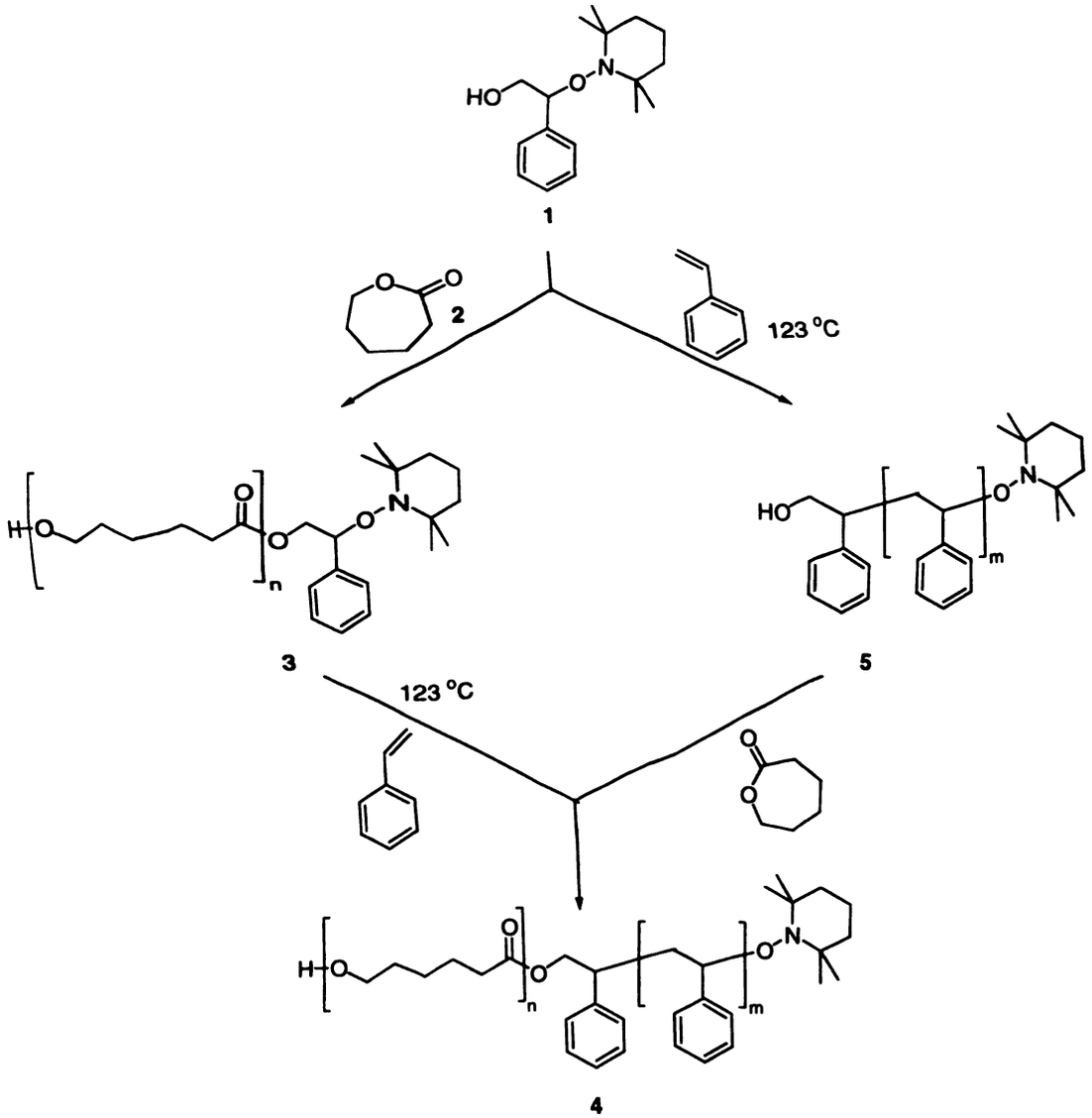

Scheme 1.18. Block copolymers of caprolactone and styrene synthesized by a difunctional initiator approach

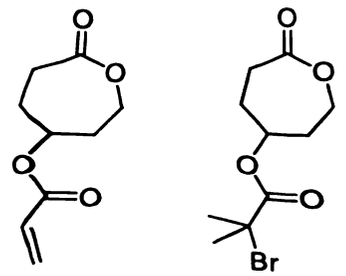

A B

Figure 1.10. Difunctional monomers used for ring opening polymerization

4) Functional macromonomers

Graft copolymers consisting of biodegradable and non-biodegradable components are interesting examples of polymers whose physical and mechanical properties are controlled by composition, distribution of the comonomers in the chains, as well as the chemical nature and length of the backbone and graft segments.

A popular route to graft copolymers is to prepare polymers with macromonomers. Using 2-hydroxyethyl (meth)acrylate as an initiator, glycolide, lactide, and caprolactone were oligomerized to give macromonomers.[132-136] Copolymerization of the macromonomers with 2-hydroxyethylmethacrylate, MMA, acrylates or itaconic anhydride by either free radical or controlled radical polymerization gave the graft architecture (**Scheme 1.19**).

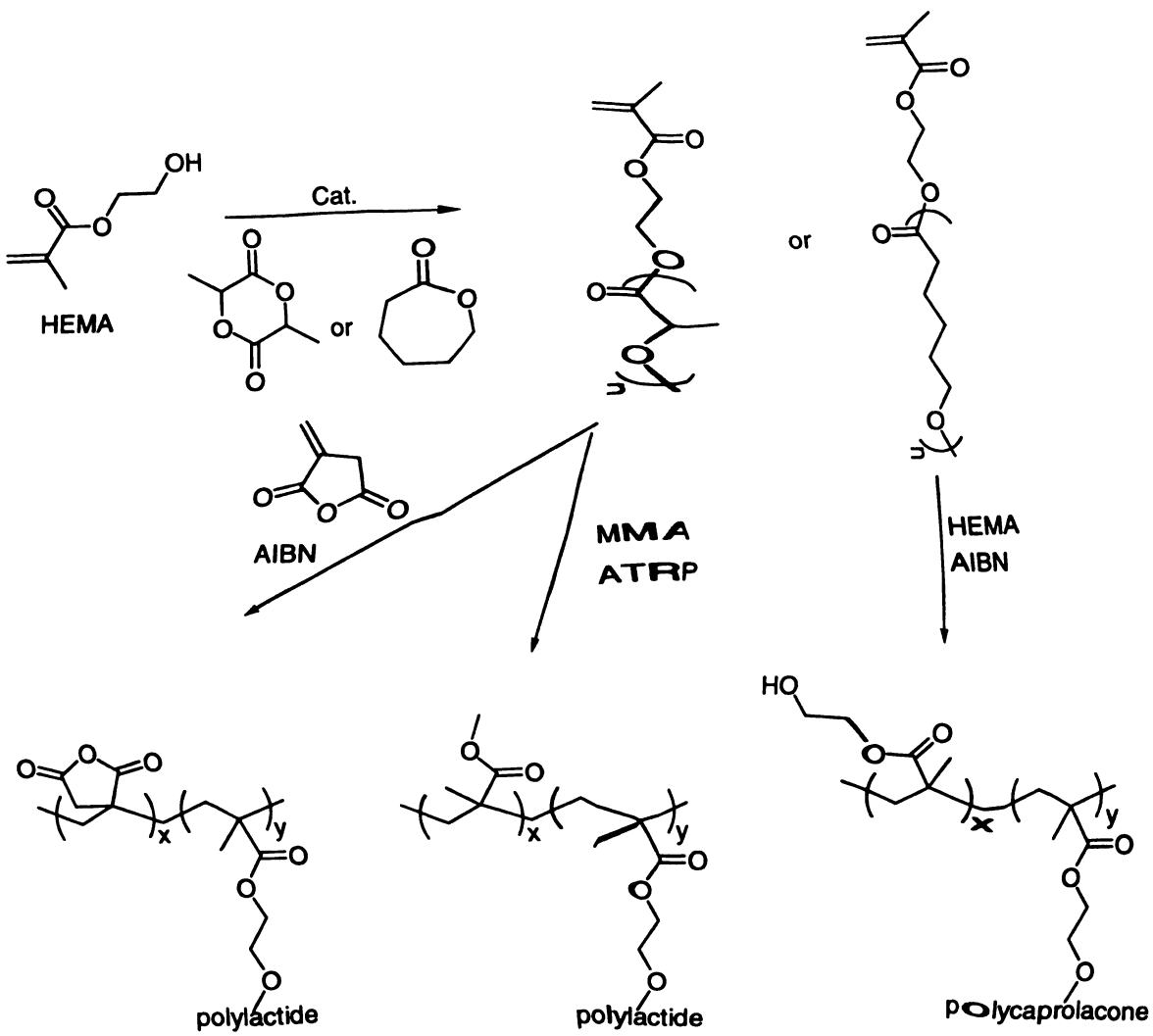

Scheme 1.19. Graft polymers synthesized by the macromonomer approach

References

1. Kinnersley, A. M.; Scott, T. C.; Yopp, J. H.; Whitten, G. H. *Plant Growth Regul.* **1990**, *9*, 137-146.

2. Bogaert, J. C.; Coszach, P. *Macromol. Symp.* **2000**, *153*, 287-303.

3. Lunt, J. *Polym. Degrad. Stabil.* **1998**, *59*, 145-152.

4. Ajioka, M.; Suizu, H.; Higuchi, C.; Kashima, T. *Polym. Degrad. Stabil.* **1998**, *59*, 137-143.

5. Woo, S. I.; Kim, B. O.; Jun, H. S.; Chang, H. N. *Polym. Bull.* **1995**, *35*, 415-421.

6. Dubois, P.; Jerome, R.; Teyssie, P. *Macromol. Symp.* **1991**, *42-3*, 103-116.

7. Ropson, N.; Dubois, P.; Jerome, R.; Teyssie, P. *Macromolecules* **1993**, *26*, 6378-6385.

8. Dubois, P.; Jerome, R.; Teyssie, P. *Polym. Bull.* **1989**, *22*, 475-482.

9. Leborgne, A.; Vincens, V.; Jouglard, M.; Spassky, N. *Macromol. Symp.* **1993**, *73*, 37-46.

10. Spassky, N.; Wisniewski, M.; Pluta, C.; LeBorgne, A. *Macromol. Chem. Phys.* **1996**, *197*, 2627-2637.

11. Ovitt, T. M.; Coates, G. W. *J. Am. Chem. Soc.* **1999**, *121*, 4072-4073.

12. Radano, C. P.; Baker, G. L.; Smith III, M. R. *J. Am. Chem. Soc.* **2000**, *122*, 1552-1553.

13. Cameron, P. A.; Jhurry, D.; Gibson, V. C.; White, A. J. P.; Williams, D. J.; Williams, S. *Macromol. Rapid Commun.* **1999**, *20*, 616-618.

14. Penczek, S.; Duda, A.; Kowalski, A.; Libiszowski, J.; Majerska, K.; Biela, T. *Macromol. Symp.* **2000**, *157*, 61-70.

15. Ryner, M.; Stridsberg, K.; Albertsson, A. C.; von Schenck, H.; Svensson, M. *Macromolecules* **2001**, *34*, 3877-3881.

16. Kricheldorf, H. R.; Lossin, M. *J. Macromol. Sci.-Pure Appl. Chem.* **1997**, *A34*, 179-189.

17. Dunsing, R.; Kricheldorf, H. R. *Polym. Bull.* **1985**, *14*, 491-495.

18. Kricheldorf, H. R.; Damrau, D. O. *Macromol. Chem. Phys.* **1997**, *198*, 1753-1766.

19. Schwach, G.; Coudane, J.; Engel, R.; Vert, M. *Polym. Int.* **1998**, *46*, 177-182.

20. Schwach, G.; Coudane, J.; Engel, R.; Vert, M. *Polym. Bull.* **1994**, *32*, 617-623.

21. Kricheldorf, H. R.; Damrau, D. O. *Macromol. Chem. Phys.* **1997**, *198*, 1767-1774.

22. O'Keefe, B. J.; Monnier, S. M.; Hillmyer, M. A.; Tolman, W. B. *J. Am. Chem. Soc.* **2001**, *123*, 339-340.

23. Simic, V.; Pensec, S.; Spassky, N. *Macromol. Symp.* **2000**, *153*, 109-121.

24. Spassky, N.; Simic, V.; Montaudo, M. S.; Hubert-Pfalzgraf, L. G. *Macromol. Chem. Phys.* **2000**, *201*, 2432-2440.

25. Yuan, M. L.; Xiong, C. D.; Li, X. H.; Deng, X. M. *J. Appl. Polym. Sci.* **1999**, *73*, 2857-2862.

26. Deng, X. M.; Yuan, M. L.; Li, X. H.; Xiong, C. D. *Eur. Polym. J.* **2000**, *36*, 1151-1156.

27. Shen, Y. Q.; Shen, Z. Q.; Zhang, Y. F.; Yao, K. M. *Macromolecules* **1996**, *29*, 8289-8295.

28. Shen, Y. Q.; Zhu, K. J.; Shen, Z. Q.; Yao, K. M. *J. Polym. Sci. Pol. Chem.* **1996**, *34*, 1799-1805.

29. Stevels, W. M.; Ankone, M. J. K.; Dijkstra, P. J.; Feijen, J. *Macromolecules* **1996**, *29*, 8296-8303.

30. Stevels, W. M.; Ankone, M. J. K.; Dijkstra, P. J.; Feijen, J. *Macromolecules* **1996**, *29*, 6132-6138.

31. Simic, V.; Spassky, N.; HubertPfalzgraf, L. G. *Macromolecules* **1997**, *30*, 7338-7340.

32. Kowalski, A.; Duda, A.; Penczek, S. *Macromolecules* **2000**, *33*, 689-695.

33. Kricheldorf, H. R.; Eggerstedt, S. *Macromol. Chem. Phys.* **1999**, *200*, 1284-1291.

34. Zhang, X. C.; Wyss, U. P.; Pichora, D.; Goosen, M. F. A. *Polym. Bull.* **1992**, *27*, 623-629.

35. Gogolewski, S.; Jovanovic, M.; Perren, S. M.; Dillon, J. G.; Hughes, M. K. *Polym. Degrad. Stabil.* **1993**, *40*, 313-322.

36. Kopinke, F. D.; Mackenzie, K. *J. Anal. Appl. Pyrolysis* **1997**, *40-1*, 43-53.

37. Wachsen, O.; Reichert, K. H.; Krueger, R. P.; Much, H.; Schulz, G. *Polym. Degrad. Stab.* **1997**, *55*, 225-231.

38. Kopinke, F. D.; Remmler, M.; Mackenzie, K.; Moder, M.; Wachsen, O. *Polym. Degrad. Stabil.* **1996**, *53*, 329-342.

39. Cam, D.; Marucci, M. *Polymer* **1997**, *38*, 1879-1884.

40. Degee, P.; Dubois, P.; Jerome, R. *Macromol. Chem. Phys.* **1997**, *198*, 1985-1995.

41. Kricheldorf, H. R.; Berl, M.; Scharnagl, N. *Macromolecules* **1988**, *21*, 286-293.

42. Noda, M.; Okuyama, H. *Chem. Pharm. Bull.* **1999**, *47*, 467-471.

43. Sodergard, A.; Nasman, J. H. *Ind. Eng. Chem. Res.* **1996**, *35*, 732-735.

44. Carlson, D.; Dubois, P.; Nie, L.; Narayan, R. *Polym. Eng. Sci.* **1998**, *38*, 311-321.

45. Wachsen, O.; Reichert, K. H.; Kruger, R. P.; Much, H.; Schulz, G. *Polym. Degrad. Stabil.* **1997**, *55*, 225-231.

46. Sparer, R. V.; Shih, C.; Ringeisen, C. D.; Himmelstein, K. J. *J. Controlled Release* **1984**, *1*, 23-32.

47. Sanders, A. J.; Li, B.; Bieniarz, C.; Harris, F. W. *Polym. Prepr. (Am. Chem. Soc., Div. Polym. Chem.)* **1999**, *40*, 888-889.

48. Li, S. M.; Garreau, H.; Vert, M. *Journal of Materials Science: Materials in Medicine* **1990**, *1*, 198-206.

49. Hyon, S. H.; Jamshidi, K.; Ikada, Y. *Polym. Int.* **1998**, *46*, 196-202.

50. Tsuji, H.; Ikada, Y. *Polym. Degrad. Stabil.* **2000**, *67*, 179-189.

51. Li, S. M.; Vert, M. *J. Biomater. Sci.-Polym. Ed.* **1996**, *7*, 817-827.

52. Li, S. M.; GirodHolland, S.; Vert, M. *J. Control. Release* **1996**, *40*, 41-53.

53. Doi, Y.; Kanesawa, Y.; Kunioka, M.; Saito, T. *Macromolecules* **1990**, *23*, 26-31.

54. Cha, Y.; Pitt, C. G. *Biomaterials* **1990**, *11*, 108-112.

55. Pitt, C. G.; Cha, Y.; Shah, S. S.; Zhu, K. J. *J. Controlled Release* **1992**, *19*, 189-199.

56. Dunne, M.; Corrigan, O. I.; Ramtoola, Z. *Biomaterials* **2000**, *21*, 1659-1668.

57. Reeve, M. S.; McCarthy, S. P.; Downey, M. J.; Gross, R. A. *Macromolecules* **1994**, *27*, 825-831.

58. Macdonald, R. T.; McCarthy, S. P.; Gross, R. A. *Macromolecules* **1996**, *29*, 7356-7361.

59. Tsuji, H.; Miyauchi, S. *Polym. Degrad. Stabil.* **2001**, *71*, 415-424.

60. Tsuji, H. I., Takeharu *Macromol. Biosci.* **2001**, *1*, 59-65.

61. Gomer, T.; Gref, R.; Michenot, D.; Sommer, F.; Tran, M. N.; Dellacherie, E. *J. Control. Release* **1999**, *57*, 259-268.

62. Lemoine, D.; Francois, C.; Kedzierewicz, F.; Preat, W.; Hoffman, M.; Maincent, P. *Biomaterials* **1996**, *17*, 2191-2197.

63. Nah, J. W.; Jeong, Y. I.; Cho, C. S. *J. Polym. Sci. Pt. B-Polym. Phys.* **1998**, *36*, 415-423.

64. Kwon, G. S.; Naito, M.; Yokoyama, M.; Okano, T.; Sakurai, Y.; Kataoka, K. *Pharm. Res.* **1995**, *12*, 192-195.

65. Lasic, D. D. *Nature* **1992**, *355*, 279-280.

66. Jeong, Y. I.; Cho, C. S.; Kim, S. H.; Ko, K. S.; Kim, S. I.; Shim, Y. H.; Nah, J. W. *J. Appl. Polym. Sci.* **2001**, *80*, 2228-2236.

67. Ruckenstein, E.; Yuan, Y. M. *J. Appl. Polym. Sci.* **1998**, *69*, 1429-1434.

68. Zhu, K. J.; Hendren, R. W.; Jensen, K.; Pitt, C. G. *Macromolecules* **1991**, *24*, 1736-1740.

69. Buchholz, B. *J. Mater. Sci.-Mater. Med.* **1993**, *4*, 381-388.

70. Schmidt, P.; Keul, H.; Hocker, H. *Macromolecules* **1996**, *29*, 3674-3680.

71. Hori, Y.; Gonda, Y.; Takahashi, Y.; Hagiwara, T. *Macromolecules* **1996**, *29*, 804-806.

72. Chen, X. H.; McCarthy, S. P.; Gross, R. A. *Macromolecules* **1998**, *31*, 662-668.

73. Chen, X. H.; McCarthy, S. P.; Gross, R. A. *Macromolecules* **1997**, *30*, 3470-3476.

74. Song, C. X.; Sun, H. F.; Feng, X. D. *Polym. J.* **1987**, *19*, 485-491.

75. HiljanenVainio, M. P.; Orava, P. A.; Seppala, J. V. *J. Biomed. Mater. Res.* **1997**, *34*, 39-46.

76. Vion, J. M.; Jerome, R.; Teyssie, P.; Aubin, M.; Prudhomme, R. E. *Macromolecules* **1986**, *19*, 1828-1838.

77. Shirahama, H.; Mizuma, K.; Umemoto, K.; Yasuda, H. *J. Polym. Sci. Pol. Chem.* **2001**, *39*, 1374-1381.

78. Mecerreyes, D.; Humes, J.; Miller, R. D.; Hedrick, J. L.; Detrembleur, C.; Lecomte, P.; Jerome, R.; San Roman, J. *Macromol. Rapid Commun.* **2000**, *21*, 779-784.

79. Barrera, D. A.; Zylstra, E.; Lansbury, P. T.; Langer, R. *Macromolecules* **1995**, *28*, 425-432.

80. Barrera, D. A.; Zylstra, E.; Lansbury, P. T.; Langer, R. *J. Am. Chem. Soc.* **1993**, *115*, 11010-11011.

81. Deng, X. M.; Yao, J. R.; Yuan, M. L.; Li, X. H.; Xiong, C. D. *Macromol. Chem. Phys.* **2000**, *201*, 2371-2376.

82. Veld, P. J. A.; Ye, W. P.; Klap, R.; Dijkstra, P. J.; Feijen, J. *Makromol. Chem.* **1992**, *193*, 1927-1942.

83. Wang, C.; Mao, Y.; Baker, G. L. *Abstr. Pap. Am. Chem. Soc.* **2000**, *220*, 305-POLY.

84. Wang, C.; Yin, E.; Baker, G. L. *Abstr. Pap. Am. Chem. Soc.* **2000**, *219*, 123-POLY.

85. Retsos, H.; Margiolaki, I.; Messaritaki, A.; Anastasiadis, S. H. *Macromolecules* **2001**, *34*, 5295-5305.

86. Chattopadhyay, S.; Sivaram, S. *Polym. Int.* **2001**, *50*, 67-75.

87. Kang, E. A.; Kim, J. H.; Kim, C. K.; Oh, S. Y.; Rhee, H. W. *Polym. Eng. Sci.* **2000**, *40*, 2374-2384.

88. Radonjic, G. *J. Appl. Polym. Sci.* **1999**, *72*, 291-307.

89. Veld, P.; Velner, E. M.; VanDeWitte, P.; Hamhuis, J.; Dijkstra, P. J.; Feijen, J. *J. Polym. Sci. Pol. Chem.* **1997**, *35*, 219-226.

90. Song, C. X.; Feng, X. D. *Macromolecules* **1984**, *17*, 2764-2767.

91. Schwach-Abdellaoui, K.; Heller, J.; Gurny, R. *Macromolecules* **1999**, *32*, 301-307.

92. Ng, S. Y.; Vandamme, T.; Taylor, M. S.; Heller, J. *Macromolecules* **1997**, *30*, 770-772.

93. Sintzel, M. B.; Heller, J.; Ng, S. Y.; Taylor, M. S.; Tabatabay, C.; Gurny, R. *Biomaterials* **1998**, *19*, 791-800.

94. Zhang, S.; Hou, Z.; Gonsalves, K. E. *J. Polym. Sci. Pol. Chem.* **1996**, *34*, 2737-2742.

95. Bachari, A.; Belorgey, G.; Helary, G.; Sauvet, G. *Macromol. Chem. Phys.* **1995**, *196*, 411-428.

96. Wang, Y. B.; Hillmyer, M. A. *Macromolecules* **2000**, *33*, 7395-7403.

97. Schmidt, S. C.; Hillmyer, M. A. *Macromolecules* **1999**, *32*, 4794-4801.

98. Wang, Y. B.; Hillmyer, M. A. *J. Polym. Sci. Pol. Chem.* **2001**, *39*, 2755-2766.

99. Deng, X. M.; Xiong, C. D.; Cheng, L. M.; Xu, R. P. *J. Polym. Sci., Part C: Polym. Lett.* **1990**, *28*, 411-416.

100. Deng, X. M.; Xiong, C. D.; Cheng, L. M.; Huang, H. H.; Xu, R. P. *J. Appl. Polym. Sci.* **1995**, *55*, 1193-1196.

101. Li, S. M.; Rashkov, I.; Espartero, J. L.; Manolova, N.; Vert, M. *Macromolecules* **1996**, *29*, 57-62.

102. Rashkov, I.; Manolova, N.; Li, S. M.; Espartero, J. L.; Vert, M. *Macromolecules* **1996**, *29*, 50-56.

103. Cerrai, P.; Tricoli, M. *Makromol. Chem., Rapid Commun* **1993**, *14*, 529-538.

104. Deng, X. M.; Zhu, Z. X.; Xiong, C. D.; Zhang, L. L. *J. Polym. Sci. Pol. Chem.* **1997**, *35*, 703-708.

105. Stevels, W. M.; Ankone, M. J. K.; Dijkstra, P. J.; Feijen, J. *Macromol. Chem. Phys.* **1995**, *196*, 3687-3694.

106. Du, Y. J.; Lemstra, P. J.; Nijenhuis, A. J.; Vanaert, H. A. M.; Bastiaansen, C. *Macromolecules* **1995**, *28*, 2124-2132.

107. Chen, X. H.; McCarthy, S. P.; Gross, R. A. *Macromolecules* **1997**, *30*, 4295-4301.

108. Jeong, B.; Kibbey, M. R.; Birnbaum, J. C.; Won, Y. Y.; Gutowska, A. *Macromolecules* **2000**, *33*, 8317-8322.

109. Cho, K. Y.; Kim, C. H.; Lee, J. W.; Park, J. K. *Macromol. Rapid Commun.* **1999**, *20*, 598-601.

110. Choi, Y. R.; Bae, Y. H.; Kim, S. W. *Macromolecules* **1998**, *31*, 8766-8774.

111. Li, Y. X.; Kissel, T. *Polymer* **1998**, *39*, 4421-4427.

112. Iijima, M.; Nagasaki, Y.; Okada, T.; Kato, M.; Kataoka, K. *Macromolecules* **1999**, *32*, 1140-1146.

113. Jeong, B.; Bae, Y. H.; Lee, D. S.; Kim, S. W. *Nature* **1997**, *388*, 860-862.

114. Fujiwara, T.; Mukose, T.; Yamaoka, T.; Yamane, H.; Sakurai, S.; Kimura, Y. *Macromol. Biosci.* **2001**, *1*, 204-208.

115. Coessens, V.; Pintauer, T.; Matyjaszewski, K. *Prog. Polym. Sci.* **2001**, *26*, 337-377.

116. Patten, T. E.; Matyjaszewski, K. *Adv. Mater.* **1998**, *10*, 901-915.

117. Matyjaszewski, K. *Chem.-Eur. J.* **1999**, *5*, 3095-3102.

118. Matyjaszewski, K.; Xia, J. *Chem. Rev.* **2001**, *101*, 2921-2990.

119. Ashford, E. J.; Naldi, V.; O'Dell, R.; Billingham, N. C.; Armes, S. P. *Chem. Commun.* **1999**, 1285-1286.

120. Davis, K. A.; Charleux, B.; Matyjaszewski, K. *J. Polym. Sci. Pol. Chem.* **2000**, *38*, 2274-2283.

121. Marsh, A.; Khan, A.; Garcia, M.; Haddleton, D. M. *Chem. Commun.* **2000**, 2083-2084.

122. Marsh, A.; Khan, A.; Haddleton, D. M.; Hannon, M. J. *Macromolecules* **1999**, *32*, 8725-8731.

123. Alkan, S.; Toppare, L.; Hepuzer, Y.; Yagci, Y. *J. Polym. Sci. Pol. Chem.* **1999**, *37*, 4218-4225.

124. Kajiwara, A.; Matyjaszewski, K. *Macromolecules* **1998**, *31*, 3489-3493.

125. Kim, J.-B.; Bruening, M. L.; Baker, G. L. *J. Am. Chem. Soc.* **2000**, *122*, 7616-7617.

126. Haddleton, D. M.; Kukulj, D.; Radigue, A. P. *Chem. Commun.* **1999**, 99-100.

127. Zhang, Q.; Remsen, E. E.; Wooley, K. L. *J. Am. Chem. Soc.* **2000**, *122*, 3642-3651.

128. Hedrick, J. L.; Trollsas, M.; Hawker, C. J.; Atthoff, B.; Claesson, H.; Heise, A.; Miller, R. D.; Mecerreyes, D.; Jerome, R.; Dubois, P. *Macromolecules* **1998**, *31*, 8691-8705.

129. Bielawski, C. W.; Morita, T.; Grubbs, R. H. *Macromolecules* **2000**, *33*, 678-680.

130. Guo, Z. R.; Wan, D. C.; Huang, J. L. *Macromol. Rapid Commun.* **2001**, *22*, 367-371.

131. Mecerreyes, D.; Atthoff, B.; Boduch, K. A.; Trollsas, M.; Hedrick, J. L. *Macromolecules* **1999**, *32*, 5175-5182.

132. Dubois, P.; Jerome, R.; Teyssie, P. *Macromolecules* **1991**, *24*, 977-981.

133. Wallach, J. A.; Huang, S. J. *Biomacromolecules* **2000**, *1*, 174-179.

134. Furch, M.; Eguiburu, J. L.; Fernandez-Berridi, M. J.; San Roman, J. *Polymer* **1998**, *39*, 1977-1982.

135. Barakat, I.; Dubois, P.; Jerome, R.; Teyssie, P.; Goethals, E. *J. Polym. Sci. Pol. Chem.* **1994**, *32*, 2099-2110.

136. Gopp, U.; Sandner, B.; Hahne, B. *Macromol. Symp.* **2000**, *153*, 321-332.

Chapter 2 Polymandelide

2.1. General

The glass transition temperature (T_g) is an important physical parameter of polymers since it defines the maximum temperature for which a polymer is suitable for structural applications. Above T_g, segmental movement of polymer chains is possible and polymers are rubbery and elastic. Below T_g, polymers are stiff and hard. The glass transition temperatures of all known substituted polylactides are < 70 °C. This is an obvious limitation for applications such as disposable packaging materials, where mechanical rigidity is important. For example, a polylactide cup used for a hot beverage such as coffee would soften and lose its original shape since the temperature of the liquid is above the glass transition of the material.

To increase the T_g of polylactides, we used a simple strategy based on the known structure-property relationships of commercial polymers as shown in **Table 2.1**. By varying the substituents attached to a polymer backbone of aliphatic carbon atoms, one can obtain polyethylene (PE), polypropylene (PP), polyvinylchloride (PVC) polystyrene (PS) and other polymers. The glass transition temperatures of these polymers range from –100 to 109 °C, and satisfy the requirements of a broad range of applications.

Since the glass transition is related to mobility of chains, increasing the chain stiffness or intermolecular interactions between chains increases T_g. Thus, either increasing the steric bulk of the substituents (e.g. methyl, and phenyl in the

Table 2.1. Glass transition temperatures of commercial polymers.

polymer	abbreviation	T_g (°C)
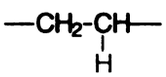	PE	-125
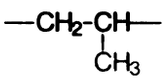	PP	-8
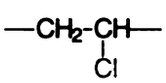	PVC	81
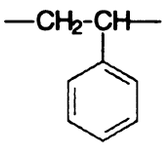	PS	109

structures shown in **Table 2.1** or incorporating dipoles (e.g. Cl) increase T_g and the chain stiffness. We expect to see the same trends in substituted polylactides. Poly(phenyllactide), where the methyl group of polylactide is replaced by benzyl, was examined as a potential high T_g material. However, the glass transition temperature of poly(phenyl lactide) is 55 °C, which is comparable to that of polylactide. The relatively low T_g can be explained by the methylene unit that links the benzene ring to the polyester backbone. The methylene unit reduces the steric barrier for rotation around the polymer backbone, thus increasing the flexibility of the polymer.

A reasonable way to increase the T_g of polylactides would be to make a simple analogy to polystyrene, eliminate the flexible methylene unit and attach a benzene ring directly to the polyester backbone. The systematic name of the resulting polymer is poly[oxy(1-oxo-2-phenyl-1,2-ethanediyl)], but polymandelide or poly(mandelic acid), common names based on the monomers used to synthesize the polymer, are more convenient. The trivial name polymandelide will be used for this degradable polystyrene mimic.

There has been minimal work on the synthesis of polymandelide and copolymers. All reported syntheses have produced low molecular weight polymers and the characterization of the polymers has been limited. Polymandelide was first obtained accidentally by Okada and Okawara[1] from the pyrolysis of a phenyl-substituted trimethyltin bromoacetate (**Scheme 2.1** entry 1). The IR and NMR spectral data for the resulting white solid are consistent with the polymandelide structure. No molecular weight data were provided, but the physical properties of the solid imply a low molecular weight product. In 1980, the reaction of the α-keto acid phenylglyoxylic acid, with 2-phenoxy-4,4,5,5-tetramethyl-1,3,2-dioxaphospholane was used by Kobayashi[2] to synthesize polymandelide (**Scheme 2.1** entry 2). The deoxy-polymerization yielded a polymer with a number average molecular weight around 2,400 g/mol as determined by vapor pressure osmometry measurements. Tighe and Smith[3] reported the first example of polymandelide synthesized by a ring opening polymerization scheme (**Scheme 2.1** entry 3). 5-Phenyl-1,3-dioxalan-2,4-dione (the anhydrocarboxylate derivative of mandelic acid) was shown to undergo ring

opening polymerization in the presence of tertiary organic bases such as pyridine to generate polymandelide and CO_2. The degree of polymerization was reported to be 25-30. Pinkus[4] (**Scheme 2.1** entry 4) prepared polymandelide by the reaction of α-bromophenyllactic acid with triethylamine. GPC and viscosity measurements indicated a degree of polymerization around 12-20, which was comparable to that obtained by other methods. Domb[5] (**Scheme 2.1** entry 6) and Whitesell[6] (**Scheme 2.1** entry 5) prepared polymandelide by polycondensation of mandelic acid and by transesterification of the methyl ester of mandelic acid. In both methods, *p*-toluenesulfonic acid was used as the catalyst and either high vacuum or a Dean-Stark trap was used to drive the equilibrium toward polymer formation. The molecular weights of the polymers obtained from the polycondensations were below 3,000 g/mol.

Low molecular weight poly(lactide-*co*-mandelide) was synthesized by a number of research groups.[7-10] The polycondensation method (**Scheme 2.2** entry 1) was used to modify the thermal and mechanical properties of polylactide as well as to achieve desired degradation profiles. A Japanese patent[11] described the first example of using mandelide, the cyclic dimmer of mandelic acid, as a comonomer to prepare poly(lactide-*co*-mandelide) (**Scheme 2.2** entry 2). Trans-4-hydroxy-L-proline was melt condensed with lactic acid or mandelic acid (**Scheme 2.2** entry 3) to obtain new biodegradable copolymers with pendant functional groups and improved degradability compared to pseudopoly(amino acid).[12] Thermal analysis showed an increase in T_g with increased incorporation of mandelic acid.

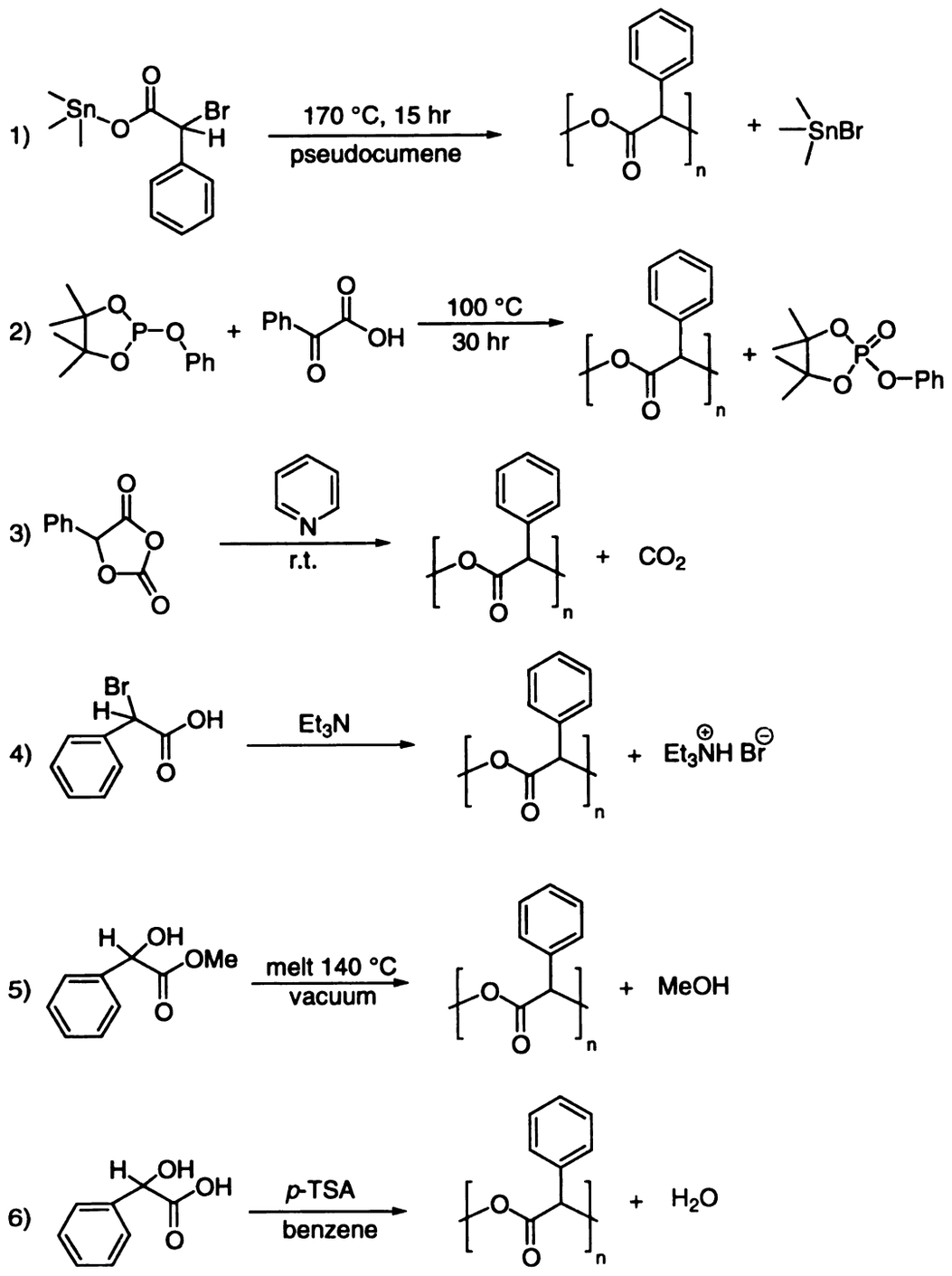

Scheme 2.1. Early examples of the synthesis of polymandelide.

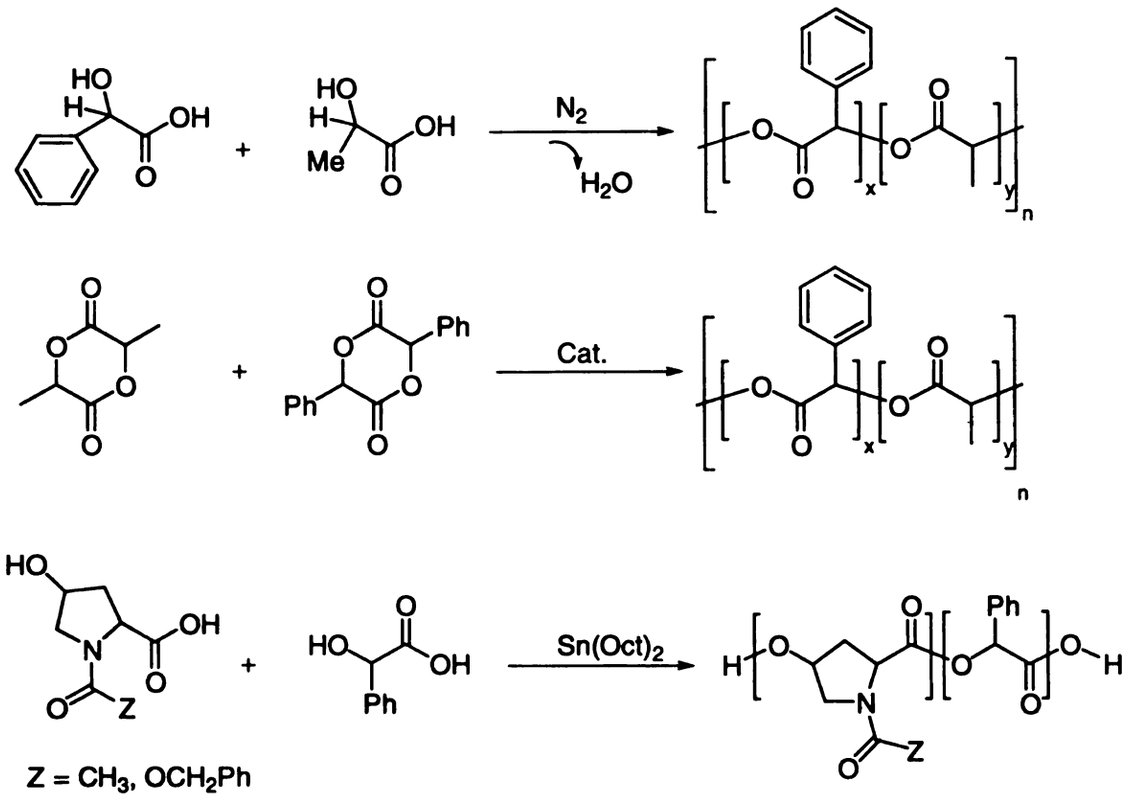

Scheme 2.2. Examples of the synthesis of mandelide copolymers

Copolymers of mandelic acid with poly(butylene succinate) and poly(ethylene adipate) were prepared by Yoon[13] using mandelic acid and the corresponding diacid and diol. Increasing the mandelic acid content decreased the crystallinity and melting temperature of the polyesters, but increased the T_g. As the mandelic acid content increased, mechanical properties such as elongation and tear strength were enhanced in the copolymers. The biodegradation rate of the poly(butylene succinate) copolymers also increased due to the disruption of crystallinity caused by incorporation of the mandelic acid monomer.

Blends of polylactide and polymandelide were prepared to study the miscibility and the effect of the low molecular weight aromatic polyester on drug release.[5] With triamcinolone (a steroid) as the model drug, the induction time for drug release from a polylactide and low molecular weight polymandelide blend decreased to half of that for pure racemic polylactide.

2.2. Monomer

2.2.1. Synthesis of mandelide

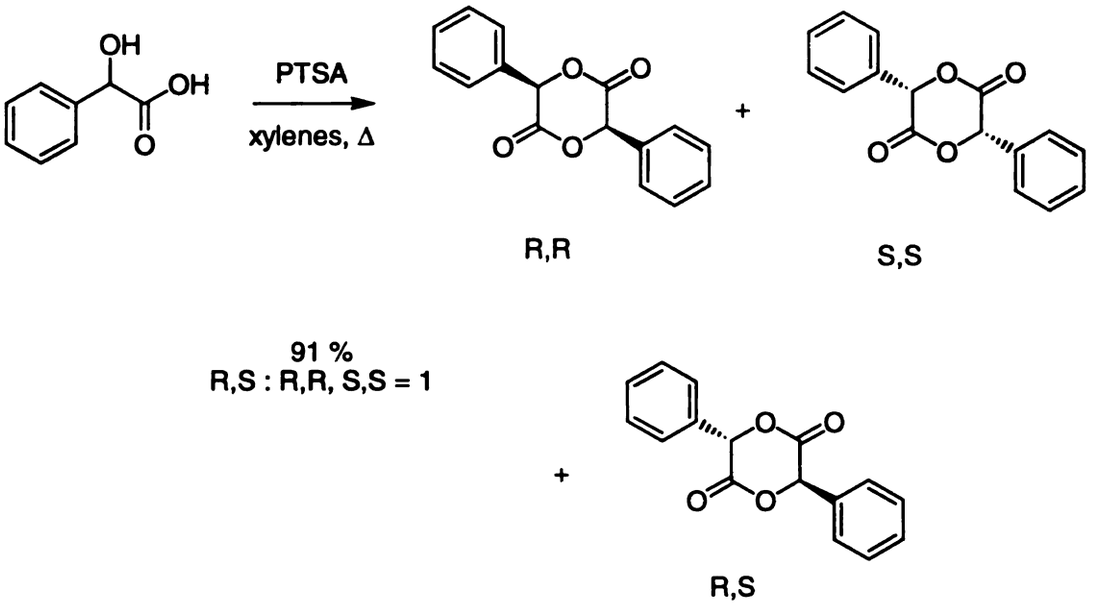

Scheme 2.3. Synthesis of mandelide from mandelic acid

Previous literature examples of mandelide syntheses were based on acid catalyzed self-esterification reactions with reported yields < 20%. A likely cause of the low yields is a high concentration of mandelic acid, which favors the formation of linear oligomers. Mandelic acid was cyclized in the presence of *p*-toluenesulfonic acid to form mandelide by a route based on literature examples and results obtained by Simmons (**Scheme 2.3**).[14] To favor intramolecular cyclization, the reaction was run in a dilute solution (< 0.1 mol/L). The reaction by-product, H_2O, was removed azeotropically using a Dean-Stark trap, and the conversion of mandelic acid could be roughly monitored by the volume of H_2O

collected in the Dean-Stark trap. Xylenes, toluene and benzene were investigated as solvents for the condensation, and xylenes gave the best results in terms of rate of the product formation and yield. Due to their low boiling points, toluene and benzene gave low yields (< 10%) of cyclic dimers even after 2 weeks at reflux. Using xylenes as solvent, mandelic acid was consumed within 3 days and gave a mixture of R,S and R,R/S,S mandelide in about a 1:1 ratio. However, when the reaction was allowed to continue for longer times (1 week) the R,S mandelide isomer slowly disappeared and the content of R,R/S,S isomers increased, eventually becoming the only cyclic dimers in the reaction system (**Scheme 2.4**).

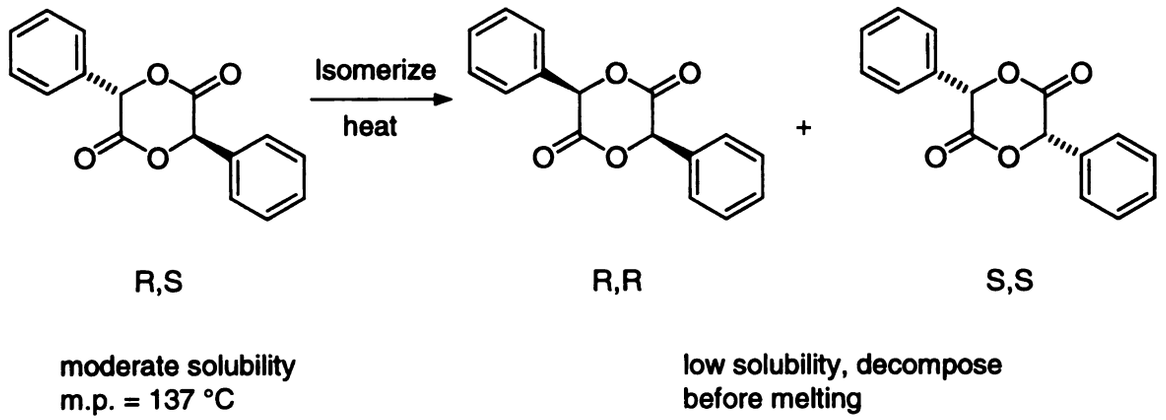

Scheme 2.4. Isomerization of R,S mandelide to R,R/S,S mandelide

2.2.2. Purification of mandelide

After cyclization, the reaction mixture contained cyclic dimers, oligomers, *p*-toluenesulfonic acid and sometimes unreacted mandelic acid. Due to their different solubilities in cold xylenes, the less soluble R,R and S,S isomers precipitated when hot xylene solutions were cooled to room temperature, while the more soluble R,S isomer and other components were soluble in the xylene filtrate. Mandelic acid and cyclic oligomers were removed by washing with sat. $NaHCO_3$ solution. The majority of the remaining off-white powder was the R,S isomer, which was then washed with hexanes and ether followed by recrystallization from ethyl acetate. Another way to remove oligomers and acids was to filter a cold xylene solution through a short pad of silica gel to remove all components but the R,S isomer. Although this separation method is faster, the yield is usually lower due to the adsorption of mandelide on silica gel.

2.2.3. Physical properties of mandelide isomers

All of the mandelides were obtained as white crystals. The R,S diastereomer melts at 137–138 °C while the R,R/S,S isomers decompose around 210 °C without melting. Addition of R,R/S,S mandelide to the R,S diastereomer decreases the melting point, as expected. The R,S isomer has relative good solubility in typical organic solvents such as THF, CH_2Cl_2, $CHCl_3$, ethyl acetate and DMSO. In contrast, the R,R/S,S isomers are poorly soluble in the same solvents, but do dissolve well in DMSO. Thus, NMR measurements were run in deuterated DMSO since it readily dissolves all the isomers.

2.3. Polymerization of mandelide

2.3.1. Melt polymerization

Mandelide, the phenyl derivative of glycolide, can be polymerized by a typical catalyst used for the ring opening polymerization of glycolide and lactide – $Sn(Oct)_2$. Due to the small amount of catalyst and initiator needed for most polymerizations, dilute stock solutions of catalyst and initiator were prepared. The desired aliquots were injected into the reaction vessels, and after removing solvents, the monomer/catalyst/initiator mixture was sealed in a tube under vacuum for melt polymerization. *t*-Butylbenzyl alcohol (BBA) was chosen as the initiator because the *t*-butyl group provides a distinct peak on NMR spectra which can be used for calculating number average molecular weights.

The sealed tubes were put into a thermostatted oil bath set at 160 °C, above the melting point of the R,S isomer. After desired intervals, tubes were removed and quenched in ice water. Despite starting with pure R,S mandelide, epimerization *in situ* generated the R,R/S,S isomers and the resulting polymandelide was amorphous. NMR analysis of partially polymerized samples showed that in the presence of $Sn(Oct)_2$, the pure R,S isomer rapidly isomerized to the R,R/S,S diastereomers. Thus melt polymerizations are complicated by the epimerization of R,S mandelide to the more stable R,R/S,S diastereomers.

Racemization of polylactide is not uncommon, especially when metal catalysts were present, and the rate of racemization increases dramatically with temperature. Kricheldorf and Serra[16] screened approximately 70 L-Lactide

polymerization systems and found that racemization was related to the basicity of the catalyst. The proposed racemization mechanism is based on an ester-hemiacetal tautomerization which is favored by the acidity of the proton α to the carbonyl (**Scheme 2.5**). Rehybridization of the asymmetric carbon atom followed by racemization has also been proposed to explain the existence of more than two lactide diastereomers from the degradation of poly(L-lactide).[17]

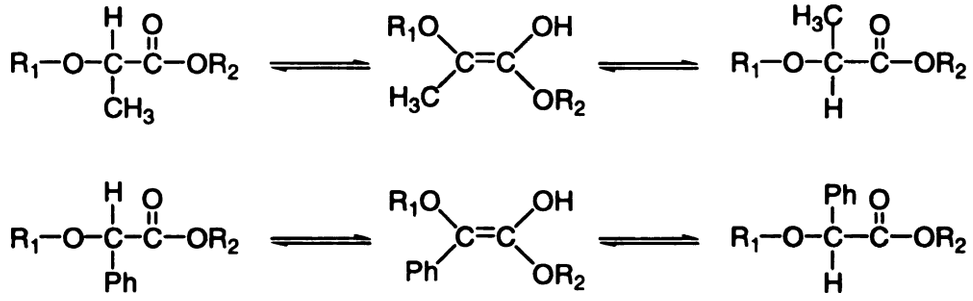

Scheme 2.5. Racemization in polylactide and polymandelide

$Sn(Oct)_2$ catalyzed polymerizations show some of the lowest rates of racemization. However, the benzene ring increases the lability of the methine C-H bond, and mandelide racemizes rapidly. Compared to lactide, epimerization should be more significant and occur at lower temperatures. In addition, even purified $Sn(Oct)_2$ contains residual ethylhexanoic acid, water and other impurities which may catalyze the racemization process.

A control experiment shows the ease of racemizing mandelide. When pure R,S mandelide was heated at 160 °C under vacuum, the solid melted completely, and then slowly resolidified within 80 minutes to give a white solid that was only slightly soluble in $CDCl_3$. NMR analysis showed that soluble

portion contained a 30/70 mixture of R,S mandelide and the R,R/S,S isomers, while an NMR spectrum of the insoluble white solid measured in DMSO showed that it was solely the R,R/S,S isomers.

The R,R/S,S isomers are the more stable mandelides, but pure R,R/S,S mandelide cannot be melt polymerized by $Sn(Oct)_2$ because they decompose at high temperature. Thus, either pure R,S mandelide or a low melting mixture of the R,R/S,S and R,S isomers were used for both melt and solution polymerization. The R,R/S,S isomers did not seem to interfere with the polymerization because they are soluble in the molten R,S isomer, and are consumed during the polymerization.

The typical purification method for lactide (e.g. multiple recystallizations) are effective in that polymerizations using purified monomer provide good control over the molecular weight by simply varying the monomer to initiator ratio. But as shown in **Table 2.2**, more vigorous drying is needed for mandelide. The first two entries were polymerizations using mandelide dried by the protocol typically used for lactide monomers. Even when no BBA was added (**Table 2.2** entry 2), $Sn(Oct)_2$ catalyzed ring opening polymerization. When the ratio of $Sn(Oct)_2$ to BBA was 1 (**Table 2.2** entry 1), the conversion was higher, but the molecular weight was only half of what was expected, an indication of excess initiator in the polymerization. When the same catalyst and initiator solutions were used for lactide polymerizations, the expected molecular weights were obtained. Thus, the low molecular weight in mandelide polymerizations can only be caused by monomer impurities such as H_2O.

The single crystal x-ray structure of S,S mandelide shows that the methine proton is in close proximity to the carbonyl oxygen and C-H···O hydrogen bonds have been suggested.[18,19] It is possible that mandelides have a strong affinity for water due to formation of H-bonds with H_2O. To obtain good control over the polymer molecular weight, mandelide monomers need to be scrupulously dried. The monomers used in entries 3-5 (**Table 2.2**) were dried under high vacuum (10^{-5} torr) at 40 - 45 °C, and the molecular weights obtained were close to the values predicted by the monomer initiator ratio. The lower than expected molecular weight for entry 5 was can be attributed to transesterification reactions becoming more prominent as the polymerization reached completion. The increased polydispersity index (1.44) is consistent with that view.

Table 2.2. Melt polymerization of mandelide at 160 °C

entry	[BBA]/[Sn(Oct)$_2$]	time (min.)	conversion	M_n (expected)	M_n (GPC)	PDI
1[a]	1	3	93.1%	12,500	6,850	1.17
2[a]	0	3	85.6%	11,470	10,400	1.19
3[b]	1	4	90.6%	12,060	11,480	1.26
4[b]	1	4	96.6%	12,950	11,430	1.29
5[b]	1	20	98.4%	13,200	8,830	1.44

(a): mandelide purified by recrystallization and drying overnight;
(b): mandelide purified as for entries 1 and 2, but further dried under vacuum (10^{-5} torr)at 40-45 °C.

2.3.2. Solution polymerization

Solution polymerizations of mandelide were run either in toluene or CH_3CN. Because of the poor solubility of the monomer, solution polymerizations have slower rates and are more likely to suffer from problems associated with equilibrium polymerization. In CH_3CN, R,S mandelide has a solubility of around 0.58 mol/L at room temperature and 1.5 mol/L at 50 °C. Although R,S mandelide is less soluble in toluene, the higher boiling point of toluene leads to faster reaction rates. The solubility of the R,R/S,S mandelides is significantly lower (0.01 mol/L in CH_3CN at room temperature). Most solution polymerizations of mandelide were run in anhydrous CH_3CN as shown below. Since, *t*-butylbenzyl alcohol and $Sn(Oct)_2$ do not dissolve in CH_3CN even at 65 °C, their toluene solutions were used in the polymerizations.

Given that mandelides readily epimerize, a mixture of the R,R/S,S mandelides with the R,S diastereomer should polymerize. This proved to be true, and thus for solution polymerizations, the R,S mandelide was isolated from condensation of mandelic acid, but with no special steps taken to remove the R,R/S,S mandelides. For the kinetic run shown in **Figures 2.1** and **2.2**, an R,S mandelide sample containing 26% of the R,R/S,S diastereomers was used, and initially the polymerization solution was colorless and clear. However, within half an hour, the reaction became heterogeneous as indicated by the formation of a precipitate. ^1H NMR showed that by the time the polymerization reached 24% conversion, the soluble mandelides had epimerized to roughly a 50:50 mixture of R,S and R,R/S,S mandelide, while the precipitate corresponded to the R,R/S,S

isomers. As the polymerization proceeded, the 1:1 ratio was maintained in solution. When the conversion reached around 70%, the solution became clear, homogeneous, and viscous. Thus the super-saturated mandelide solution provided a constant supply of the R,R/S,S isomers, which either were directly incorporated into the polymer, or epimerized and polymerized.

The linear relationship shown in **Figure 2.1** is consistent with the polymerization being first order with respect to the monomer concentration. Compared to lactide under the same polymerization conditions, the rate is 4 times slower, as would be expected from the larger steric bulk of the phenyl group compared the methyl group of lactide. **Figure 2.2** shows that the molecular weight of the polymer increased linearly with conversion, and the PDI decreased with conversion, which indicates the "living" character of the polymerization. However, when the reaction reached completion (97% conversion) and was allowed to run longer times (5 days), the molecular weight decreased, and the PDI increased to 1.5. This is consistent with intra and intermolecular transesterification becoming more prominent as the available monomer diminishes. Some discoloration of the polymer was observed for long polymerization times, but the degradation pathway was not identified.

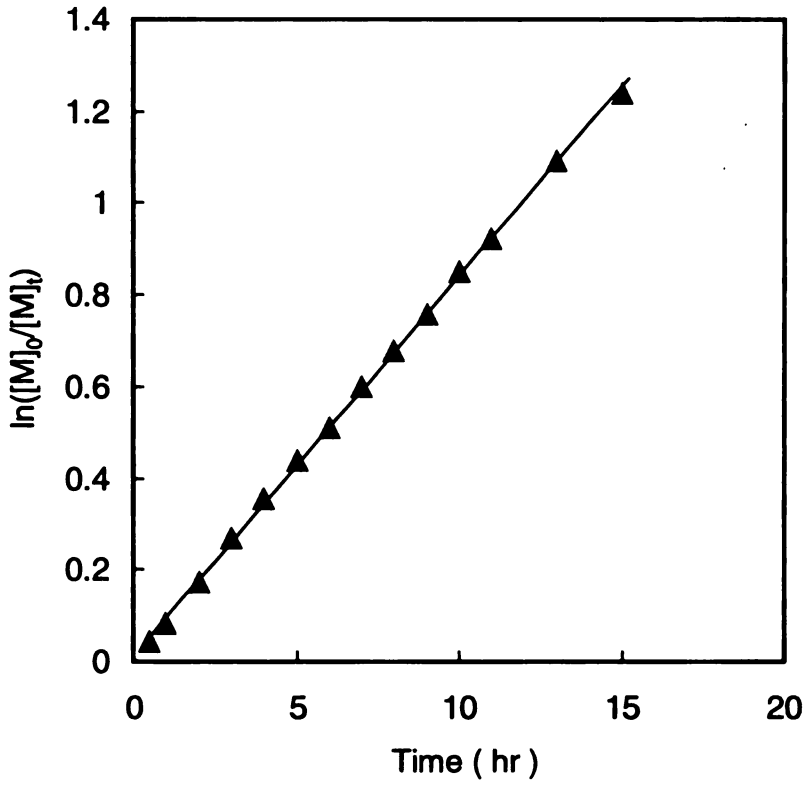

Figure 2.1. Kinetics of solution polymerization of mandelide in CH_3CN at 70 °C under argon. [mandelide]:[$Sn(Oct)_2$]:[BBA] = 100:1:1; [mandelide]= 0.93 mol/L (75% R,S mandelide and 25% R,R/S,S mandelide)

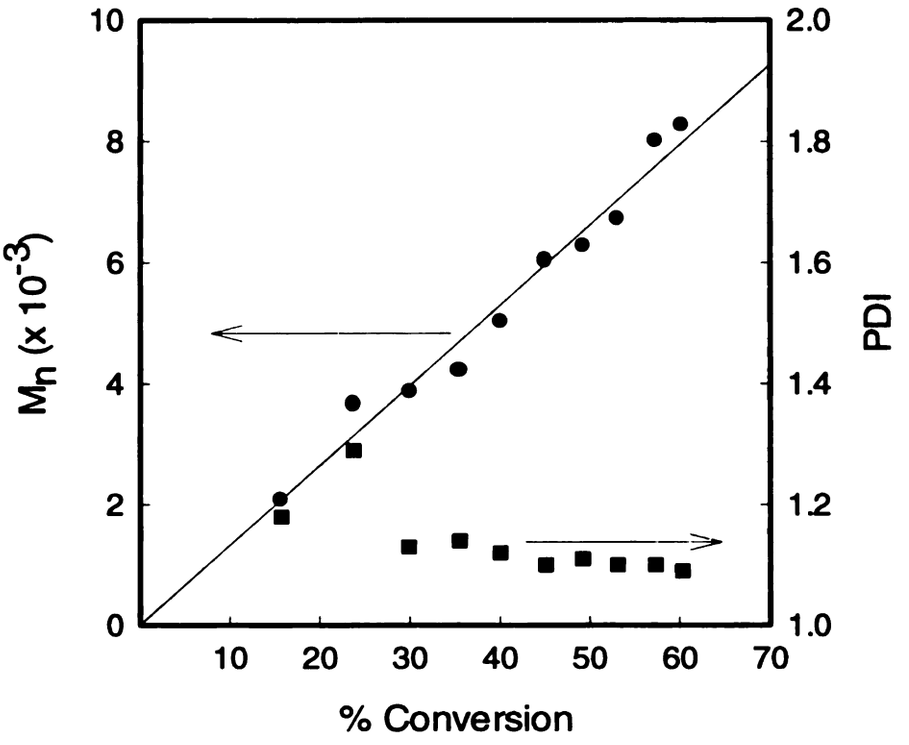

Figure 2.2. Molecular weight versus conversion during solution polymerization of mandelide in CH_3CN at 70°C under argon. [mandelide]:[$Sn(Oct)_2$]:[BBA] =100:1:1; [mandelide]= 0.93 mol/L(75% R,S mandelide and 25% R,R/S,S mandelide)

2.3.3. Purification of polymandelide

The most widely used polymer purification methods are dissolution–precipitation schemes, where a solution of the polymer in a good solvent is slowly dripped into a non-solvent. Ideally the polymer precipitates into thread-like pieces of polymer that are easily collected by filtration, while the impurities remain in solution. The solubility of polymandelide is similar to that of polystyrene, and polymandelide dissolves in THF, toluene, CH_2Cl_2, chloroform, ethyl acetate and DMSO. Non-solvents for polymandelide include hexanes, ether and methanol. The initial dissolution–precipitation scheme was based on a CH_2Cl_2/methanol solvent pair. The precipitation experiments resulted in milky solutions, regardless of molecular weight of the polymers, and the polymer was collected by centrifugation in low yield. If the milky solution was allowed to stand for two days, thin white films of polymandelide formed as the solvent slowly evaporated. As the amount of CH_2Cl_2 or toluene needed to dissolve the crude polymandelide was much larger than for crude polylactide samples of similar weight, the concentration of polymandelide in CH_2Cl_2 or toluene may be too low to form good precipitates. Further investigation showed that residual R,R/S,S mandelides complicate the precipitation scheme. A crude polymandelide sample was washed with a small amount of CH_2Cl_2. NMR analysis showed that the CH_2Cl_2 solution contained monomer and polymer, while the CH_2Cl_2 insoluble portion consisted only of the RR/SS mandelide. Thus, the excess CH_2Cl_2 needed to dissolve the crude polymer was due solely to the presence of unreacted R,R/S,S mandelide. It is important to remove residual R,R/S,S

mandelide from incomplete polymerizations in order to recover purified polymandelide in reasonable yields. By using less CH_2Cl_2, pre-filtering to remove the R,R/S,S mandelide followed by normal precipitation, the yields of recovered polymandelide were more than 80% and the polymer was recovered in a form that could be easily collected by filtration. The precipitated polymer was then heated to 60-90 °C under vacuum until a constant weight was obtained. Methanol and residual water were removed under vacuum, and residual monomer can be further removed by sublimation under high vacuum.

Using the above protocol, NMR analyses showed that we isolated polymandelide free of monomer. However, based on the characterization of polylactide purified by precipitation alone, other impurities such as residual metal catalysts may still be present in the polymer samples. As described in the Introduction, residual metals can catalyze transesterification reactions leading to the formation of cyclic dimers or oligomers. For practical purposes, it is also essential to remove metal residues from products intended for medical applications. A common way to remove metal residues from polylactide samples is to dissolve the polymer in an organic solvent and wash the organic solution with dilute HCl. The same method was applied to polymandelide. A solution of polymandelide in methylene chloride or toluene was washed several times with dilute HCl, followed by washes with distilled water until the water layer was neutral. The resulting solution was then treated as usual to afford white polymer samples. GPC analysis of the polymer before and after the extractions showed no change in molecular weight, confirming that no significant chain scission

occurred during the process. Therefore, extraction using dilute acid is a safe method for removing residual metals from polymandelide.

2.3.4. Characterization of polymandelide

Polymandelide can be cast from toluene or THF to give clear, colorless films. Melt pressed films prepared at ~140 °C are clear but have a light yellow color. The density of the polymer, obtained by flotation measurements of films in aqueous salt solutions was ~1.25 g/cm^3.

Polymandelide was characterized by FT-IR, NMR, DSC, X-ray powder diffraction and TGA. The IR spectrum (**Figure 2.3**) obtained on a polymandelide sample spin cast on a gold-coated silicon substrate shows two bands that are diagnostic for esters, a strong band at 1766 cm^{-1} (C=O stretching) and a broad band around 1200 cm^{-1}. Weak absorptions around 1456, 1498, 1605 and 3055 cm^{-1} are characteristics of aromatic compounds.

Given the mixture of diastereomers present in a polymerization of mandelide, it is not surprising that ^{13}C NMR spectrum of polymandelide is complicated (**Figure 2.4**). Broad peaks resulting from complex polymer tacticities were observed for each carbon resonance. Multiple peaks were also observed in ^{1}H NMR for methine and aromatic protons. Since no authentic samples of stereoregular polymandelide are known, no attempt was made to assign the stereochemical sequences.

DSC analysis of polymandelide samples shows only a single glass transition, and no crystalline transitions. Powder X-ray diffraction experiments

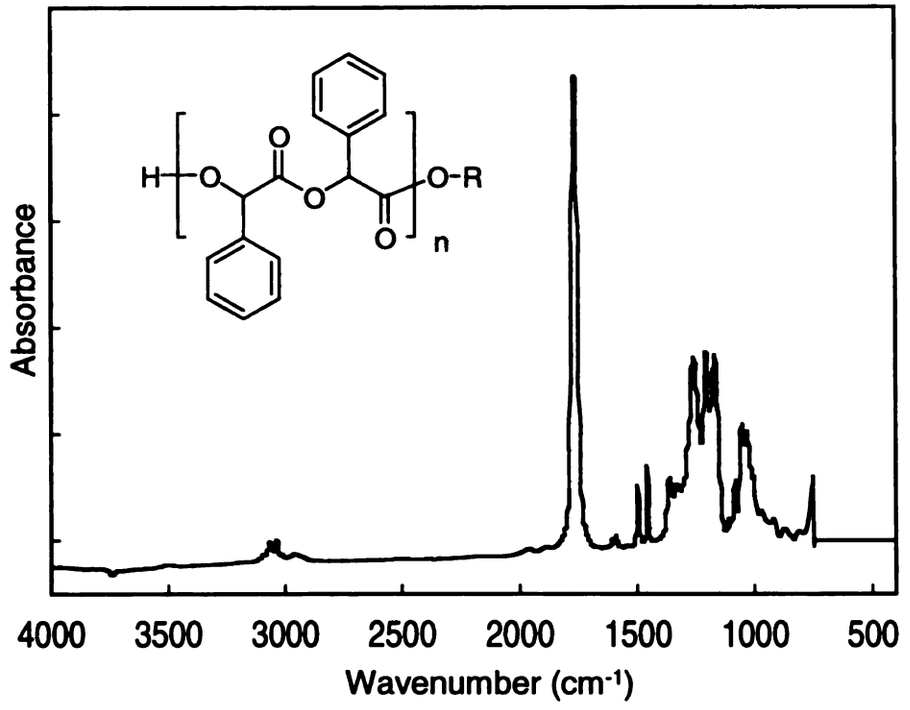

Figure 2.3. FTIR of a polymandelide film spin-coated on a gold-coated silicon wafer.

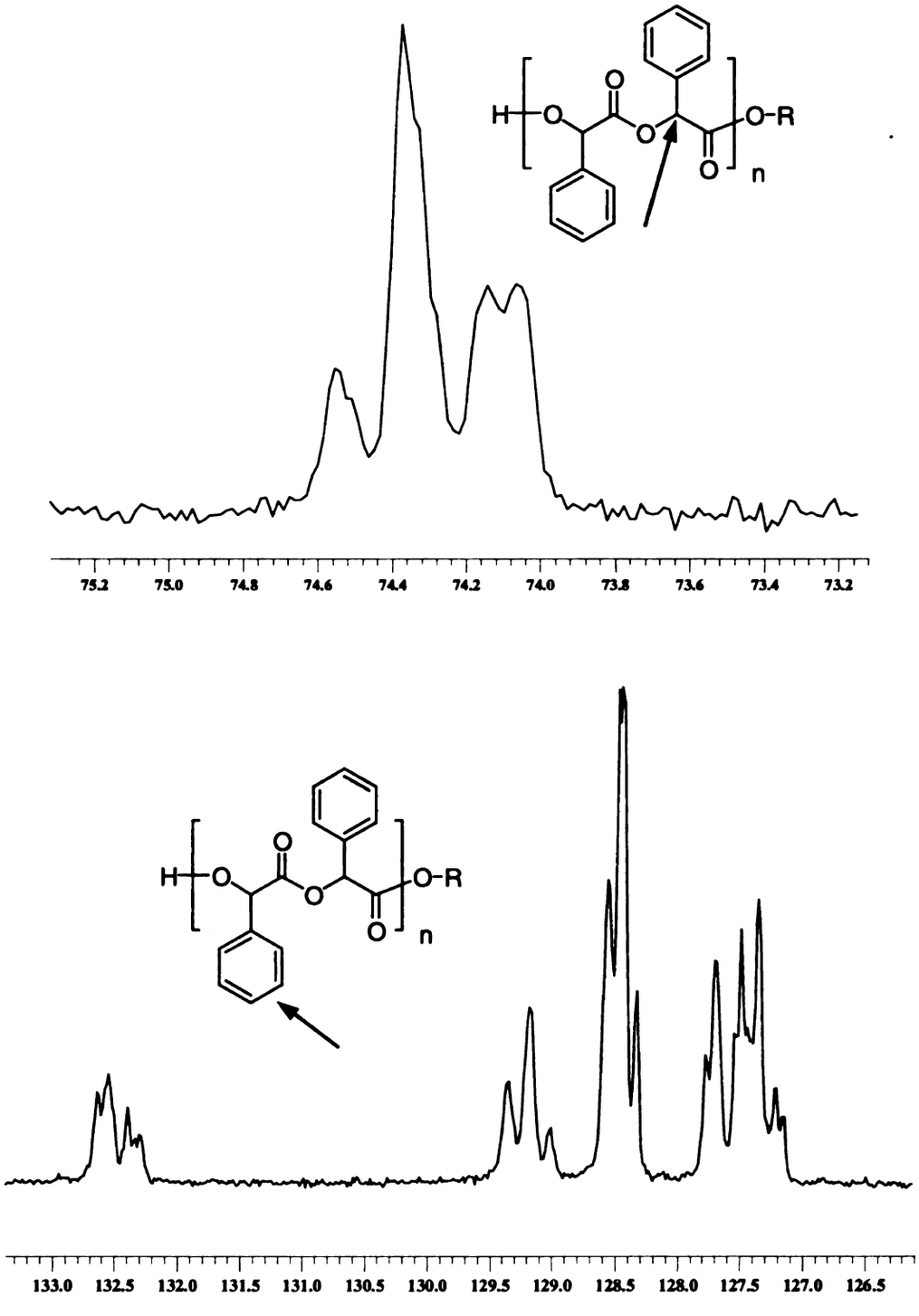

Figure 2.4. ^{13}C NMR of polymandelide in d^6-DMSO

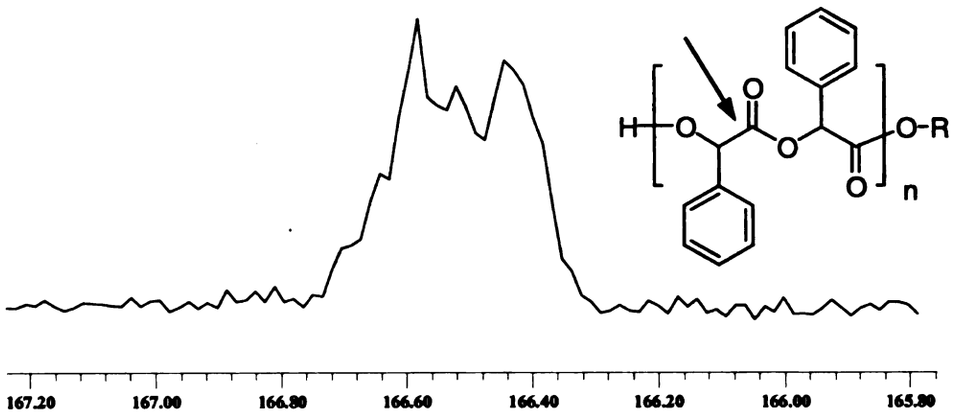

Figure 2.4. ^{13}C NMR of polymandelide in d^6-DMSO (cont'd)

concur, and show only amorphous scattering and no evidence of crystallinity. Smith and Tighe also reported that their low molecular weight polymandelide samples produced from either racemic or optically active precursors were also amorphous.[3] Like other polymers, the T_g of polymandelide depends on the molecular weight of the polymer, and eventually becomes independent of chain length at high molecular weights. The shift in T_g is related to the concentration of chain ends in the polymer. Chain ends have larger degrees of freedom compared to other chain segments, and because the chain end concentration decreases with increased molecular weight, T_g increases and then plateaus at high molecular weights. According to the literature,[7] a polymandelide sample with M_n ~ 1,100 g/mol afforded a T_g of ~ 75 °C. In a higher molecular weight polymandelide sample (M_n= 16,000 g/mol) the T_g shifted to ~ 95 °C, and it

eventually reached 100 °C when M_n= 60,000 g/mol (**Figure 2.5**). This value is similar to that of polystyrene (109 °C) making the analogy between polymandelide and polystyrene even stronger.

The thermal decomposition of polymandelide was characterized by TGA under nitrogen. As mentioned in the Introduction, the decomposition of polylactide in the presence of residue metal catalysts is considered to be a series transesterification reactions that generate volatile cyclic dimers or oligomers. After removing catalyst residues from polylactide samples, the onset for decomposition shifts to higher temperatures. Presumably, polymandelide should undergo the same degradation processes, and show a similar dependence of the thermal stability on purity.

Polymandelide and polylactide samples were purified by simple precipitation into a non-solvent. For these samples, the onset for thermal degradation of polymandelide occurred at higher temperatures than that of polylactide (**Figure 2.6**). However, after both samples were purified by washing with dilute HCl, the order was reversed (**Figure 2.7**). In terms of the onset of decomposition, no significant change was found for polymandelide samples before and after acid treatment (**Figure 2.8**), but the stability of the polylactide sample improved significantly.

If the two polymers degrade by the same depolymerization mechanism, one would expect that polymandelide would have an onset for degradation at higher temperatures due to the lower volatility of mandelide compared to lactide.

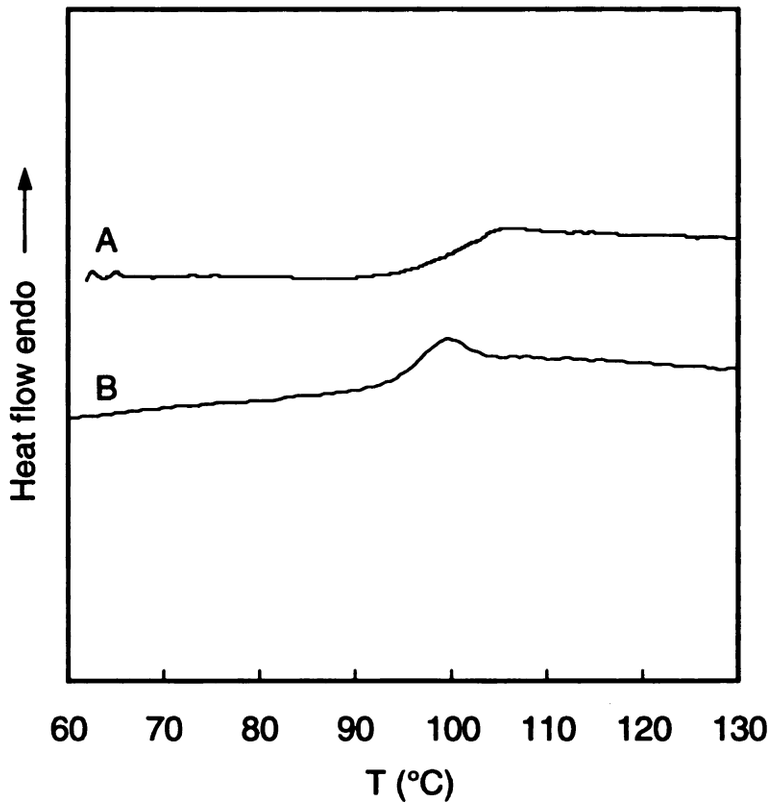

Figure 2.5. DSC of polymandelide samples, showing the molecular weight dependence of T_g. A: M_n = 60,000 g/mol; B: 16,000 g/mol. Samples were heated at 10 °/min under helium.

It is possible that the methine protons in polymandelide are more labile and radical pathways are more favorable in the mandelide system. A less plausible explanation would be that catalyst is removed far more efficiently from polymandelide than polylactide.

To test these possibilities, a polymandelide sample free of monomer was sealed in a glass ampoule and heated in a 200 °C oil bath for 24 hours. NMR confirmed that the polymer had not degraded significantly, and there was no evidence for the formation of mandelide. However, GPC traces confirmed a large decrease in molecular weight and a singlet in the ^{1}H NMR at 10.0 ppm suggested the formation of benzaldehyde, which can be formed from the radical cleavage of the polymer backbone. Smith and Tighe[3] reported that the onset for polymandelide decomposition occurred at about 205 °C and carbon monoxide and benzaldehyde were the principal decomposition products seen in their thermogravimetric experiment.

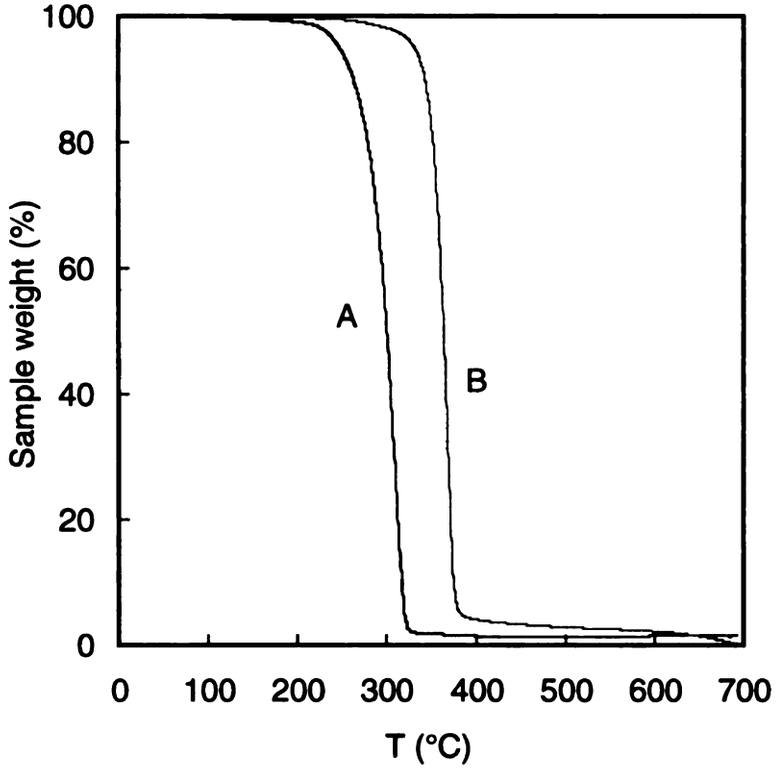

Figure 2.6. Thermal Gravimetric Analysis of polylactide (A) and polymandelide (B) before washing with dilute HCl. Samples were heated at 40°C/min under N_2

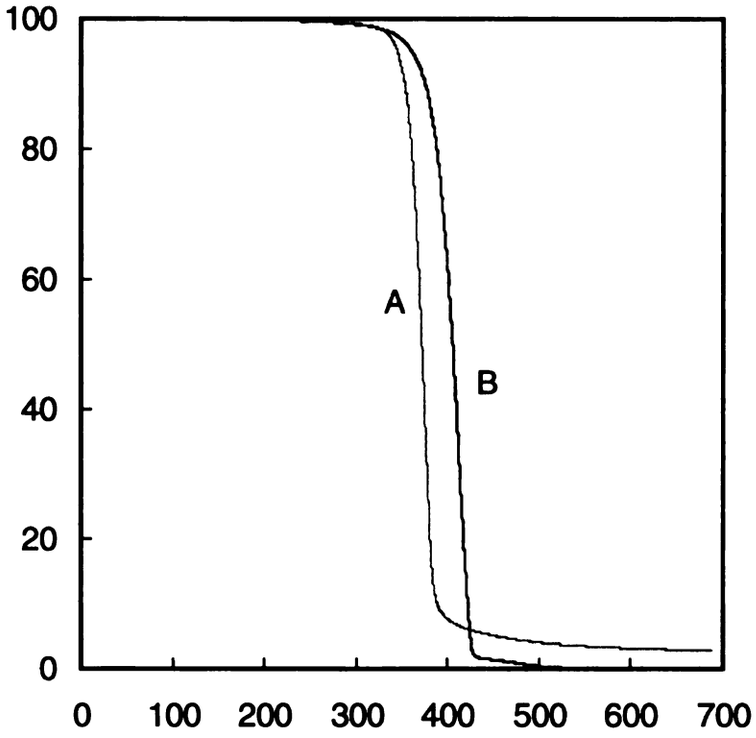

Figure 2.7. Thermal Gravimetric Analysis of polymandelide (A) and polylactide (B) after washing with dilute HCl. Heating rate: 40°C/min. under N_2

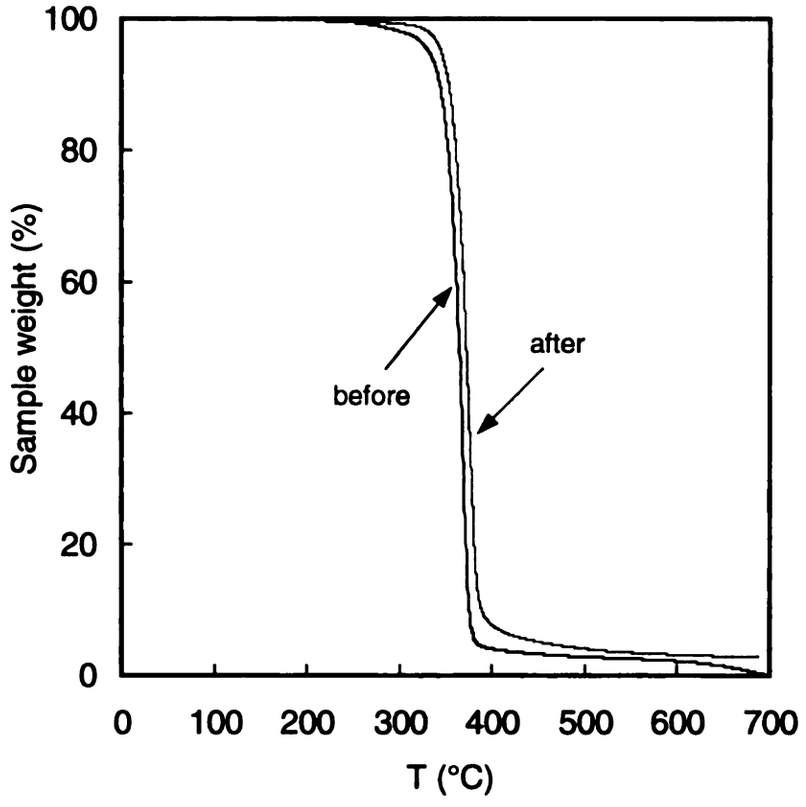

Figure 2.8. Thermal Gravimetric Analysis of polymandelide before and after washing with dilute HCl. Samples were heated at 40°C/min under N_2

2.4. Copolymerization of mandelide with lactide

To expand the range of end use temperatures available from biodegradable polymers, a series of random copolymers were prepared by copolymerizing mandelide with *rac*-lactide and L-lactide. Polymerizing *rac*-lactide with mandelide should provide a series of glassy materials, while incorporation of mandelide in poly(L-lactide) should affect the crystallization of poly(L-lactide). Depending on the degree of crystallinity in the copolymer, these materials may mimic various toughened thermoplastics and thermoplastic elastomers.

Poly(*rac*-lactide-*co*-mandelide) copolymers were prepared by bulk copolymerization at 130 °C using $Sn(Oct)_2$ as the catalyst and BBA as the initiator. The polymers were purified as described earlier. The molar composition of the copolymers as determined by ^1H NMR had mandelide to lactide mole ratios of 11:89, 25:75, 45:55, 75:25 and 89:11 (**Table 2.3**), which were close to the feed ratios.

DSC measurements of the copolymers showed a single glass transition temperature for each copolymer. As shown in **Figure 2.9**, the T_gs range from 48 °C to 100 °C, with the lower and upper limits corresponding to the T_g of the L-lactide and mandelide homopolymers respectively. The dramatic increase in the glass transition temperature with mandelide content is caused by the introduction of bulky phenyl substituents on the polymer backbone that reduce chain mobility. Since the polymers are homogeneous (single T_g), the glass transition temperatures should follow the Fox equation, (**Eq. 2.1**).

$$1/T = W_1/T_1 + W_2/T_2 \qquad \text{Eq 2.1}$$

where T, T_1 and T_2 are the glass transition temperature of the copolymer, polymandelide and polylactide homopolymers respectively, and W_1 and W_2 are the weight fractions of two components in the copolymer. A good fit to the Fox equation was observed, with the primary deviation apparently coming from a "too low" value for the T_g of polylactide (**Figure 2.10**). This behavior has been observed previously, for other lactide copolymers, but its origin is unclear.

L-lactide and mandelide were copolymerized to study the effect of mandelide content on the crystallization of polylactide. Copolymers were synthesized with mandelide to lactide mole ratios of 2:98, 5:95, 12:88, 20:80 and 45:55 (**Table 2.4.**). As the polymerizations were allowed to run to high conversions at 160 °C, the ratio of mandelide to lactide in each copolymer was close to the feed ratio.

DSC experiments were run on purified copolymers. Only one glass transition temperature was observed for each copolymer, and the T_g increased as the mandelide content increased. The first scan (10 °C/min) used polymer directly after precipitation and drying, and only two copolymers (mandelide:lactide = 2:98 and 5:95) afforded a melting peak. As the mandelide content in the copolymers increased, the melting temperature decreased from 172, to 160 and to 151 °C (**Figure 2.11**).

Despite annealing poly(L-lactide-*co*-mandelide) (mandelide:lactide = 12:88) in the DSC for 18 hours at 130 °C, no melting peak was detected when the sample was heated to 185 °C. The result is reasonable when compared to

data for poly(L-lactide). Polylactide derived from > 93% L-lactic acid usually crystallizes, while polylactide prepared from 50-93% L-lactic acid is generally amorphous. In the lactide case, R-lactic acid residues in the polymer chain act as defects that interfere with crystallization. Mandelide serves the same function in poly(L-lactide-*co*-mandelide). A recent report also described similar data; incorportation of > 10 mol% mandelic acid in L-lactide polymerizations gave amorphous materials.[10]

Based on the thermal degradation results described earlier for polymandelide and polylactide, the degradation of poly(lactide-*co*-mandelide) as measured by TGA should be sensitive to impurities in the polymer. For samples contaminated with catalyst residues, the onset temperature for weight loss did not correlate with polymer composition. However, when the samples were treated with dilute HCl, the onset temperature increased as expected as the fraction of lactide in the copolymer increased (**Figure 2.12.**).

Table 2.3. Poly(mandelide-*co*-*rac*-lactide) copolymers prepared by bulk polymerization catalyzed by $Sn(Oct)_2$ at 130 °C

Entry	Mandelide/lactide (mol:mol)		M_n[(b)]	PDI[(b)]	T_g (°C)[(c)]
	feed ratio	copolymer ratio[(a)]			
1	100:0	100:0	68,000	1.63	100.3
2	90:10	89:11	37,000	1.45	94.5
3	75:25	75:25	42,000	1.60	90.0
4	50:50	45:55	58,000	1.47	82.1
5	25:75	24:76	80,000	1.65	66.9
6	10:90	11:89	98,000	1.65	61.3
7	0:100	0:100	20,000	1.47	46.5

(a): determined by ^1H NMR;
(b): determined by GPC in THF and reported relative to polystyrene standards;
(c): measured at 10 °C/min under helium.

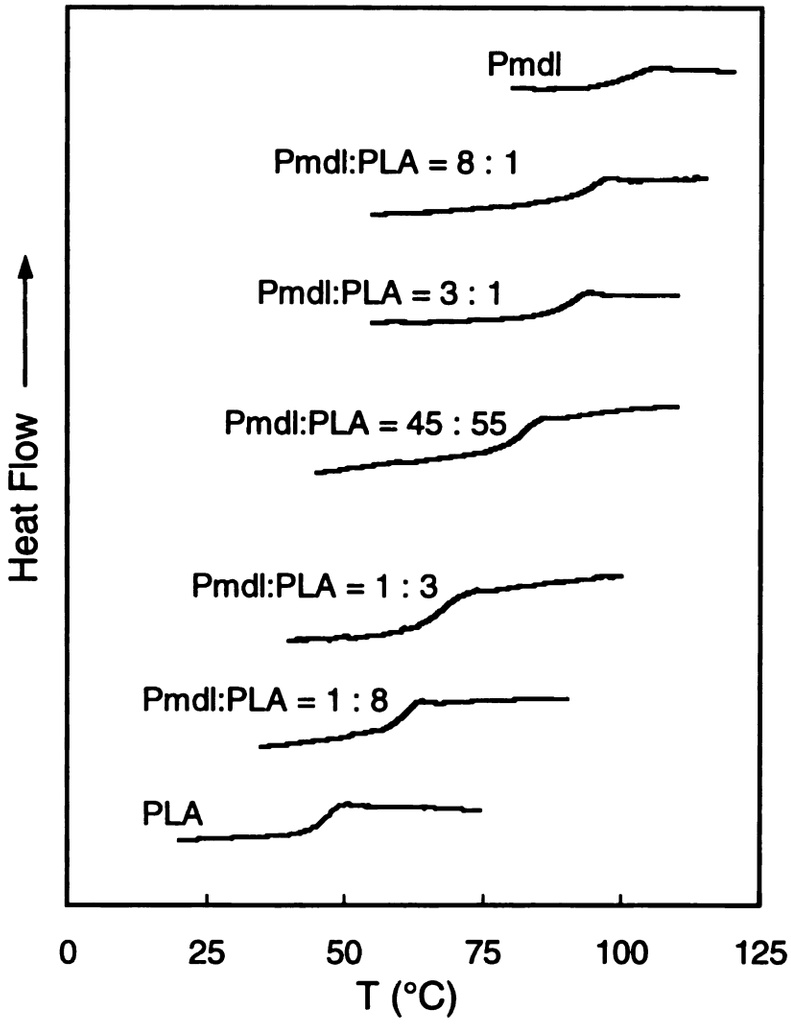

Figure 2.9. Glass transition temperatures of poly(mandelide-*co*-*rac*-lactide) copolymers. Samples were heated at 10 °C/min under helium

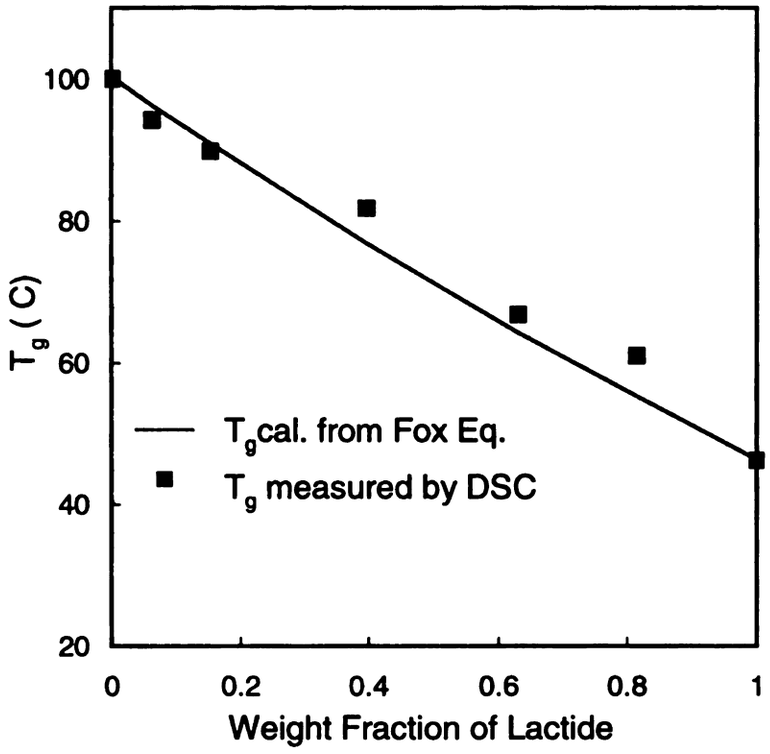

Figure 2.10. Glass transition temperatures of poly(mandelide-*co*-*rac*-lactide) copolymers fitted to the Fox Equation

Table 2.4. Poly(mandelide-*co*-L-lactide) copolymers prepared by bulk polymerization at 160 °C

Entry	Mandelide:L-lactide (mol:mol)		M_n[(b)]	PDI[(b)]	T_m(°C)[(c)]	$\Delta H_{(fusion)}$ (J/g)[(c)]
	feed ratio	copolymer ratio[(a)]				
1	0:100	0:100	21,800	1.47	172	50.7
2	2:98	2:98	66,000	1.20	160	31.2
3	5:95	5:95	48,100	1.25	153	23.8
4	10:90	12:88	59,900	1.47	—	—
5	20:80	20:80	48,150	1.23	—	—
6	45:55	49:51	42,100	1.23	—	—

(a): determined by ^{1}H NMR;
(b): determined by GPC in THF and reported relative to polystyrene standards;
(c): measured at 10 °C/min under helium.

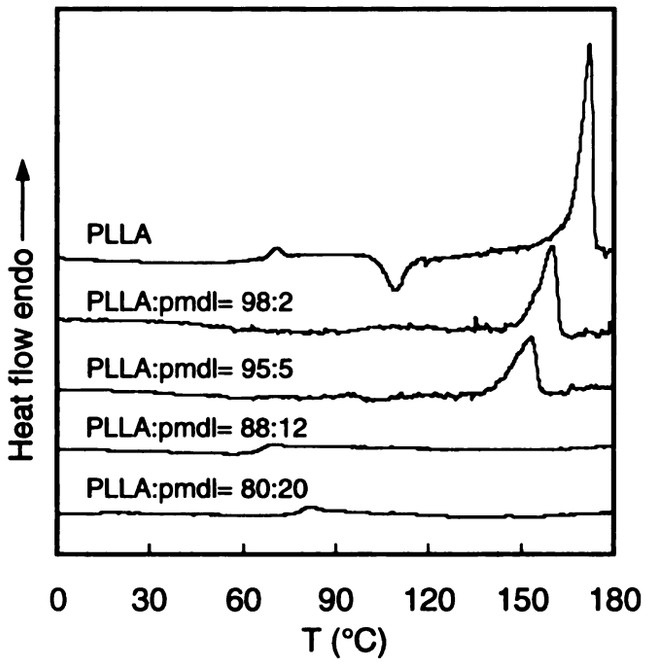

Figure 2.11. Thermal properties of poly(mandelide-*co*-L-lactide) copolymers. Samples were heated at 10 °C/min under helium

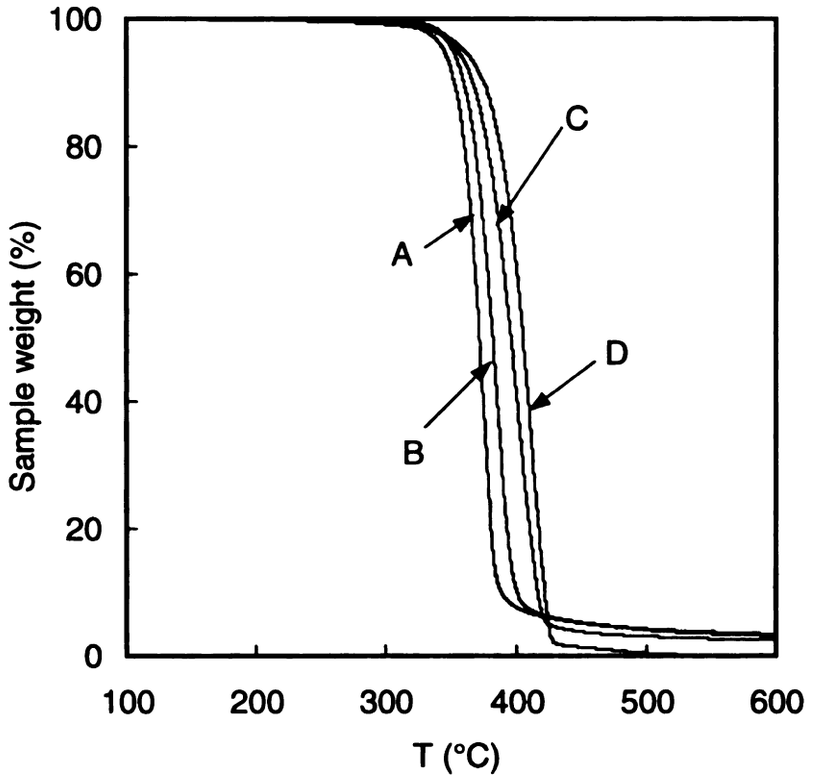

Figure 2.12. Thermal Gravimetric Analysis of poly(mandelide-*co*-*rac*-lactide) copolymers. A: polymandelide; B: mandelide:lactide = 3:1; C: mandelide:lactide = 1:3; D: polylactide. Samples were washed with dilute HCl after precipitation and heated at 40 °C/min under N_2

2.5. Hydrolytic degradation of polymandelide

One of the most interesting and important features of biodegradable polymers is their degradability. Like polylactide, polymandelide contains hydrolyzable ester linkages in the polymer backbone and differs only in that the pendant methyl groups of polylactide are replaced by phenyl groups. The aromatic rings make the polymer more hydrophobic than polylactide and should lead to a slower degradation rate.

Copolymers of L-lactic acid and mandelic acid obtained via polycondensation schemes have been subjected to *in vitro*[7] and *in vivo*[8,9] degradation studies. *In vitro* studies show that the mandelic acid content has a large affect on the degradation profile. As the mandelic acid content increased, the profile shifted from being parabola-like, characterized by an initial rapid degradation followed by gradual erosion of the polymer, to an "S"-type degradation profile, which is characterized by initial swelling followed by degradation of the ester linkages in the swollen state. Similar changes were observed *in vivo*. To date, no data had been obtained on the hydrolytic degradation of high molecular weight polymandelide. The rate is expected to be slow, since a low molecular weight polymandelide sample (1,300 g/mol) showed no weight loss during 15 weeks of hydrolytic degradation.

The conditions used to study the degradation of polymandelide (phosphate buffered solution at pH 7.4 and 55 °C) were identical to those used to characterize the degradation rates of other substituted polylactides. Carrying out the degradation at 55 °C allows for completion of the degradation in several

months. In addition, the degradation rates of poly(L-lactide) measured in phosphate buffered solutions have been shown to mirror those measured *in vivo*.[20,21] Powdered samples (~ 1 mm in size) were allowed to age in the phosphate buffer without stirring to simulate the low flow rates of body fluids in smooth and hard tissues.[22]

The initial M_n of the polymandelide sample was 78,200 g/mol. The molecular weight decrease fits the random chain model with a rate 1/120th that of lactide degraded under the same conditions. Weight loss began after 80 days, and thus the random chain scission is not relevant after 80 days (**Table 2.5**). The delay in the onset for weight loss relative to the loss in M_n is consistent with a bulk erosion mechanism, where carboxylic acid groups generated by ester hydrolysis catalyze further degradation of the polymer. Carboxylic acids near the surface of the sample can be neutralized by the phosphate buffer, but acid end groups inside the sample cannot escape or be neutralized, leading to faster degradation in the core of the material. An alternative mechanism, surface erosion, would require that sample weight loss precede substantial loss in molecular weight.

A slight shoulder appeared in the GPC trace of the polymer sample after 97 days of degradation as shown in **Figure 2.13**. The shoulder grew more prominent with time, until a bimodal molecular weight distribution became obvious. Such a distribution is characteristic of heterogeneous degradation, in which the surface and core of the sample degrade at different rates, resulting in two distinct molecular weight distributions. This surface-core differentiation with

its characteristic biomodal molecular weight distribution is a common feature in the degradation of polylactide samples > 50 μm in size.[23] However, a bimodal distribution was not observed for polylactide and polyphenyllactide degraded at 55 °C, presumably because the degradation temperature was higher than the T_g of the polylactide and nearly identical to the T_g of polyphenyllactide. For both cases, the polymer chains should have enough mobility to allow low molecular weight oligomers bearing acid end groups to diffuse out of the sample, especially as the polymers partially hydrolyze and become more hydrophilic. As shown in **Figure 2.14** the molecular weight of polymandelide was plotted against degradation time according to the random chain scission model. A linear trend was observed before any significant weight loss (up to 97 days). After 97 days, the data dramatically deviated from the random chain scission model due to the heterogeneous nature of polymandelide's degradation. The rate of polymandelide hydrolytic degradation before 97 days was calculated to be ~ 120 times slower than amorphous polylactide under identical degradation conditions. The result can be explained by the large difference in T_g.

A large drop in molecular weight in parallel with a constant sample weight has been observed for polylactide and other substituted polyglycolides. For autocatalyzed degradation, significant weight loss requires the formation of water soluble oligomers, which only occurs after extensive hydrolysis of the polymer chains. This behavior can be fit by the Prout Tompkins model described in the introduction (**Figure 2.15**) which was based on autocatalytic thermal

decomposition of potassium permanganate and has been applied to evaluate mass loss from poly(lactide-*co*-glycolide) particles.[24]

Table 2.5. Weight and molecular weight change during hydrolytic degradation of polymandelide in phosphate buffer (pH= 7.4) at 55 °C

Degradation time (days)	Weight percent of remaining polymer	M_n(GPC)	PDI
0	100	78,200	1.61
12	96.0	73,800	1.62
20	0.964	66,860	1.64
40	98.6	58,900	1.67
64	96.1	49,100	1.67
97	92.4	33,800	1.80
161	78.3	13,300	2.48
188	62.8	6,980	4.19
225	51.2	4,590	4.84
304	26.2	—[a]	—[a]

a: the molecular weight was too broad to be determined

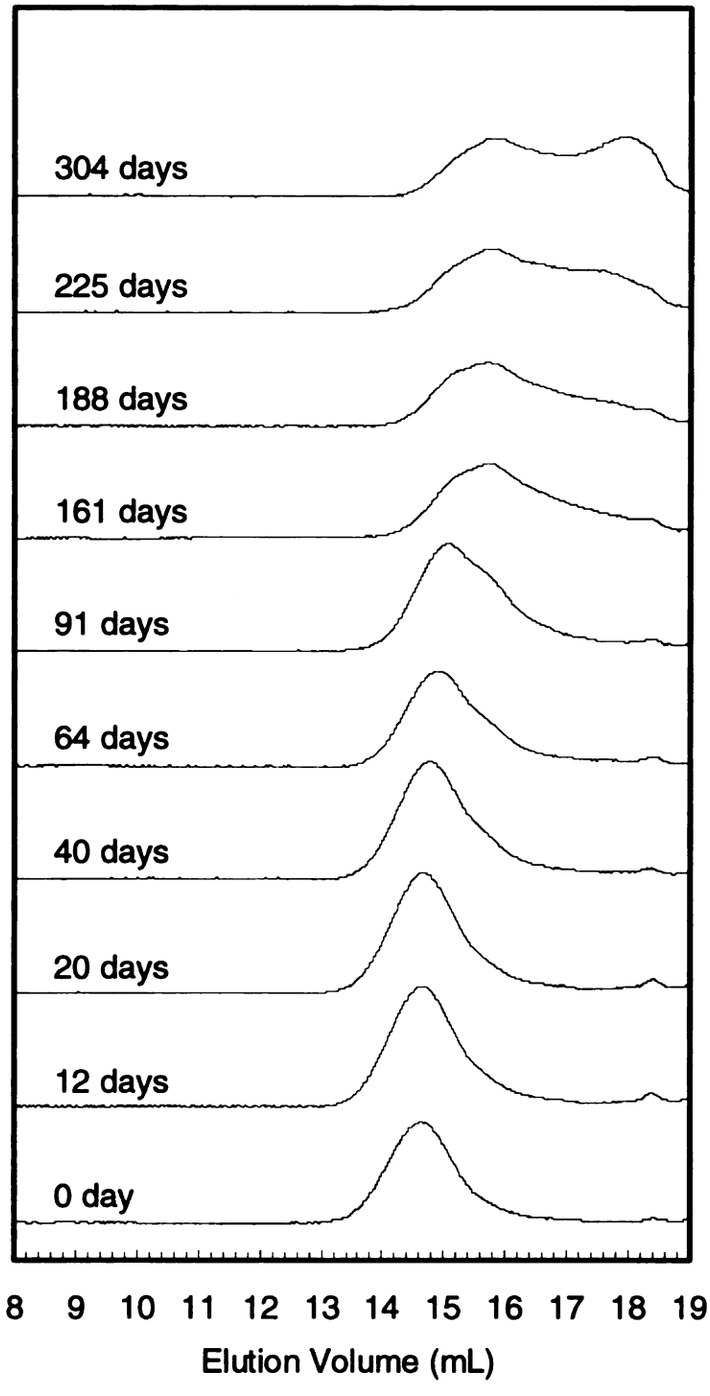

Figure 2.13. GPC traces of polymandelide samples during hydrolytic degradation at pH=7.4 and 55 °C

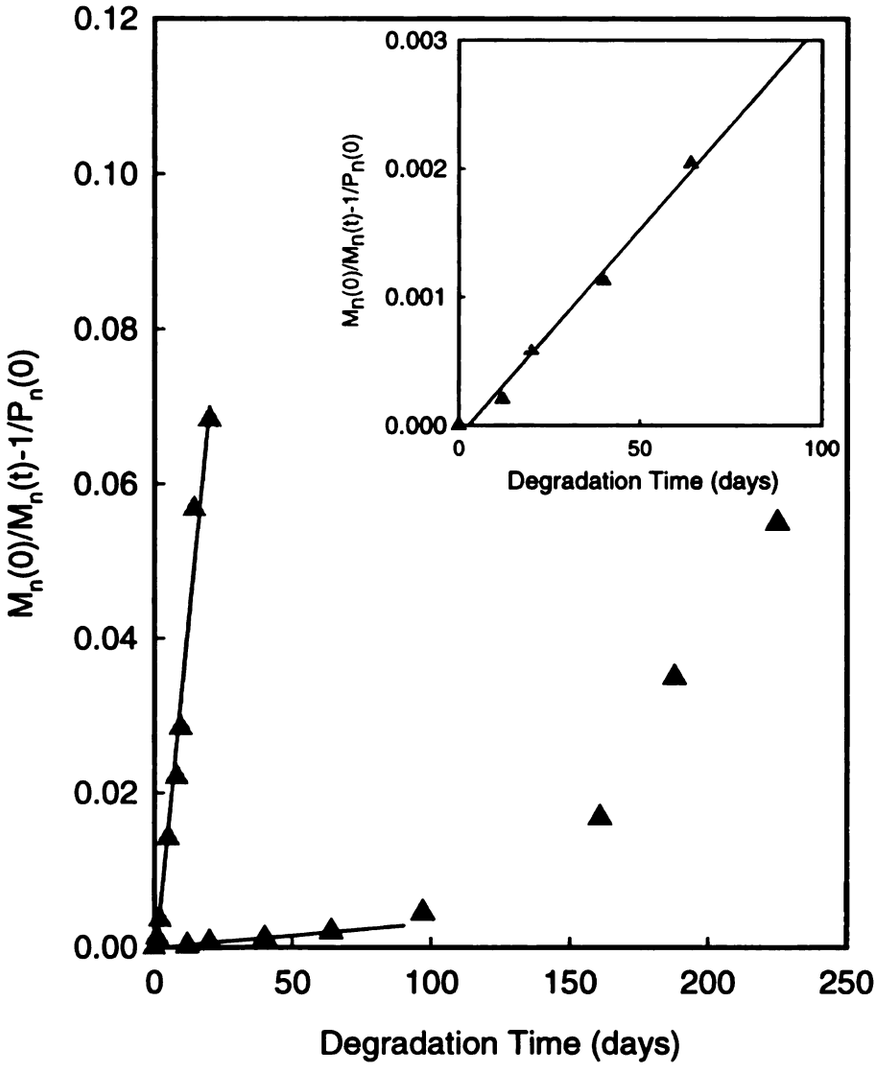

Figure 2.14. Molecular weight change of polymandelide (▲) and polylactide (▲) during hydrolytic degradation in phosphate buffer at 55 °C. The lines are fit to a random chain scission model. The inset shows the molecular weight data before 97 days.

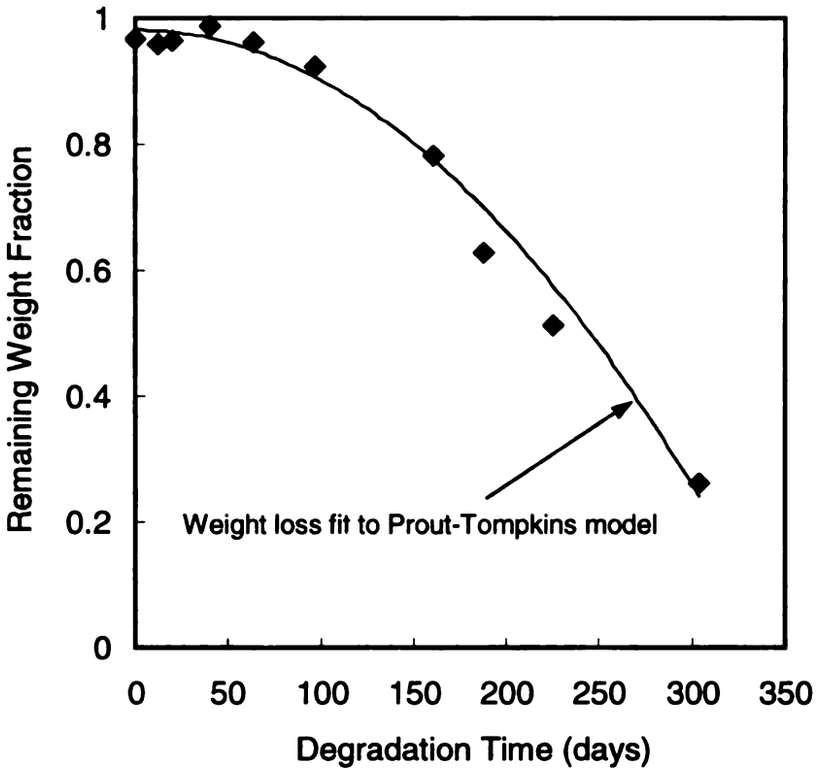

Figure 2.15. Weight loss during hydrolytic degradation of polymandelide in phosphate buffer (pH=7.4) at 55 °C

2.6. Experimental section

General. Unless otherwise specified, ACS reagent grade starting materials were used as received from commercial suppliers. THF was distilled over CaH_2, and then was distilled from sodium benzophenone ketyl under nitrogen. Toluene was freshly distilled from sodium benzophenone ketyl under nitrogen. Anhydrous acetonitrile was obtained from Aldrich and used as received.

Characterization ^1H and ^{13}C NMR analyses were performed at room temperature in $CDCl_3$ on a Varian Gemini-300 spectrometer using TMS as the chemical shift standard unless otherwise specified. Reflectance FTIR spectra were obtained under nitrogen using a Nicolet Magna-560 FTIR spectrometer containing a PIKE grazing angle (80°) attachment. Typically, 256 scans were collected using a MCT detector. Polymer molecular weights were measured by gel permeation chromatography at 35 °C in THF using a Plgel 20μ Mixed column at a flow rate of 1 mL/min. Two detectors were used, a Waters R410 Differential Refractometer and a Waters 996 Photodiode Array. The concentration of the polymer samples was 1 mg/mL, and each solution was filtered through a Whatman 0.2 μm PTFE filter before injection. The molecular weights are reported relative to monodisperse polystyrene standards. Differential scanning calorimetry (DSC) data were obtained with a Perkin Elmer DSC 7 instrument calibrated with indium and hexyl bromide standards. The samples were placed in aluminum pans, and were heated at 10 °C/min under a helium atmosphere. Liquid nitrogen was used as the coolant. Thermogravimetric analysis (TGA) data

were obtained from a Perkin Elmer TGA 7 instrument at a heating rate of 40 °C/min under nitrogen. Reported melting points were measured with an Electrothermal Melting Point Apparatus and are uncorrected. The densities of solutions were measured using a series of hydrometers (Curtin Matheson Scientific. Inc).

Synthesis of mandelide Racemic mandelic acid (6.03 g, 39.7 mmol) and a catalytic amount of *p*-toluenesulfonic acid (0.20 g, 1.2 mmol) were dissolved in xylenes (600 mL). The solution was refluxed for 3 days and water was removed via a Dean Stark trap. The conversion of the reaction was monitored by NMR and by the amount of water that collected in the trap. The solution was allowed to cool to room temperature and most of the R,R/S,S mandelide precipitated from solution and was collected by filtration to give 1.3 g (47%) of a 1:1 mixture of the R,R and S,S isomers (mp 193 °C (decomposes)). The filtrate was washed three times with saturated aqueous $NaHCO_3$ and the solvent was dried and removed by rotary evaporation. The crude mixture of R,S, R,R and S,S mandelide was recrystallized three times from ethyl acetate to give 1.5 g (53%) of R,S-mandelide, mp 137 °C. The R,S-mandelide could also be purified by passing the crude filtrate through a layer of silica gel, followed by solvent removal and recrystallization. This method gave a lower yield of product.

R,S mandelide: ^1H NMR (300 MHz, d^6-DMSO) δ 6.44 (s, 1H), 7.35-7.62 (m, 5H); ^{13}C NMR (75 MHz, d^6-DMSO) δ 164.71, 133.23, 129.56, 128.94, 127.56, 77.56.

R,S/S,S mandelide: ^{1}H NMR (300 MHz, d^6-DMSO) δ 6.61 (s, 1H), 7.35-7.58 (m, 5H); ^{13}C NMR (125 MHz, d^6-DMSO) δ 166.47, 132.32, 129.28, 128.35, 128.29, 77.47

Melt polymerization of mandelide. Stock solutions of $Sn(Oct)_2$ and BBA in anhydrous toluene were prepared in a dry box, fitted with vacuum adapters and removed from the box. Mandelide was loaded into small glass ampoules (~ 3 mL) with stir bars and connected to a vacuum line through a vacuum adapter. After evacuating the ampoule for 2 hours, the ampoule was backfilled with argon, and a syringe was used to add a predetermined amount of the $Sn(Oct)_2$ and BBA solutions to ampoules though the adaptor. After solvent removal, the glass ampoules were sealed under vacuum. The ampoules were added to a thermostatted silicon oil bath, and after desired time intervals, ampoules were removed from the bath and were quenched with ice water. The ampoules were then broken and the residue was extracted with methylene chloride or THF. Filtration and removal of the solvent *in vacuo* gave crude polymandelide as an off-white or light brown colored sold. The conversion of the polymerization was measured by ^{1}H NMR.

Purification of polymandelide Crude polymandelide was dissolved in methylene chloride and the insoluble portion (R,R/S,S mandelide) was removed by filtration. The polymer solution was concentrated to ~ 10 wt%, and was slowly dripped into a well-stirred cold methanol solution. The polymer precipitate was collected on a fritted glass funnel and was dried under vacuum at 60-70 °C. If necessary, the precipitation procedure was repeated.

Polymandelide: ^{1}H NMR (300 MHz d^{6}-DMSO): δ 6.0-6.26 (m, 1H), 7.42-7.9 (m, 5H); ^{13}C NMR (125 MHz, d^{6}-DMSO): δ 166.5, 132.5, 129.3, 128.4, 127.5, 74.3.

Solution polymerization of mandelide Mandelide (2.50 g, 9.32 mmol) was placed in a Schlenk flask and dried under vacuum. After transferring the flask into a drybox, anhydrous acetonitrile (10 mL) was added to the flask. The flask was then connected to a vacuum line and heated to 70 °C under argon. $Sn(Oct)_2$ (93.2 μmol) and BBA (93.2 μmol) solutions were added into the flask by syringe under argon to initiate polymerization. At predetermined intervals, a syringe was used to remove aliquots of the reaction solution, which were analyzed by NMR and GPC to determine the conversion and molecular weight of the polymer.

Density measurement. Polymandelide powder obtained from precipitation of the polymer was melt pressed at 140 °C. Chunks of polymer that were free of air bubbles were selected for density measurements. The samples were added to a graduated cylinder filled with distilled water. The polymer sample sank to the bottom, and NaCl was added to increase the density of the solution to the point that the polymandelide remained suspended in the solution. The density of the solution (equivalent to the density of the polymer) was measured by a hydrometer.

Hydrolytic degradation of polymandelide A pH 7.4 phosphate buffer solution was prepared by adding dilute NaOH solution into commercially available phosphate buffer (pH=7.0) at 55 °C. Around 50 mg of the polymer

power (~ 1 mm in size) was placed inside a test tube with a screw cap and 15 mL of pH of 7.4 phosphate buffer solution was added. Multiple samples were prepared and placed into a water/ethylene glycol bath thermostatted at 55 ± 0.2 °C. At desired times, the test tubes were removed from the bath. The solutions were then filtered through a pre-weighed fritted glass funnel, and the collected polymer powder was rinsed repeatedly with a large amount of distilled water. The polymer and the funnel were dried under vacuum at 70 °C until constant weight was obtained.

References

1. Okada, T.; Okawara, R. *J. Organometal. Chem.* **1973**, *54*, 149-152.

2. Kobayashi, S.; Yokoyama, T.; Kawabe, K.; Saegusa, T. *Polym. Bull.* **1980**, *3*, 585-591.

3. Smith, I. J.; Tighe, B. J. *Macromol. Chem. Phys.***1981**, *182*, 313-324.

4. Pinkus, A. G.; Subramanyam, R.; Clough, S. L.; Lairmore, T. C. *J. Polym. Sci. Pol. Chem.* **1989**, *27*, 4291-4296.

5. Domb, A. J. *J. Polym. Sci. Pol. Chem.* **1993**, *31*, 1973-1981.

6. Whitesell, J. K.; Pojman, J. A. *Chem. Mat.* **1990**, *2*, 248-254.

7. Fukuzaki, H.; Aiba, Y.; Yoshida, M.; Asano, M.; Kumakura, M. *Makromol. Chem.* **1989**, *190*, 2407-2415.

8. Fukuzaki, H.; Yoshida, M.; Asano, M.; M., K.; Imasaka, K.; Nagai, T.; Mashimo, T.; Yuasa, H.; Imai, K.; Yamanaka, H. *Eur. Polym. J.* **1990**, *26*, 1273-1277.

9. Imasaka, K.; Yoshida, M.; Fukuzaki, H.; Asano, M.; Kumakura, M.; Mashimo, T.; Yamanaka, H.; Nagai, T. *Int. J. Pharm.* **1992**, *81*, 31-38.

10. Kim, W. J.; Kim, J. H.; Kim, S. H.; Kim, Y. H. *Polym.-Korea* **2000**, *24*, 431-436.

11. Kimura, Y. In *Chem. Abst. 1993, 118, 255577r.* Japan, 1993

12. Lee, R. S.; Yang, J. M. *J. Polym. Sci. Pol. Chem.* **2001**, *39*, 724-731.

13. Jin, H. J.; Lee, B. Y.; Kim, M. N.; Yoon, J. S. *J. Polym. Sci. Pt. B-Polym. Phys.* **2000**, *38*, 1504-1511.

14. Simmons, T. Dissertation, Michigan State University, **2000**, 66-78.

15. Cerrai, P.; Tricoli, M. *Makromol. Chem., Rapid Commun.* **1993**, *14*, 529-538.

16. Witzke, D. R.; Narayan, R. *Abstr. Pap. Am. Chem. Soc.* **1998**, *216*, U11-U12.

17. Kopinke, F. D.; Remmler, M.; Mackenzie, K.; Moder, M.; Wachsen, O. *Polym. Degrad. Stabil.* **1996**, *53*, 329-342.

18. Lynch, V. M.; Pojman, J.; Whitesell, J. K.; Davis, B. E. *Acta Crystallogr., Sect. C: Cryst. Struct. Commun.* **1990**, *C46*, 1125-1127.

19. Taylor, R.; Kennard, O. *J. Am. Chem. Soc.* **1982**, *104*, 5063-5070.

20. Matsusue, Y.; Yamamuro, T.; Oka, M.; Shikinami, Y.; Hyon, S. H.; Ikada, Y. *J. Biomed. Mater. Res.* **1992**, *26*, 1553-1567.

21. Therin, M.; Christel, P.; Li, S. M.; Garreau, H.; Vert, M. *Biomaterials* **1992**, *13*, 594-600.

22. Li, S. *J. Biomed. Mater. Res.* **1999**, *48*, 342-353.

23. Grizzi, I.; Garreau, H.; Li, S.; Vert, M. *Biomaterials* **1995**, *16*, 305-311.

24. Dunne, M.; Corrigan, O. I.; Ramtoola, Z. *Biomaterials* **2000**, *21*, 1659-1668.

Chapter 3 Block copolymers of lactide and methyl methacrylate (MMA)

3.1. General

Due to its biocompatibility, biodegradability and non-toxicity, polylactide is an important material for medical applications such as surgical sutures,[1] implants,[2] tissue scaffolds[3] and drug delivery matrices.[4] A more recent research emphasis has been the development of polylactide as a commodity polymer for packaging materials, coatings and fibers.[5] For many applications, the properties of polylactide need to be fine-tuned. For example, better control over its degradation rate is needed for medical applications,[6] and improved impact strength is needed to overcome polylactide's brittleness. Blends,[9,10] copolymers,[11-13] and composites,[14] were synthesized to extend the properties of polylactide and the range of applications for which polylactide is suitable. For example, polylactide has been blended or copolymerized with ε-caprolactone,[15] glycolide,[16] and ethylene glycol[17,18] to achieve a wider range of degradation rates, while block copolymers that combine polylactide with a rubbery block such as polyisoprene[19,20] or polybutadiene[21] lead to toughened materials. Interesting polymer architectures were prepared by using a hydrophilic polymer, poly(2-hydroxyethyl methacrylate) (polyHEMA), as a polymer initiator from which lactide was polymerized to give a comb polymer with polylactide teeth.[22] Matyjaszewski also reported the polymerization of methacrylate-terminated polylactide to give poly(methyl methacrylate)-*g*-poly(lactic acid).[23]

Poly(methyl methacrylate) (PMMA) is a commodity polymer with good optical and mechanical properties. It also has been used in medical implants,[24-26] drug delivery systems[27] and hard contact lenses due to its biocompatibility. Polylactide and PMMA have been combined in various ways to yield new materials with unique properties. Composite biomaterials[28] that combine good mechanical properties with partial biodegradability were prepared by the free radical polymerization of MMA in the presence of α-Al_2O_3 and low molecular weight crystalline polylactide. These composite materials were considered for structural applications in orthopedic surgery. Poly(β-hydroxybutyric acid) is significantly toughened when it is "reactive blended" with PMMA,[29] but the same blending strategy applied to crystalline polylactide gave a highly interconnected network structure.[31]

A useful biocompatible and partially biodegradable system would be a toughened polylactide prepared by the combination of polylactide and PMMA in a block copolymer architecture. Because the synthesis of the two blocks are "mechanistically incompatible", the polymerization mechanism must be transformed to chemically connect the two blocks. In order to obtain well-defined block copolymers with low polydispersities, "living" or "controlled" polymerization methods are preferred.

Polylactide can be prepared by the direct condensation of lactic acid or by ring opening polymerization (ROP) of lactide, the cyclic dimer of lactic acid. Most research has focused on ROP because it offers a high polymerization rate and easy control over molecular weights ranging from several thousands to several

millions.[32] Atom Transfer Radical Polymerization (ATRP) of MMA has been intensively investigated since it leads to well-defined polymers with low polydispersities.[33] The characteristic feature of ATRP is a fast dynamic equilibrium between the active and dormant species[34] which ensures a low radical concentration, and minimizes bimolecular termination reactions.

There are examples of complex polymer architectures that have been synthesized via a combination of ROP and ATRP.[35] Interesting star and graft copolymers of poly(caprolactone) and PMMA were prepared by end-group transformation and by the use of monomers that contain an ATRP initiator.[36] Shell cross-linked nanoparticles with poly(caprolactone) as the core and poly(acrylic acid) as the shell were synthesized using a difunctional aluminum catalyst.[37] A difunctional initiator, 2,2,2-tribromoethanol,[38] has been used in a one-step (simultaneous) block copolymerization of caprolactone and MMA. In this study, we employed both end-group transformation and the use of a difunctional initiator to synthesize block copolymers of lactide and MMA. Different polymer properties were observed for copolymers synthesized by the two approaches. The miscibility of the two blocks and the effect of the amorphous PMMA block on the thermal properties and crystallization of polylactide were investigated.

3.2. Results and discussion

3.2.1 Synthesis of polylactide macroinitaitors

Lactide and MMA are polymerized by different mechanisms, the former by ring opening polymerization and the later by radical or anionic polymerization. To synthesize well defined PMMA/polylactide block copolymers, one must employ two different "living" or "controlled" polymerization methods. In the work we describe here, we used ring opening polymerization to prepare polylactide blocks and ATRP for the PMMA blocks. The polymerization mechanisms were combined in two different ways, which differ in the way the polylactide block is synthesized. In the first approach, polylactide was synthesized using a $Sn(Oct)_2$ catalyst with *t*-butyl benzyl alcohol as the initiator, and the resulting polymer was capped with an α-bromoacyl bromide that can be used to initiate ATRP. In the second approach, the polylactide block was synthesized with $Sn(Oct)_2$ and a difunctional initiator that can initiate both ROP and ATRP.

Using the first strategy, lactide was polymerized in toluene using $Sn(Oct)_2$ as the catalyst and *t*-butylbenzyl alcohol as the initiator. *t*-Butylbenzyl alcohol was chosen as the initiator because the *t*-butyl group provides a distinct ^1H NMR peak useful for end group analysis. The polylactide chain was then converted to an ATRP macroinitiator using *α*-bromoisobutyryl bromide (**Scheme 3.1**). The ^1H NMR spectrum of the macroinitiator is shown in **Figure 3.1**. Two signals are diagnostic for the end groups, two peaks at 1.94 ppm (c) due to the diastereotopic methyl groups on the carbon α to the carbonyl group at the capped end of the polymer chain, and a singlet at 1.3 ppm (a) due to the *t*-butyl

group. A quartet at 5.15 ppm (d) from the methine proton on the polylactide chain, and a doublet at 1.6 ppm (b) serve as markers for the polylactide chain. The M_n of the macroinitiator was calculated from the NMR data in two ways, from the integration ratio of protons d and c, or from the ratio of the d and a protons. Both methods gave comparable results ((d/c): M_n = 5,500; (d/a): M_n = 5,250), which suggests a high end-capping efficiency.

The second strategy uses a difunctional initiator that can initiate both ROP and ATRP. As shown in **Scheme 3.2**, the initiator is readily synthesized from a difunctional alcohol and an α-bromoacyl bromide.[39] In principle, this initiator could support simultaneous ATRP of MMA and ROP of lactide, but in this study, lactide was polymerized first to afford a polylactide macroinitiator. Thus, the two approaches yield two different polylactide macroinitiators for ATRP of MMA. The key difference between the two macrominitiators is that the macroinitiator prepared by the end capping approach has an α-bromo ester group as the chain end, while the macroinitiator prepared from the difunctional initiator is terminated with a hydroxy group. As seen later, the difference in the chemical nature of the chain ends lead to dramatic differences in the thermal properties of the polymer.

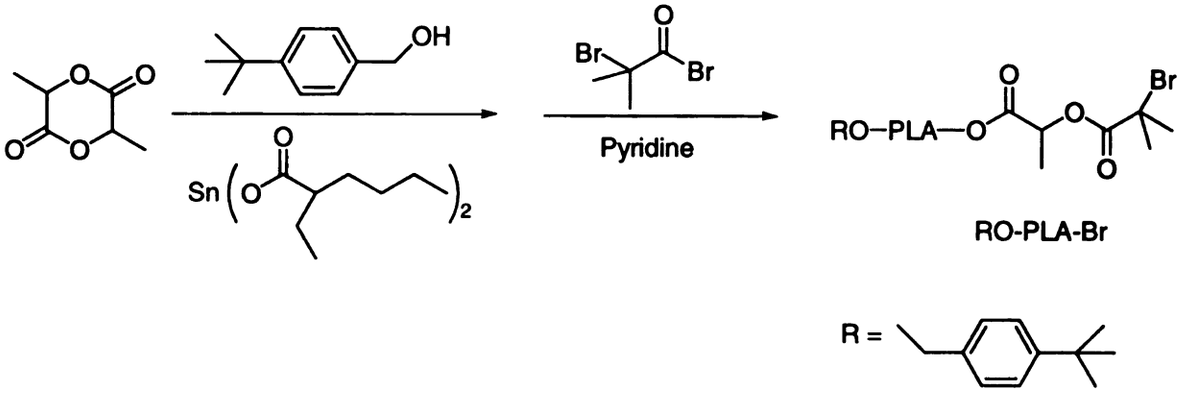

Scheme 3.1. Synthesis of end-capped polylactide initiator (RO-PLA-Br)

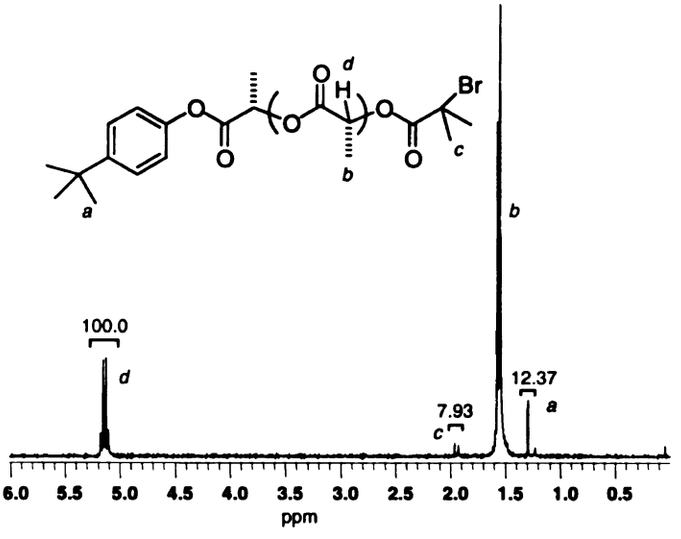

Figure 3.1. ^{1}H NMR of polylactide end capped with α-bromoisobutyryl bromide

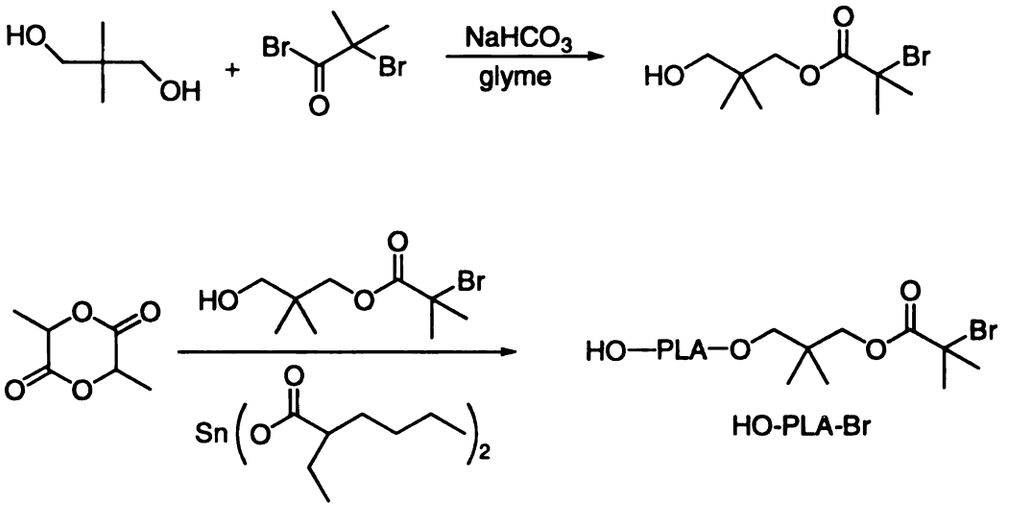

Scheme 3.2. Synthesis of polyactide prepolymer (HO-PLA-Br) from a difunctional initiator

3.2.2. Synthesis of polylactide-*b*-PMMA

The two polylactide macroinitiators were used to initiate the solution ATRP of MMA to give the corresponding linear diblock copolymers. The solvents used were toluene and anisole, with the more polar anisole being the preferred solvent for macroinitiators based on crystalline poly(L-lactide). ATRP of MMA was carried out at ambient and elevated temperatures to study the effect of polymerization temperature on the final composition of the block copolymers. For ATRP at high temperatures (e.g. 70 °C), the catalyst was CuBr with bipyridine as the ligand (**Scheme 3.3**). ATRP at ambient temperature required a more active catalyst, CuBr paired with Me_6TREN.[40] Both sets of conditions afforded soluble block copolymers with good control over molecular weight and polydispersity. However, a disadvantage of ambient temperature polymerization was significantly longer polymerization times, even when run in bulk, and as a result, most polymerizations were run at 70 °C using bipyridine as the ligand. At the end of the polymerization, the reaction vessel was opened to the air, and the polymerization solution changed from dark red to green as Cu(I) oxidized to Cu(II). The catalyst was removed by treatment with activated carbon followed by filtration. Residual copper catalyst in the organic layer could also be removed by extraction with an aqueous solution of EDTA (ethylenediaminetetraacetic acid disodium salt). After the extraction, the organic layer was colorless. The usual method for removing the copper catalyst is by filtration through silica gel and neutral alumina,[41] but when this method was used, the yield of recovered

polymer was low, possibly due to strong adsorption of the polymer to silica or alumina.

Figure 3.2 shows typical GPC traces for the polylactide macroinitiator and the block copolymer. Both "controlled" polymerization products had monomodal distributions with low polydispersities, and there was no evidence that the block copolymer was contaminated by polylactide or PMMA homopolymer. The polymer characterization data appear in **Table 3.1**. The molecular weights of the block copolymers were obtained by two methods, from the GPC analysis and by directly calculating M_n from the ^1H NMR data. Shown in **Figure 3.3** is a typical ^1H NMR spectrum of the block copolymer. For the case shown in **Figure 3.2**, M_n for the starting polylactide was 4,740 g/mol. Comparing the integrated intensities for peaks **a** and **e** gives 1:2.2 as the molar ratio of the two blocks, which corresponds to M_n = 19,200 g/mol. M_n calculated from the GPC data was 20,500 g/mol. The reflectance FTIR spectrum of the block copolymer, measured for a film spin-coated on a Au-coated silicon wafer, is shown in **Figure 3.4**. As expected for block copolymers, the spectrum appears as the linear sum of the two homopolymer spectra. C=O peaks were detected at 1767 cm^{-1} and 1745 cm^{-1}, corresponding to polylactide C=O and PMMA C=O stretching respectively. These data and the monomodal GPC traces further confirm the formation of the block copolymer.

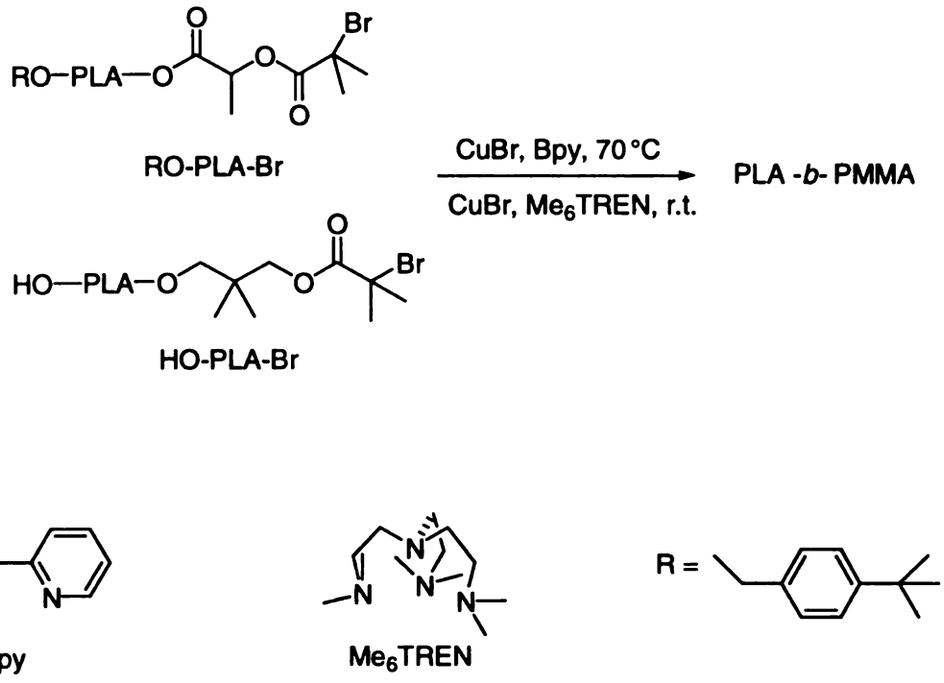

Scheme 3.3. Synthesis of poly(lactide-*b*-MMA) copolymers using polylactide macroinitiators derived from end-capping polylactide (RO-PLA-Br) and from a difunctional initiator (HO-PLA-Br).

Table 3.1. Glass transition temperatures of amorphous poly(*rac*-lactide-*b*-MMA) copolymers.

Copolymer composition (molar ratio) lactide: MMA	100:0	67:33	31:69	0:100
M_n	20,000	31,700	17,900	12,000
PDI	1.47	1.52	1.30	1.04
T_g (°C)	47	61	90	110

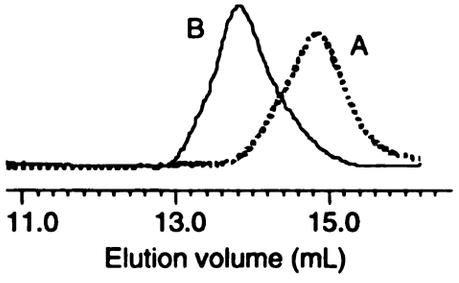

Figure 3.2. GPC traces of the polylactide macroinitiator and the resulting block copolymer. A: RO-PLA-Br (M_n= 7,200, PDI=1.24); B: poly(lactide-*b*-MMA) (M_n= 20,500, PDI=1.31).

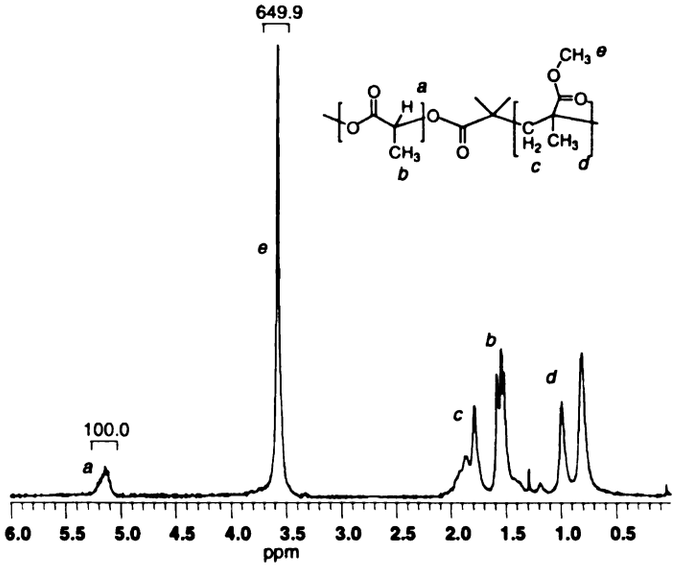

Figure 3.3. ^{1}H NMR of poly(lactide-*b*-MMA)

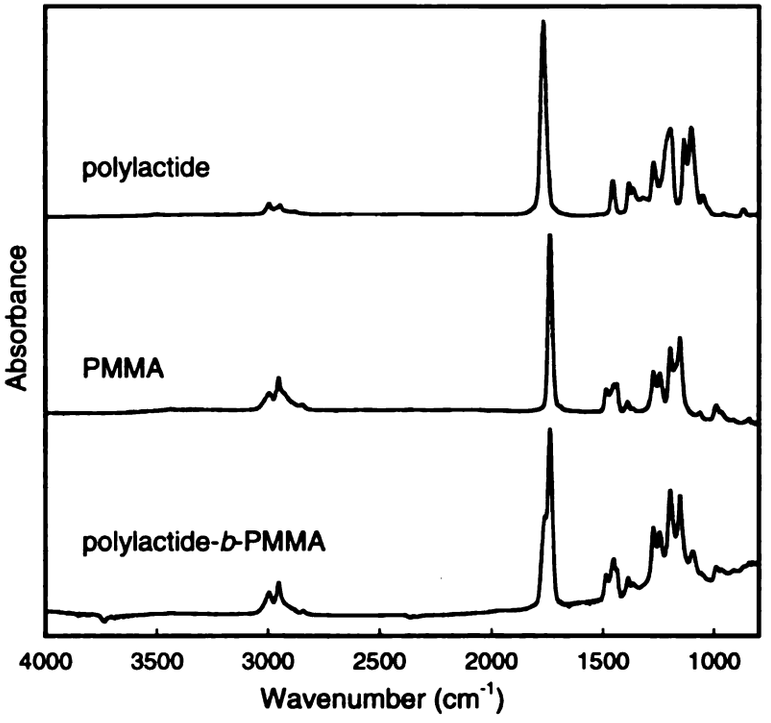

Figure 3.4. FT-IR spectra of polylactide, PMMA, and poly(lactide-*b*-MMA) films spin-coated on gold-coated silicon wafers.

3.2.3. Kinetics of the ATRP of MMA using polylactide macroinitiators

A crystalline polylactide macroinitiator synthesized from the difunctional initiator was used to study the kinetics of the ATRP of MMA. Anisole was used as the solvent since the crystalline polylactide, the copper catalyst, and the block copolymer all have good solubility in anisole. The kinetic data in **Figure 3.5** show a linear relationship, confirming that the ATRP of MMA initiated by polylactide was first order with respect to the monomer concentration as expected, and that the concentration of the active chains in the reaction was constant. M_n for the copolymers was calculated from the NMR data as described earlier, and as shown in **Figure 3.6**, a plot of the molecular weights of the copolymers vs. conversion is linear and parallels the corresponding GPC data. The slight off-set for the two sets of data reflects the fact that GPC is a relative method and the molecular weights are calibrated using polystyrene standards. The linearity of the molecular weight vs. conversion data shows that ATRP initiated by the polylactide initiator is a "controlled" process.

It is possible that the polymeric nature of the initiator may affect the polymerization kinetics and lead to slower ATRP than is seen for low molecular weight initiators. However, a control experiment designed to test for this effect gave unexpected results. When ethyl-2-bromoisobutyrate, a common ATRP initiator, was used to polymerize MMA under the same conditions used for the macroinitiator, we observed poor control over the molecular weight and a slow polymerization rate. Two additional control experiments helped explain this apparent contradiction. When a small amount of $Sn(Oct)_2$ was added to the

system, we observed a color change from dark red to orange-red, and fast consumption of MMA. When polylactide homopolymer (synthesized from BBA and $Sn(Oct)_2$ and not capped with an ATRP initiator) was added in the reaction as a spectator, we again observed a good control over the kinetics (**Figure 3.7**). Both observations point to $Sn(Oct)_2$ as a modifier of the ATRP reaction.

Aluminum isopropoxide has been used as a modifier in ATRP[41,42] to ensure good kinetic control. It was proposed that aluminum isopropoxide, a Lewis acid, could coordinate with the initiator or the dormant polymer species and lower the dissociation energy of the carbon-halogen bond, thus facilitating the halogen transfer in the ATRP equilibrium. In our case, the same effect could result from tin catalyst residues in the macroinitiator and the spectator polylactide that were not removed by precipitation into cold methanol. Washing the polymer with dilute acid is more efficient at removing catalyst residues, but it is not favored by most researchers due to possible chain scission. A polylactide sample was washed with dilute HCl and then water. After precipitation into methanol, the dried polymer was added to an ATRP of MMA. After 28 hours, the conversion of MMA to polymer (15%) was comparable to a parallel polymerization run in the absence of added polylactide.

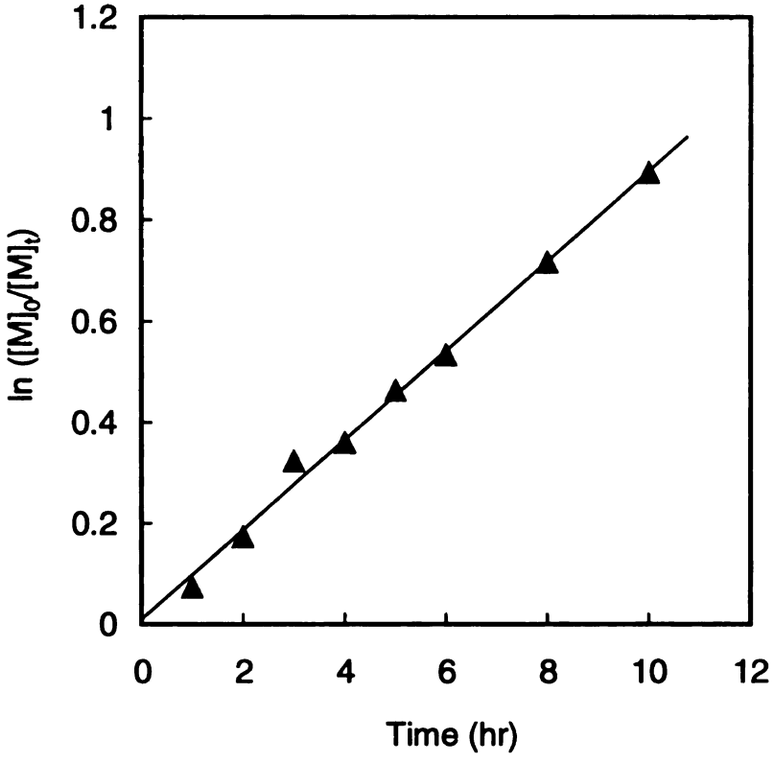

Figure 3.5. Semi-logarithmic kinetic plot of the solution ATRP of MMA in anisole at 70 °C using a polylactide macroinitiator. [MMA]=0.474 mol/L, [MMA]: [polylactide]: [CuBr]: [Bipy] = 300 : 1 : 1 : 2.5

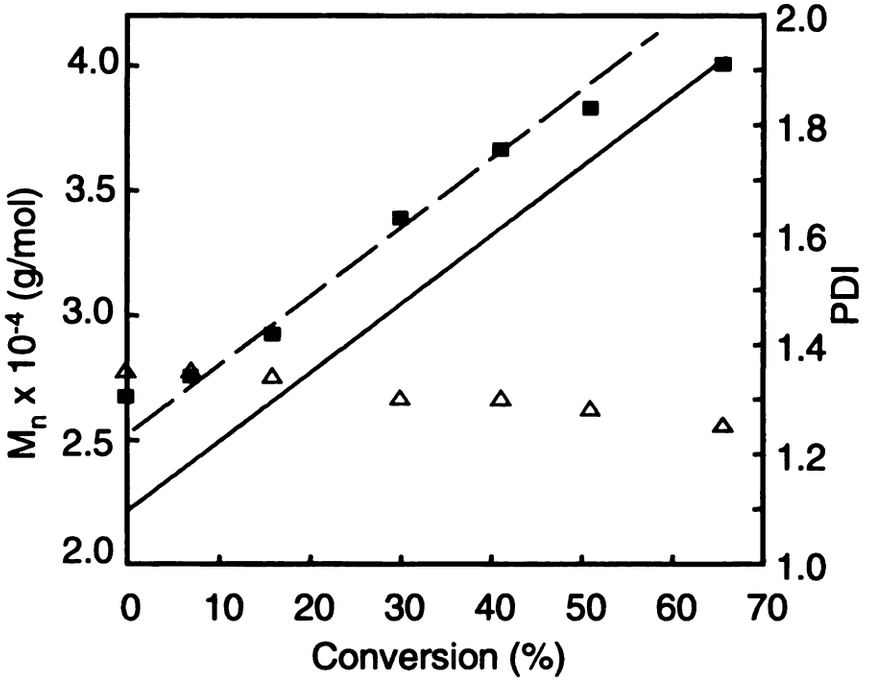

Figure 3.6. Molecular weight of block copolymers vs. monomer conversion.

▪: Molecular weight measured from GPC using polystyrene as standard;
△: PDI of copolymers; —— : Molecular weight of copolymers calculated from NMR integration; — — — : a guide to the eye drawn line parallel to the solid line

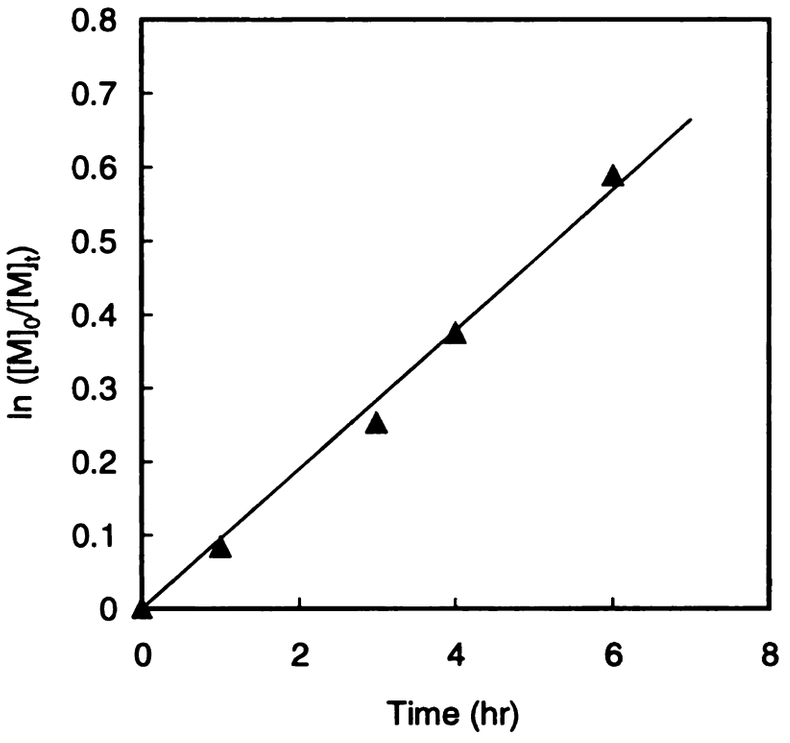

Figure 3.7. ATRP kinetics of MMA in anisole initiated by ethyl-2-bromoisobutyrate with polylactide ($Sn(Oct)_2$ and BBA) as the spectator. [MMA]=0.474 mol/L, [MMA]:[ethyl-2-bromoisobutyrate]:[CuBr]:[Bipy] = 300:1:1:2.5; M_n(polylactide)= 21,400g/mol, PDI = 1.47

3.2.4. Thermal properties of polylactide macroinitiators and block copolymers

Macroinitiators synthesized by the end-capping scheme and by using a difunctional initiator have different thermal properties. In the $Sn(Oct)_2$ catalyzed ROP of lactide, the alcohol initiator forms an ester at one end of the chain, with the other end terminated in a tin alkoxide. During workup in protic solvents, the tin alkoxide is usually hydrolyzed, and thus the polylactide macroinitiator synthesized from a difunctional initiator has a hydroxy chain end. In the end-capping approach, the macroinitiator is not terminated with a hydroxy group since tin alkoxide is replaced by an α-bromo ester. The difference in end groups is manifested in the thermal properties of the two polylactide macroinitiators. As shown in **Figure 3.8**, the onset for thermal degradation of end-capped polylactide is ~100 ° higher than for the hydroxy terminated macroinitiator.

As described in the Introduction, a variety of degradation mechanisms have been proposed for polylactide, including intramolecular transesterification, *cis*-elimination and radical chain scission. Intramolecular transesterification to give volatile cyclic dimers or oligomers is generally accepted as the dominant thermal degradation pathway since both *cis*-elimination and homolytic cleavage reactions have higher activation energies and should become significant only at higher temperatures.[43-45] Further favoring intramolecular transesterification are catalyst residues that often contaminate polylactides, even after washing with dilute HCl.[46] However, if hydroxy chain end of polylactide is capped, then intramolecular transesterification is kinetically inaccessible and polylactide will

remain intact until the onset of alternate degradation pathways at much higher temperatures. Other research groups have observed similar enhancements in the thermal stability of polylactide by blocking or capping hydroxy end groups.[47-49]

The thermal degradation profiles of the polylactide macroinitiators are transferred to the corresponding block copolymers. As shown in **Figure 3.9**, the copolymer derived from an end-capped polylactide macroinitiator had a higher onset for thermal degradation and degraded in a single step. In contrast, the copolymer derived from the difunctional initiator showed an earlier degradation and displayed a stepwise weight loss. These steps were shown to correspond to the degradation of polylactide and PMMA respectively by heating a sample to 390 °C, and then analyzing the residue by ^{1}H NMR. Only PMMA was present in the colored residue and no polylactide resonances were detected. Thus the hydroxy end groups facilitated polylactide degradation by intramolecular transesterification at low temperatures, which was followed by the degradation of PMMA at a higher temperature by a radical pathway.

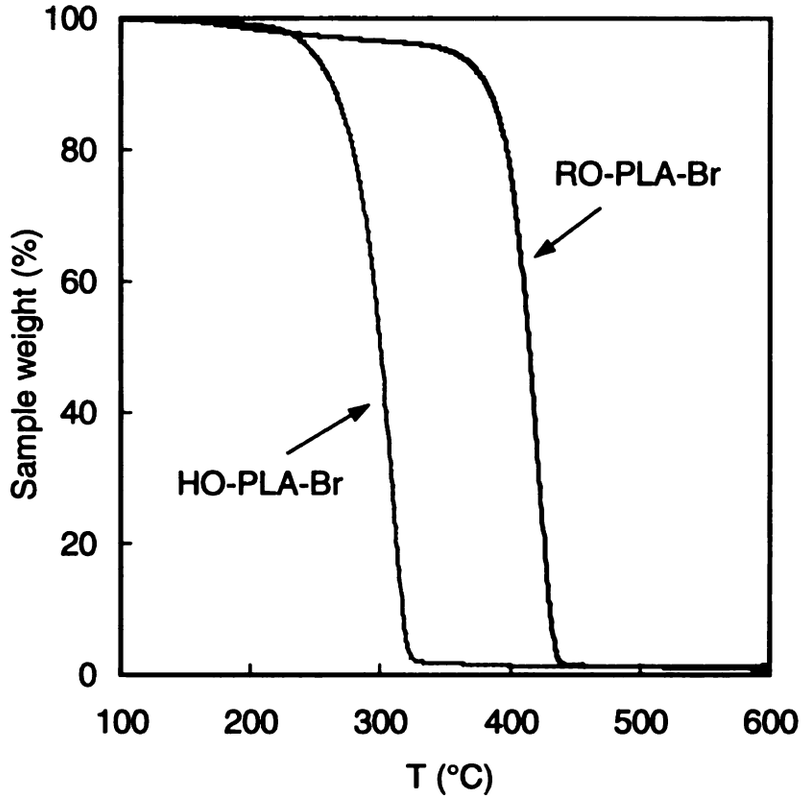

Figure 3.8. Thermal Gravimetric Analysis of polylactide macroinitiators synthesized by the end capping (RO-PLA-Br) and difunctional initiator strategies (HO-PLA-Br). Heating rate: 40 °C/min. under N_2.

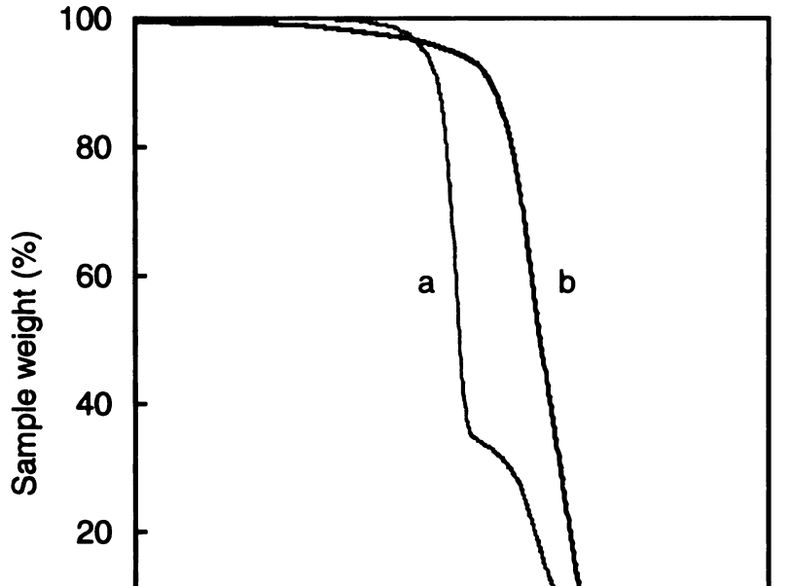

Figure 3.9. Thermal Gravimetric Analysis of poly(lactide-*b*-MMA) copolymers prepared from macroinitiators: a, HO-PLA-Br; b, RO-PLA-Br. Heating rate: 40 °C under N_2

3.2.5. Miscibility and crystallization of poly(L-lactide) blocks in the copolymers.

Poly(*rac*-lactide-*b*-MMA) and poly(L-lactide-*b*-MMA) copolymers were synthesized to study the miscibility of polylactide and PMMA blocks, and the effect that the PMMA block has on the crystallization of poly(L-lactide). As shown in **Table 3.1**, DSC runs detected only one T_g for each poly(*rac*-lactide-*b*-MMA) copolymer, and the T_g increased as the PMMA block length increased. Thus, the two blocks are miscible, consistent with the data on blends of polylactide and PMMA.[50]

For poly(L-lactide-*b*-MMA), three different compositions were synthesized (molar ratio: 72:28, 54:46, 32:68) with the crystalline polylactide block constant in molecular weight (M_n = 21,800). The semicrystalline polylactide macroinitiator was used as a control. Both the pure poly(L-lactide) and the 72:28 sample readily crystallized under a variety of conditions. The DSC scans of **Figure 3.10** are second heating scans recorded at 10 °C/min after each sample was first melted at 180 °C, and cooled to –20 °C at a rate of 10 °C/min. Samples 54:46 and 32:68 failed to crystallize under these conditions. However, after annealing sample 54:46 overnight at 130 °C, the sample did crystallize as shown in **Figure 3.11**. The 32:68 sample has the lowest poly(L-lactide) content and DSC did not detect crystallinity even after 36 hours of annealing. However, a low degree of crystallinity was observed by polarized optical microscopy. Despite the differences in crystallinity, all samples displayed a single glass transition that increased as the content of PMMA increased, which is consistent with a two-

phase mixture of crystalline poly(L-lactide) and a homogeneous mixture of PMMA and polylactide.

Polarized optical microscopy was used to study the crystalline morphology as well as the relative crystallization rate. Pure poly(L-lactide) and sample 72:28 were melted at 180 °C and then annealed at 140 °C. As shown in the micrographs **Figures 3.12** and **3.13**, pure poly(L-lactide) had the highest crystallization rate. Within ten minutes, two spherulites formed in the field of view and grew rapidly until they impinged upon each other. Sample 72:28 crystallized more slowly, and consistent with a slower growth rate, more spherulites nucleated in the optical field. Despite difference in the rate of crystallization from the melt, both samples were highly crystalline and eventually the entire field of view was filled with spherulites. The different rates of crystallization can be understood in terms of kinetic barriers to crystallization caused by the methacrylate block. Two factors are at play. First, the polylactide block has the same length in all of the poly(L-lactide-*b*-MMA) copolymers, and the longer chains in the 72:28 polymer should lead to increased chain entanglements and a slower crystallization rate. In addition, the crystallization process must exclude the PMMA chains from the crystal lattice, imposing another restraint on the growth rate. (Wide-angle X-ray scattering (**Figure 3.14**) showed that poly(L-lactide) block in the copolymer (72:28) had the same diffraction pattern as pure poly(L-lactide). The most intense peaks at 2θ values of 16.3 and 18.7 ° agree with those reported for the α from of optically pure poly(L-lactide).[51] These effects also show up in the DSC runs shown in **Figure 3.10** as a shift of the

crystallization exotherm for the 72:28 sample to a higher temperature than for pure poly(L-lactide). Because the PMMA block is chemically bonded to the poly(L-lactide) block and polarized optical microscopy shows no evidence of PMMA aggregation (dark regions), the PMMA blocks in 72:28 must be located between lamellae in the spherulites.

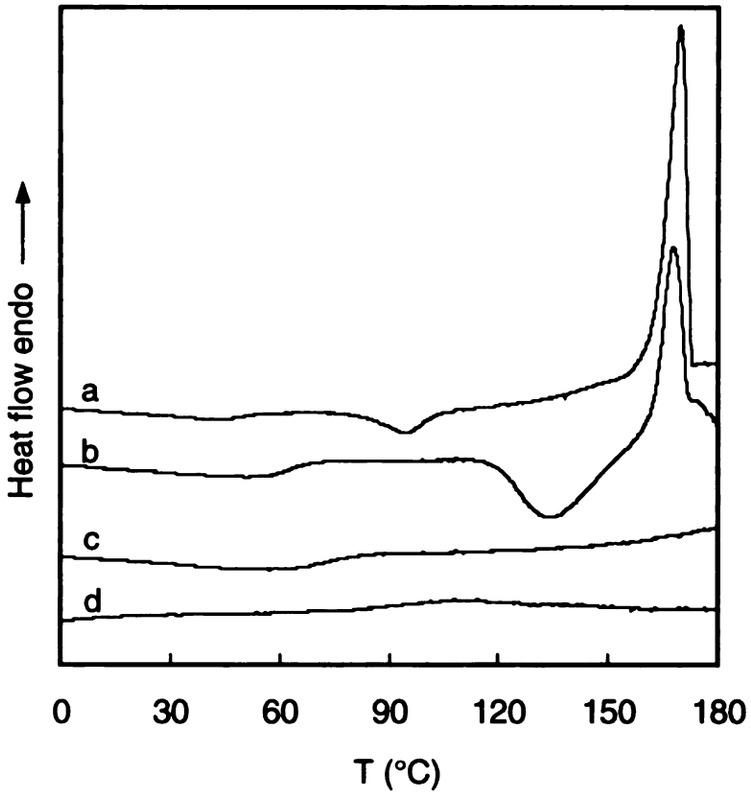

Figure 3.10. DSC second heating scans of poly(L-lactide-*b*-MMA) copolymers taken after cooling from 180 °C at 10 °C/min. Samples were heated at 10 °C/min. under helium. a: PLLA 100 (pure PLLA); b: PLLA 72 (PLLA:PMMA= 72:28); c: PLLA 54 (PLLA:PMMA= 54:46); d: PLLA 32 (PLLA:PMMA= 32:68)

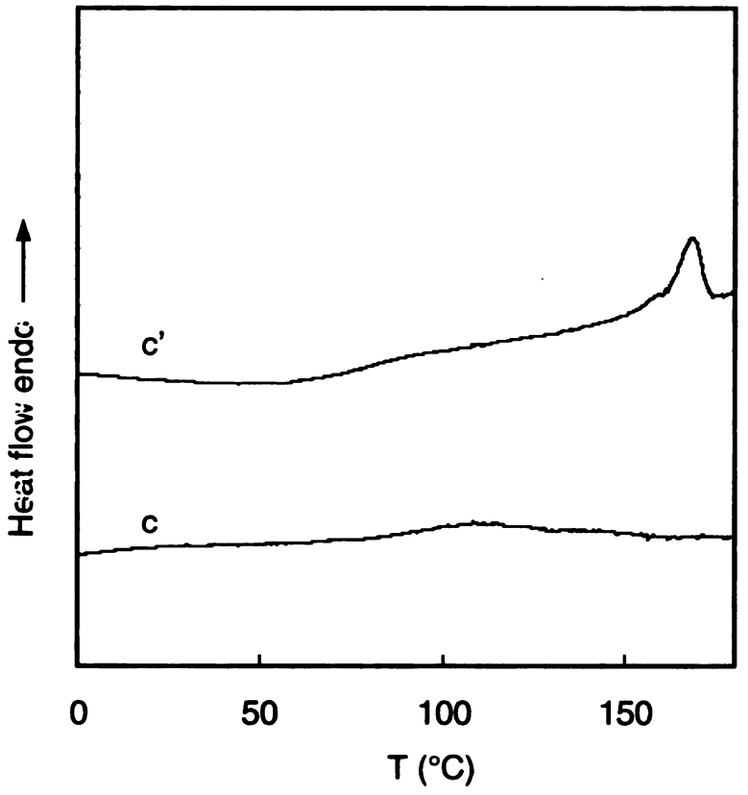

Figure 3.11. Normalized DSC heating scans of poly(L-lactide-*b*-MMA) (54:46). Samples were heated at 10 °C/min. under helium. c: after cooling at 10 °C/min from 180 °C; c': taken after annealing overnight at 130 °C

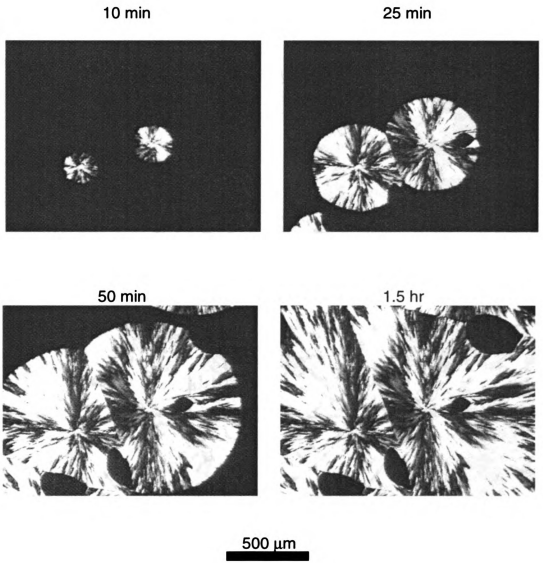

Figure 3.12. Optical micrograph of pure poly(L-lactide) (M_n= 21,800) annealed at 140 °C and observed through cross polarizers (black regions were due to air bubbles)

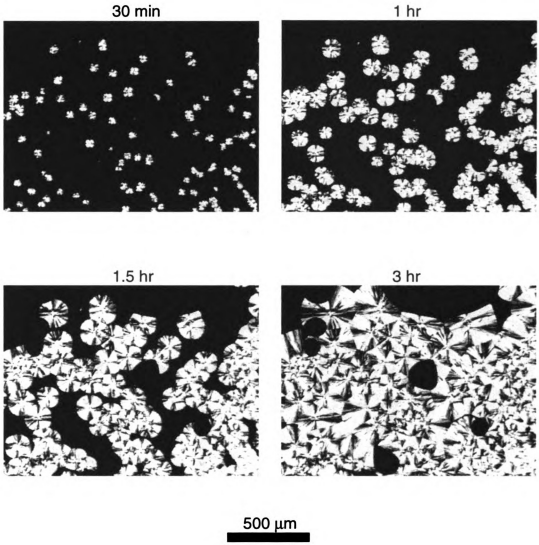

Figure 3.13. Optical micrograph of PLLA 72 (PLLA: PMMA= 72:28) annealed at 140 °C and observed through cross polarizers(black regions were due to air bubbles)

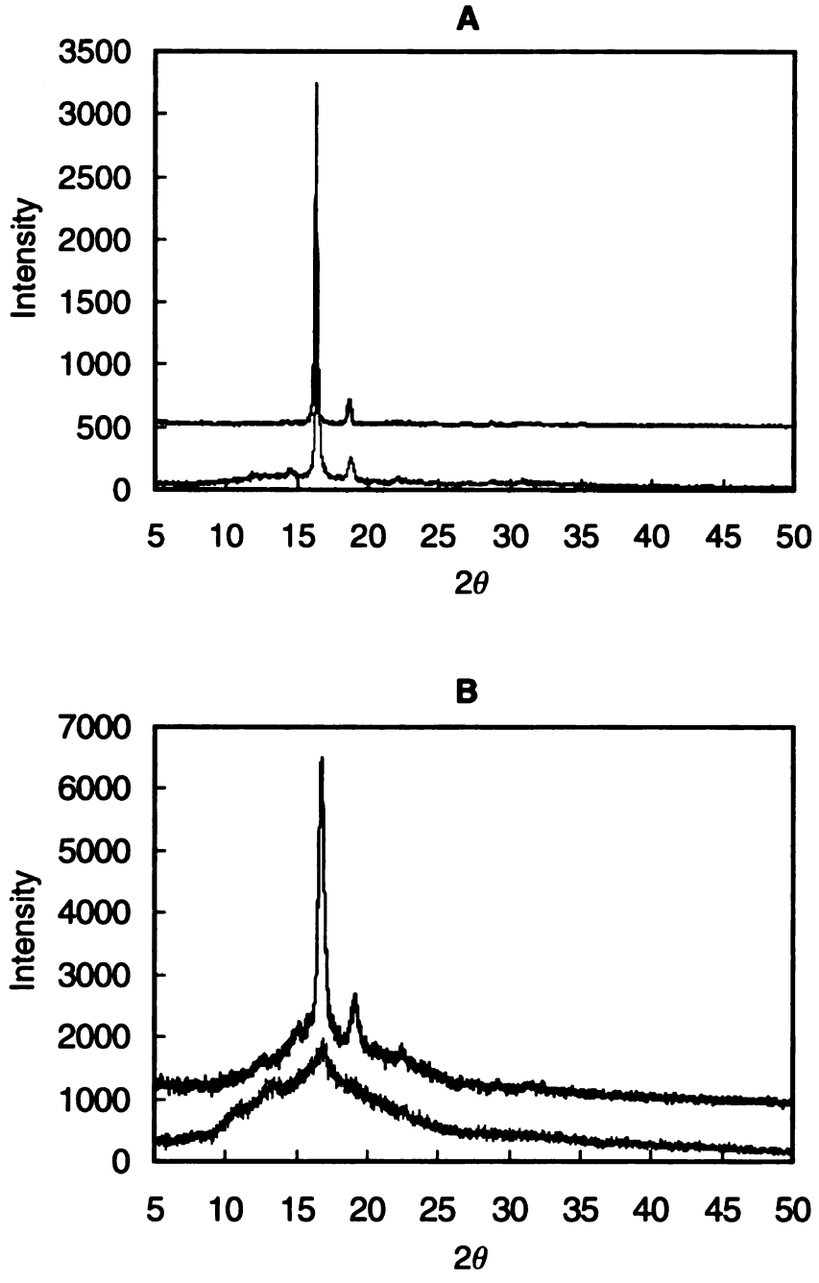

Figure 3.14. Wide-angle X-ray diffraction pattern of poly(L-lactide) and poly(L-lactide-*b*-MMA) (72:28) after annealing at 130 °C overnight. (A) as precipitated from solution (B). — polylactide; — block copolymer

3.3. Experimental Section

General. Unless otherwise specified, ACS reagent grade starting materials were used as received from commercial suppliers. Toluene was freshly distilled from sodium benzophenone ketyl under nitrogen. Methyl methacrylate (MMA) was distilled over KOH and powdered calcium hydride and was stored in a freezer at –17 °C in a drybox. 1,2-dimethoxyethane (glyme) was distilled from calcium hydride. Racemic and L-lactide were recrystallized three times from ethyl acetate before use.

Characterization ^{1}H and ^{13}C NMR analyses were performed at room temperature in $CDCl_3$ on a Varian Gemini-300 spectrometer using TMS as the chemical shift standard unless otherwise specified. Reflectance FTIR spectra were obtained under nitrogen using a Nicolet Magna-560 FTIR spectrometer containing a PIKE grazing angle (80°) attachment. Typically, 256 scans were collected using a MCT detector. Polymer molecular weights were measured by gel permeation chromatography (GPC) at 35 °C in THF using a Plgel 20μ Mixed column at a flow rate of 1 mL/min. Two detectors were used, a Waters R410 Differential Refractometer and a Waters 996 Photodiode Array. The concentration of the polymer samples was 1 mg/mL, and each solution was filtered through a Whatman 0.2 μm PTFE filter before injection. The molecular weights are reported relative to monodisperse polystyrene standards. Differential scanning calorimetry (DSC) data were obtained with a Perkin Elmer DSC 7 instrument calibrated with indium and hexyl bromide standards. The samples were placed in aluminum pans, and were heated at 10 °C/min under a helium

atmosphere. Liquid nitrogen was used as the coolant. Thermogravimetric analysis (TGA) data were obtained from a Perkin Elmer TGA 7 instrument at a heating rate of 40 °C/min under nitrogen. Optical microscopy experiments were carried out on a Nikon OPTIPHOT-2-POL microscope equipped with a Mettler FP82-HT hot stage.

Synthesis of 2,2-Dimethyl-3-hydroxypropyl α-bromoisobutyrate. To a well-stirred suspension of 3.5 g of sodium bicarbonate in 19.5 g of dry glyme was added 18.75 g (0.18 mol) neopentyl glycol. α-Bromoisobutyryl bromide (9.2 g, 0.04 mol) was added to the mixture dropwise and stirring was continued for 20 minutes. The mixture was filtered through filter paper, and the filtrate was concentrated using a rotary evaporator. Ether (100 mL) was added, and the milky solution was washed with water several times to remove excess neopentyl glycol. The ether layer was dried with sodium sulfate and concentrated under vacuum. Vacuum distillation of the residual oil afforded 5.3 g (52%) of the difunctional initiator as a colorless liquid: bp 76 °C (0.1 mm); IR bands at 3400 and 1720 cm^{-1}; ^1H NMR (300 MHz $CDCl_3$): δ 0.94 (s, 6H), 1.91 (s, 6H), 3.36 (s, 2H), 4.0 (s, 2H), 5.2(b, 1H); ^{13}C NMR (75 MHz $CDCl_3$): δ 172.04, 70.76, 68.07, 55.82, 36.59, 30.69, 21.33; MS (EI) m/z=253.0 (M); Anal. Cal. for $C_9H_{17}BrO_3$: C, 42.7; H, 6.8. Found: C, 41.75; H, 6.85.

Bulk ring opening polymerization of lactide using the difunctional initiator Racemic or L-lactide was dried under vacuum overnight before ring opening polymerization. A predetermined amount of lactide (5.00 g, 347 mmol) was added to a Schlenk flask. The flask was connected to a vacuum line and

was evacuated and refilled with argon three times. Toluene solutions of $Sn(Oct)_2$ (1.60 mL, 0.217 mol/L) and the difunctional initiator (2.82 mL, 0.123 mol/L) were added to the monomer by syringe. After removing the toluene, the Schlenk flask was refilled with argon and was heated at 140 °C in a thermostatted oil bath. After one half hour, the flask was removed from the oil bath and cooled to room temperature. A small amount of toluene or dichloromethane was used to dissolve the polymer sample, and the polymer solution was added drop-wise to a large volume of well-stirred cold methanol. After filtration, the polylactide sample was dried under vacuum at 50-60 °C until it reached constant weight.

Synthesis of end-capped polylactide macroinitiators. Racemic or L-lactide (4.32 g, 0.030 mol) was dissolved in 40 mL of toluene under argon at 90 °C. Toluene solutions of $Sn(Oct)_2$ (4.29 mL, 0.233 mol/L) and *t*-butyl benzyl alcohol (BBA) (9.42 mL, 0.106 mol/L) were added to start the polymerization. Using a syringe, small samples were removed and characterized by NMR to monitor the conversion of monomer to polymer. Upon reaching completion, the polymer solution was cooled to room temperature, and α-bromoisobutyryl bromide (3.71 mL, 0.027 mol) and pyridine (2.45 mL, 0.030 mol) were added. After stirring for half an hour, the mixture was filtered and the filtrate was concentrated using a rotary evaporator. Then the polymer solution was precipitated into a large amount of cold methanol, filtered and dried under vacuum at 50-60 °C before use.

Synthesis of polylactide-*b*-PMMA using CuBr catalyst Polylactide prepared from the difunctional initiator and end-capped polylactide were used as

ATRP initiators. CuBr/bpy was used as the catalyst at 70 °C, and CuBr/Me_6TREN was used for ambient temperature ATRP. ATRP was run either in bulk or in solution (toluene, anisole) in helium filled drybox. In a typical run, polylactide macroinitiator (0.63 g, 0.029 mmol) was first dissolved in 10 g of anisole at 70 °C, followed by CuBr (0.0090 g, 0.063 mmol) and bipyridine (0.0224 g, 0.143 mmol) to start the polymerization. The conversion of the polymerization was monitored by NMR. The polymerization was stopped by taking the reaction flask out of the drybox and opening it to the air. The polymer solution was diluted with toluene or dichloromethane and activated charcoal was added. After filtration, the polymer solution was concentrated and precipitated into a large amount of cold methanol. The purified block copolymer was then filtered and dried as usual.

References

1. Jain, R. A. *Biomaterials* **2000**, *21*, 2475-2490.

2. Middleton, J. C.; Tipton, A. J. *Biomaterials* **2000**, *21*, 2335-2346.

3. Sheridan, M. H.; Shea, L. D.; Peters, M. C.; Mooney, D. J. *J. Control. Release* **2000**, *64*, 91-102.

4. Uhrich, K. E.; Cannizzaro, S. M.; Langer, R. S.; Shakesheff, K. M. *Chem. Rev.* **1999**, *99*, 3181-3198.

5. Drumright, R. E.; Gruber, P. R.; Henton, D. E. *Adv. Mater.* **2000**, *12*, 1841-1846.

6. Bergsma, J. E.; Debruijn, W. C.; Rozema, F. R.; Bos, R. R. M.; Boering, G. *Biomaterials* **1995**, *16*, 25-31.

7. Wachsen, O.; Platkowski, K.; Reichert, K. H. *Polym. Degrad. Stabil.* **1997**, *57*, 87-94.

8. Gogolewski, S.; Jovanovic, M.; Perren, S. M.; Dillon, J. G.; Hughes, M. K. *Polym. Degrad. Stabil.* **1993**, *40*, 313-322.

9. Cleek, R. L.; Ting, K. C.; Eskin, S. G.; Mikos, A. G. *J. Control. Release* **1997**, *48*, 259-268.

10. Tsuji, H.; Mizuno, A.; Ikada, Y. *J. Appl. Polym. Sci.* **1998**, *70*, 2259-2268.

11. Yin, M.; Baker, G. L. *Macromolecules* **1999**, *32*, 7711-7718.

12. Wang, D.; Feng, X. D. *Macromolecules* **1997**, *30*, 5688-5692.

13. Joziasse, C. A. P.; Grablowitz, H.; Pennings, A. J. *Macromol. Chem. Phys.* **2000**, *201*, 107-112.

14. Kasuga, T.; Ota, Y.; Nogami, M.; Abe, Y. *Biomaterials* **2001**, *22*, 19-23.

15. Qian, H. T.; Bei, J. Z.; Wang, S. G. *Polym. Degrad. Stabil.* **2000**, *68*, 423-429.

16. Li, Y. X.; Kissel, T. *Polymer* **1998**, *39*, 4421-4427.

17. Chen, X. H.; McCarthy, S. P.; Gross, R. A. *Macromolecules* **1997**, *30*, 4295-4301.

18. Celikkaya, E.; Denkbas, E. B.; Piskin, E. *J. Appl. Polym. Sci.* **1996**, *61*, 1439-1446.

19. Frick, E. M.; Hillmyer, M. A. *Macromol. Rapid Commun.* **2000**, *21*, 1317-1322.

20. Schmidt, S. C.; Hillmyer, M. A. *Macromolecules* **1999**, *32*, 4794-4801.

21. Wang, Y. B.; Hillmyer, M. A. *Macromolecules* **2000**, *33*, 7395-7403.

22. Barakat, I.; Dubois, P.; Jerome, R.; Teyssie, P.; Goethals, E. *J. Polym. Sci. Pol. Chem.* **1994**, *32*, 2099-2110.

23. Shinoda, H.; Matyjaszewski, K. *Macromolecules* **2001**, *34*, 6243-6248.

24. Mousa, W. F.; Kobayashi, M.; Shinzato, S.; Kamimura, M.; Neo, M.; Yoshihara, S.; Nakamura, T. *Biomaterials* **2000**, *21*, 2137-2146.

25. Shinzato, S.; Kobayashi, M.; Mousa, W. F.; Kamimura, M.; Neo, M.; Kitamura, Y.; Kokubo, T.; Nakamura, T. *J. Biomed. Mater. Res.* **2000**, *51*, 258-272.

26. Miller, D. J.; Lang, F. F.; Walsh, G. L.; Abi-Said, D.; Wildrick, D. M.; Gokaslan, Z. L. *J. Neurosurg.* **2000**, *92*, 181-190.

27. Vallet-Regi, M.; Granado, S.; Arcos, D.; Gordo, M.; Cabanas, M. V.; Ragel, C. V.; Salinas, A. J.; Doadrio, A. L.; San Roman, J. *J. Biomed. Mater. Res.* **1998**, *39*, 423-428.

28. RodriguezLorenzo, L. M.; Salinas, A. J.; ValletRegi, M.; Roman, J. S. *J. Biomed. Mater. Res.* **1996**, *30*, 515-522.

29. Avella, M.; Errico, M. E.; Immirzi, B.; Malinconico, M.; Falcigno, L.; Paolillo, L. *Macromol. Chem. Phys.* **1998**, *199*, 1901-1907.

30. He, Y.; Shuai, X.; Cao, A. M.; Kasuya, K.; Doi, Y.; Inoue, Y. *Macromol. Rapid Commun.* **2000**, *21*, 1277-1281.

31. Avella, M.; Errico, M. E.; Immirzi, B.; Malinconico, M.; Falcigno, L.; Paolillo, L. *Macromol. Chem. Phys.* **2000**, *201*, 1295-1302.

32. Hyon, S. H.; Jamshidi, K.; Ikada, Y. *Biomaterials* **1997**, *18*, 1503-1508.

33. Coessens, V.; Pintauer, T.; Matyjaszewski, K. *Prog. Polym. Sci.* **2001**, *26*, 337-377.

34. Greszta, D.; Mardare, D.; Matyjaszewski, K. *Macromolecules* **1994**, *27*, 638-644.

35. Hedrick, J. L.; Trollsas, M.; Hawker, C. J.; Atthoff, B.; Claesson, H.; Heise, A.; Miller, R. D.; Mecerreyes, D.; Jerome, R.; Dubois, P. *Macromolecules* **1998**, *31*, 8691-8705.

36. Mecerreyes, D.; Trollsas, M.; Hedrick, J. L. *Macromolecules* **1999**, *32*, 8753-8759.

37. Zhang, Q.; Remsen, E. E.; Wooley, K. L. *J. Am. Chem. Soc.* **2000**, *122*, 3642-3651.

38. Mecerreyes, D.; Moineau, G.; Dubois, P.; Jerome, R.; Hedrick, J. L.; Hawker, C. J.; Malmstrom, E. E.; Trollsas, M. *Angew. Chem.-Int. Edit.* **1998**, *37*, 1274-1276.

39. Newman, M. S.; Kilbourn, E. *J. Org. Chem.* **1970**, *35*, 3186-3188.

40. Ciampolini, M.; Nardi, N. *Inorg. Chem.* **1966**, *5*, 41-44.

41. Guo, J. H.; Han, Z. W.; Wu, P. P. *J. Mol. Catal. A-Chem.* **2000**, *159*, 77-83.

42. Schubert, U. S.; Hochwimmer, G.; Spindler, C. E.; Nuyken, O. *Macromol. Rapid Commun.* **1999**, *20*, 351-355.

43. Kopinke, F. D.; Remmler, M.; Mackenzie, K.; Moder, M.; Wachsen, O. *Polym. Degrad. Stabil.* **1996**, *53*, 329-342.

44. Kopinke, F. D.; Mackenzie, K. *J. Anal. Appl. Pyrolysis* **1997**, *40-1*, 43-53.

45. Wachsen, O.; Reichert, K. H.; Kruger, R. P.; Much, H.; Schulz, G. *Polym. Degrad. Stabil.* **1997**, *55*, 225-231.

46. Cam, D.; Marucci, M. *Polymer* **1997**, *38*, 1879-1884.

47. Lee, W. K.; Losito, I.; Gardella, J. A.; Hicks, W. L. *Macromolecules* **2001**, *34*, 3000-3006.

48. Lee, S. H.; Kim, S. H.; Han, Y. K.; Kim, Y. H. *J. Polym. Sci. Pol. Chem.* **2001**, *39*, 973-985.

49. Jamshidi, K.; Hyon, S. H.; Ikada, Y. *Polymer* **1988**, *29*, 2229-2234.

50. Eguiburu, J. L.; Iruin, J. J.; Fernandez-Berridi, M. J.; Roman, J. S. *Polymer* **1998**, *39*, 6891-6897.

51. Ikada, Y.; Jamshidi, K.; Tsuji, H.; Hyon, S. H. *Macromolecules* **1987**, *20*, 904-906.

Chapter 4 Block copolymers of lactide and OEGMA

4.1. General

Polylactide is the most prominent biodegradable material in the packaging, pharmaceutical and medical fields. However, polylactide is brittle with a low impact resistance, and articles made from polylactide tend to shatter. Another limitation of polylactide is its hydrophobic nature, which leads a to slow biodegradation that is undesirable in some medical applications. In drug delivery systems, carriers with a better hydrophobic/hydrophilic balance are desired to achieve faster water uptake and more rapid drug release at early stages in the degradation process. Amphiphilic copolymers systems that include lactide and ethylene oxide have been synthesized to address both problems.

Methoxy-capped oligo(ethylene oxide) methacrylate (OEGMA) is a commercially available hydrophilic monomer. Polymerization of OEGMA gives a polymer with the same backbone as PMMA, but with hydrophilic side chains composed of ethylene oxide oligomers. The side chains bear some of the same characteristics of PEO, such as hydrophilicity, biocompatibility and good resistance to protein adsorption and cell adhesion.[1-3] Poly(OEGMA) (POEGMA) has been widely used in coatings[2,4] hydrogels[5] and drug delivery nanospheres[6] as a hydrophilic and biocompatible material. Block polymers of lactide and OEGMA are a new amphiphilic biocompatible polymer system.

Previous studies of lactide/PEO block copolymers were limited to the PEO block lengths that are available from commercial suppliers. In lactide/OEGMA

block copolymers, the length of each block can be controlled simply by adjusting monomer to initiator ratio and the reaction time since two "controlled" polymerization methods can be applied, just as in the case of lactide/methyl methacrylate block copolymers. Another advantage of using OEGMA is that each monomer contains an average of 5 ethylene oxide units, which means that many ethylene oxide units are incorporated into copolymers even for relatively short OEGMA block lengths. In aqueous solutions, OEGMA is known to polymerize rapidly and in a controlled fashion using ATRP since both monomer and polymer are soluble in water. POEGMA also has good solubility in typical organic solvents.

In the scheme described here, polylactide was polymerized first using a difunctional initiator for ease of molecular weight control. Then the macroinitiator was used to polymerize OEGMA in toluene or anisole in the presence of CuBr and bipyridine.

4.2. Results and discussions

4.2.1. Polymerization of lactide and OEGMA

As shown in **Scheme 4.1**, lactide was polymerized by $Sn(Oct)_2$ and a difunctional initiator, 2-bromo-2-methylpropionic acid 3-hydroxy-2,2-dimethyl-propyl ester. The resulting macroinitiator was purified by dissolution in CH_2Cl_2, and precipitation into methanol, followed by drying under vacuum at 50 °C. For ATRP, a predetermined amount of macroinitiator, CuBr/bipyridine, OEGMA and

toluene were used in the system. The polylactide macroinitiator was first dissolved in toluene at 70 °C, and then OEGMA with the CuBr/bipyridine catalyst were added to start the polymerization. Parallel reactions were set up that could be stopped at desired intervals and conversions to give copolymers of different composition. As seen from entries 2-4 in **Table 4.1**, the degree of polymerization increased and the polydispersity index decreased as the POEGMA block length increased. This behavior is consistent with well-controlled ATRP, where the polydispersity index decreases as the conversion increases.[7]

Block copolymer formation was confirmed by GPC and spectroscopic data for the copolymers. GPC measurements show a single peak for the polylactide block that shifts to higher molecular weights (**Figure 4.1**). There is no evidence of polylactide or POEGMA homopolymer in the GPC trace of the block copolymer. FTIR (**Figure 4.2.**) and ^{1}H NMR (**Figure 4.3.**) spectroscopy of polylactide, POEGMA and the block copolymers confirmed the presence and composition of both blocks in the resulting copolymers.

Table 4.1. Block copolymers of polylactide-*b*-POEGMA

entry	M_n(PLA)	ratio of two blocks PLA:POEGMA	M_n(calc.from NMR ratio)	M_n (GPC)	PDI
1	18,700[a]	100:45	53,760	54,750	1.65
2	30,000[b]	100:12.5	45,600	58,900	1.59
3	30,000[b]	100:35	73,750	70,900	1.40
4	30,000[b]	100:40	80,000	76,530	1.33

a: obtained by NMR, M_n = 25,500, PDI= 1.55 (by GPC)
b: obtained by NMR, M_n = 46,500, PDI= 1.58 (by GPC)

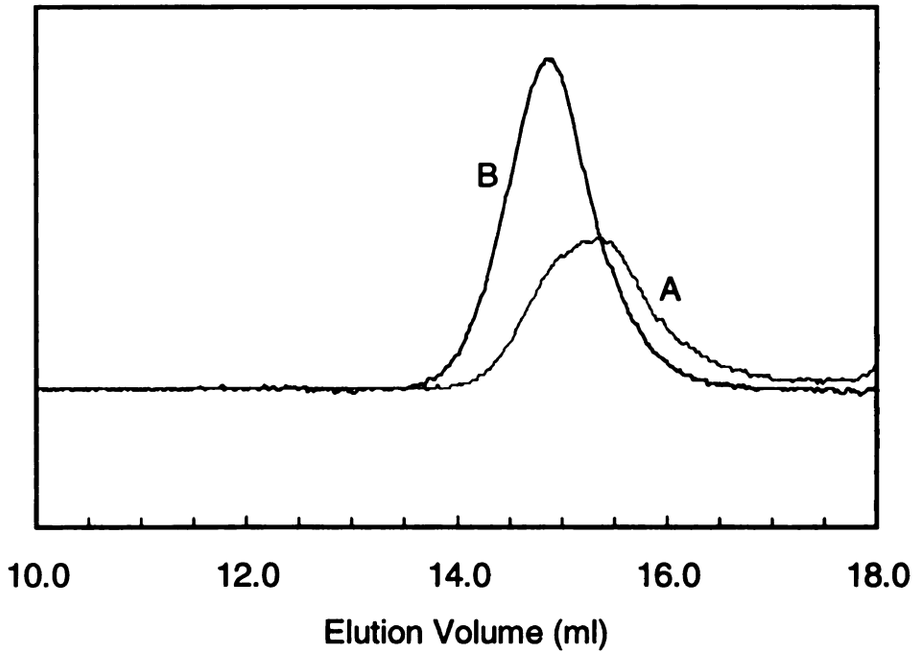

Figure 4.1. GPC traces of polylactide macroinitiator (A: M_n= 26,150, PDI= 1.47) and polylactide-*b*-POEGMA (B: M_n= 45,790, PDI= 1.39)

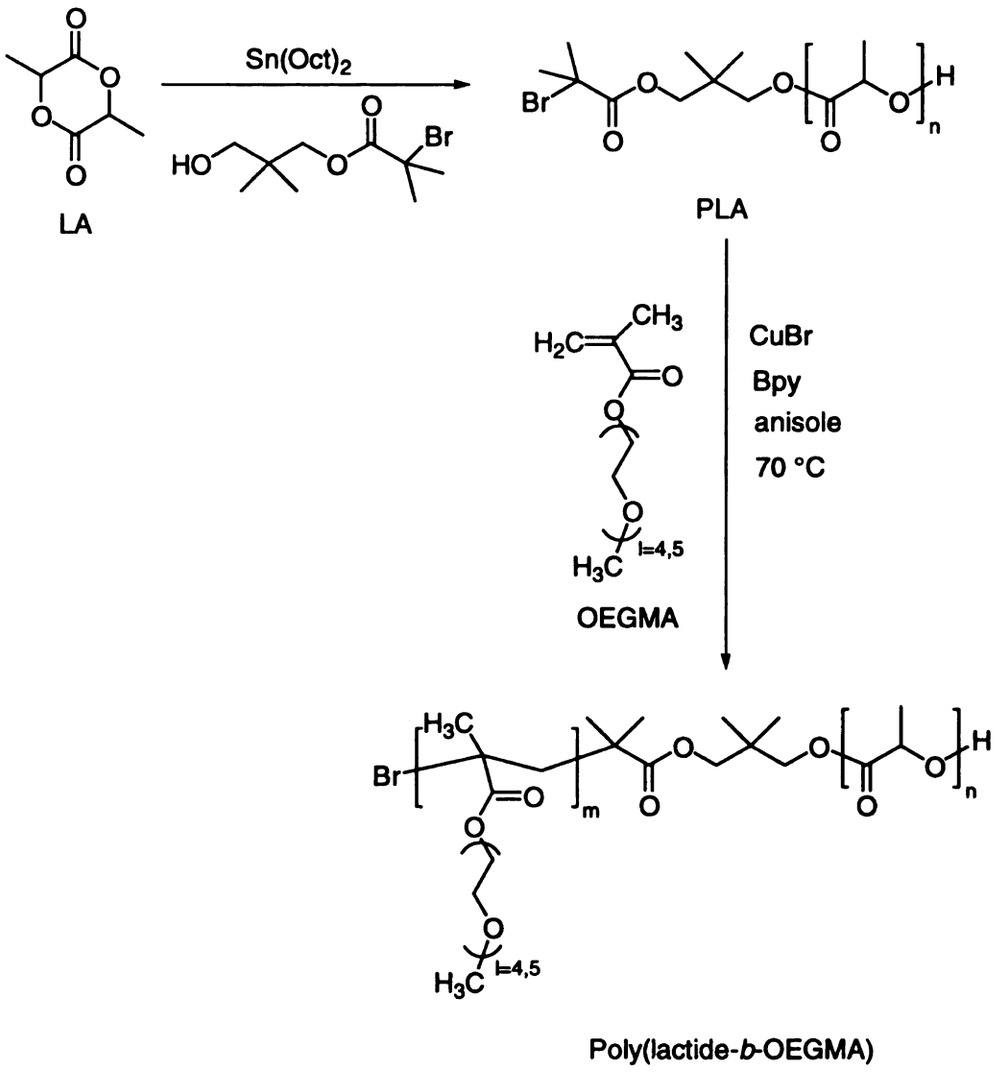

Scheme 4.1. Synthesis of poly(lactide-*b*-OEGMA)

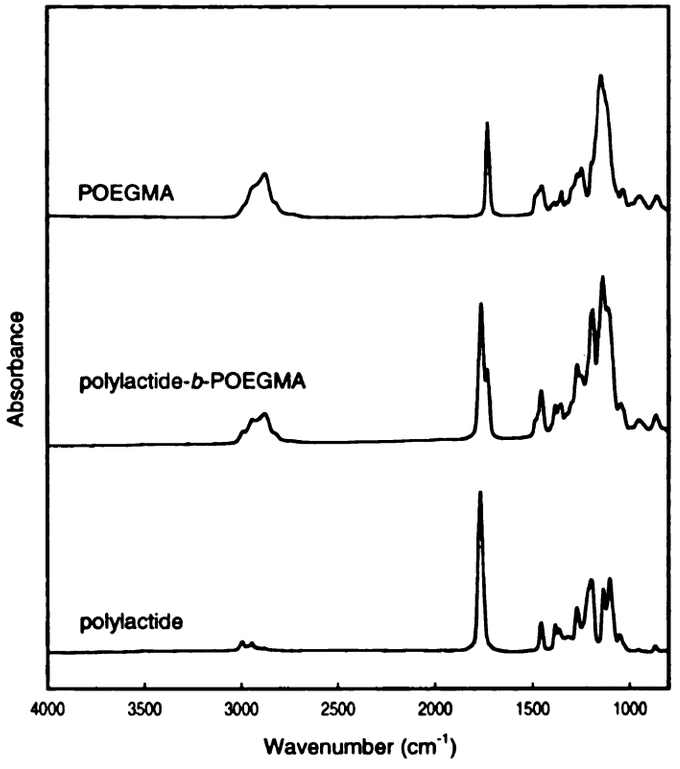

Figure 4.2. FTIR spectra of polylactide, POEGMA and polylactide-*b*-POEGMA) films spin coated on gold-coated silicon substrates.

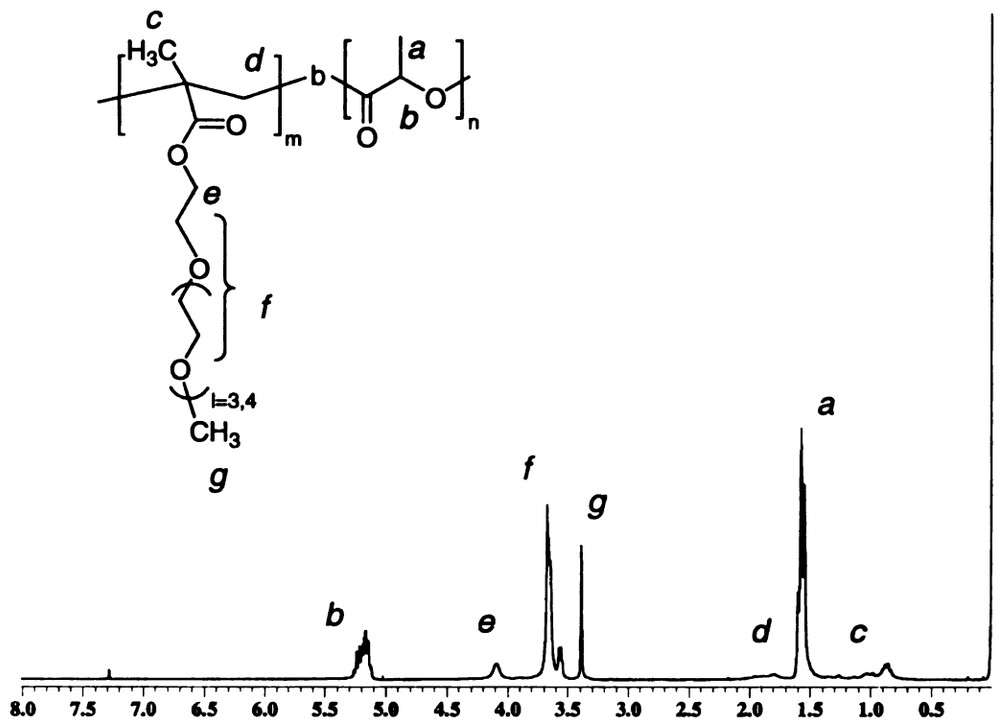

Figure 4.3. NMR spectrum of polylactide-*b*-POEGMA

4.2.2. Purification of block copolymers

Upon exposure to air, the polymer solutions changed from the brownish red of a typical ATRP system to green, paralleling the oxidation Cu(I) to Cu(II) by oxygen. Activated carbon failed to remove residual copper catalysts despite lengthy filtrations using 0.2 μm filters. Centrifugation gave clear but tinted solutions. EDTA is an excellent chelating agent for heavy metal ions, and washing the polymer solution with saturated aqueous EDTA solution proved effective at removing residual copper. After two or three extractions, the blue color of the copper containing organic phase was completely clear. Washing with distilled water followed by removal of the solvent yielded the copolymers as white solids.

The copolymers were purified by removing residual OEGMA from the crude polymer samples. OEGMA is soluble in hexanes, but the copolymers are insoluble. NMR spectra of the copolymer showed that washing the crude polymer with hexanes several times gave OEGMA-free polymer. L-lactide/OEGMA block copolymers were also purified by dissolution in toluene or methylene chloride followed by precipitation into cold methanol.

4.2.3. Thermal properties of lactide and OEGMA copolymers

POEGMA, poly(*rac*-lactide), and poly(*rac*-lactide)-*b*-poly(OEGMA) copolymers containing 9 and 28.5 mol % OEGMA were analyzed by DSC (**Figure 4.4**). The polylactide block in both copolymers and the polylactide homopolymer had the same length (polylactide M_n = 30,000, PDI = 1.58). POEGMA, a viscous liquid at room temperature, has the lowest T_g –50 °C, while that of polylactide is the highest (48 °C). The T_gs of the block copolymers fall between those two extremes. The copolymer containing 28.5% OEGMA showed a broad glass transition temperature below 0 °C, which is consistent with partial miscibility of the two blocks. The narrower transition for the 9% OEGMA copolymer (T_g = 25 °C) suggests improved miscibility for shorter OEGMA block lengths. Both block copolymers are elastic rubbery materials, but the block copolymer consisting of 9% OEGMA is stiffer.

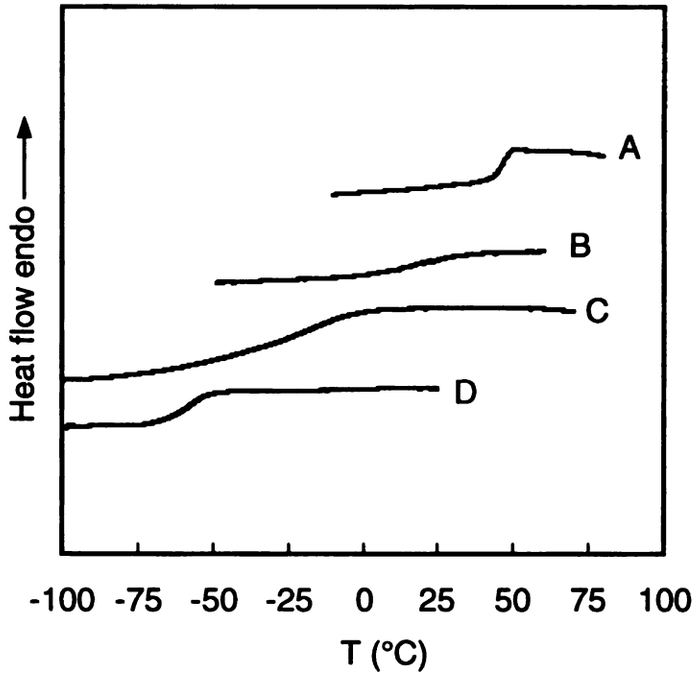

Figure 4.4. Differential Scanning Calorimetry of poly(*rac*-lactide), poly(OEGMA), and poly(*rac*-lactide)-*b*-poly(OEGMA) copolymers. A: polylactide; B: poly(*rac*-lactide)-*b*-poly(OEGMA) (9% OEGMA); C: poly(*rac*-lactide)-*b*-poly(OEGMA) (28.5% OEGMA); D: poly(OEGMA)

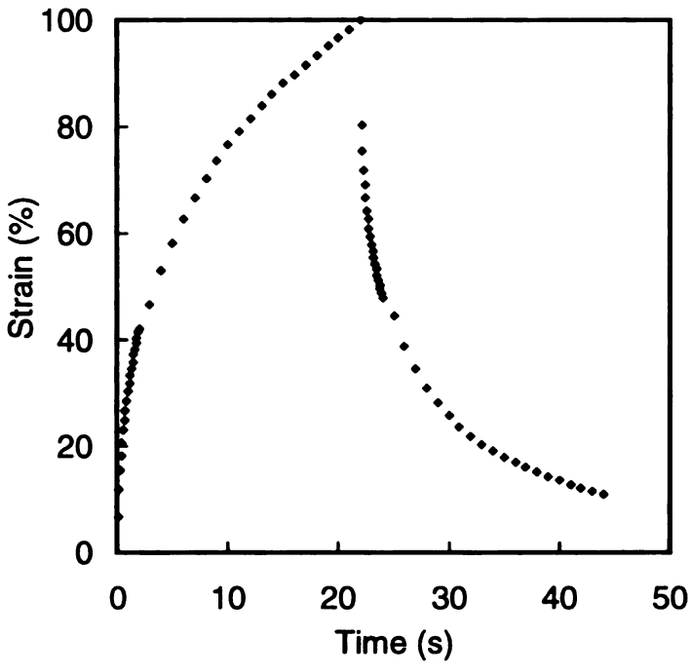

Figure 4.5. Strain recovery of poly(*rac*-lactide)-*b*-poly(OEGMA) (9% OEGMA) at 37 °C. Stress was applied for the first 22 seconds.

The mechanical properties of the block copolymer containing 9% OEGMA was characterized by a strain recovery test. A circular shaped sample (~ 1" in diameter) was sheared axially in a rheometer at 37 °C to 100% strain in 22 seconds. The load was removed, and the strain recovery was measured during the next 22 seconds. The strain recovery plot, (**Figure 4.5**) shows that ~90% of the strain was recovered leaving only 10% residual strain. The residual strain is irreversible deformation that typically results from viscous flow in the sample. Experiments run at 30 °C, closer to the T_g of the polymer, showed more rubbery behavior, with almost complete strain recovery. A shear modulus of 1.6×10^4 Pa

was calculated from the stress-strain curve for the copolymer measured at a frequency of 1 Hz at 37 °C (**Figure 4.6**), while common rubbery materials have average shear moduli of ~10^5 Pa at 25 °C. At 30 °C, the modulus increased to 2.2×10^4 Pa.

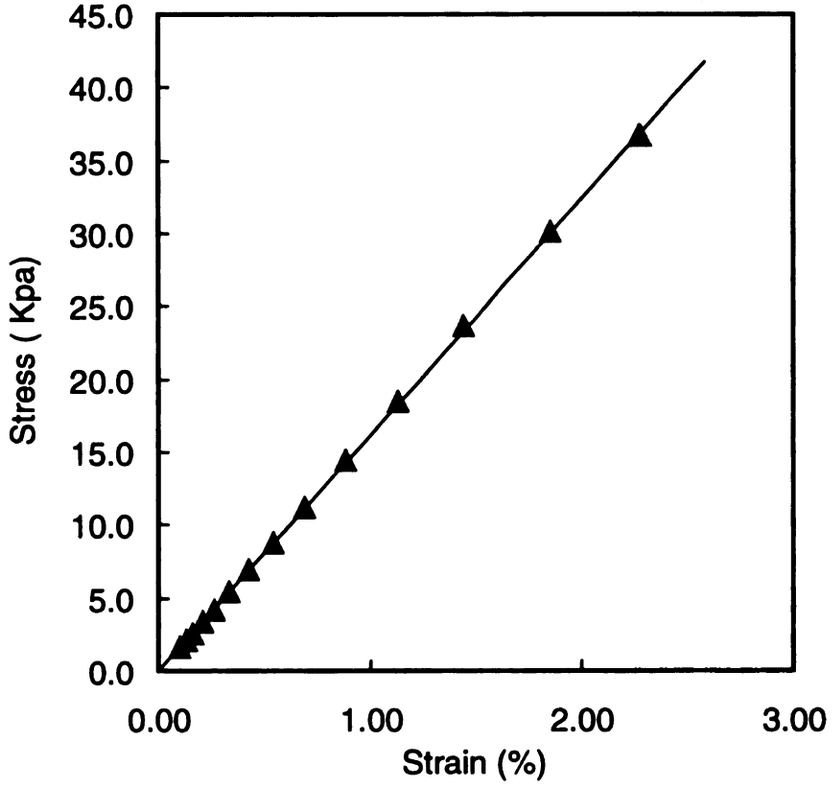

Figure 4.6. Stress-strain curve of poly(*rac*-lactide)-*b*-poly(OEGMA) (9% OEGMA) measured at a frequency of 1Hz at 37 °C

4.3. Preparation of polylactide-*b*-POEGMA nanoparticles

Polylactide-*b*-POEGMA copolymers contain both hydrophilic and hydrophobic blocks, and thus they should be ideal candidates for nano-sized drug carriers. The hydrophobic block can incorporate hydrophobic drugs while the hydrophilic block stabilizes the nanoparticles in the aqueous phase and prevents coagulation. Because block copolymers of *rac*-lactide and OEGMA are rubbery around room temperature, copolymers of L-lactide and OEGMA were used because their higher T_g leads to nanoparticles that better maintain their shape. A poly(L-lactide) macroinitiator with a molecular weight of 18,900 g/mol was used to initiate the ATRP of OEGMA in anisole at 70 °C. Poly(L-lactide)-*b*-poly(OEGMA) (6 mol% OEGMA) was used to form nanoparticles.

Due to its simplicity, the dialysis method was used to prepare the nanoparticles. Block copolymers were dissolved in dioxane, loaded in a dialysis tube with a molecular weight cut off of ~ 3,000 g/mol, and then the dialysis tube was immersed in a water bath for 24 hours (**Figure 4.7**). The clear block copolymer solution became translucent as water diffused into the tube and dioxane out of the tube. A portion of the translucent solution was then dripped onto a gold-coated silicon wafer and freeze dried. Imaging by AFM and ESEM gave images with poor resolution, but SEM measurement of uncoated nanoparticles taken at a high scan rate revealed spherical sub-micron particles (**Figure 4.8**). The nanoparticles were not robust in the electron beam and readily degraded, especially at slower scan rates.

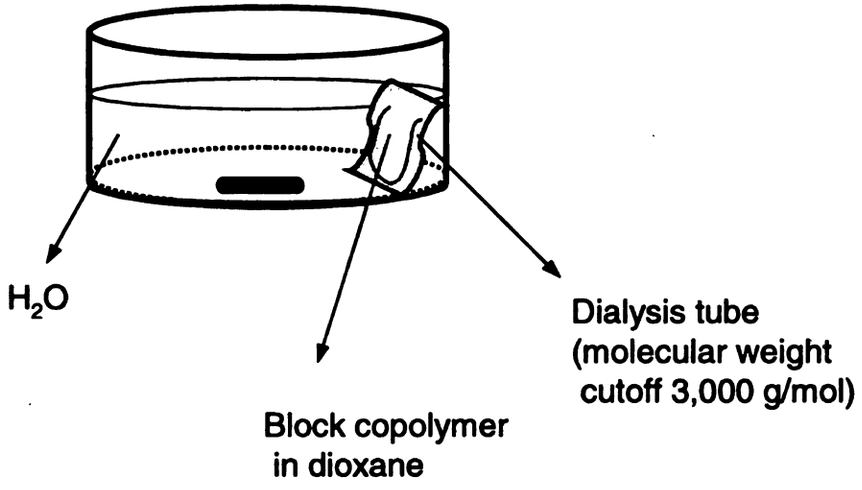

Figure 4.7. Preparation of poly(L-lactide)-*b*-poly(OEGMA) nanoparticles via dialysis.

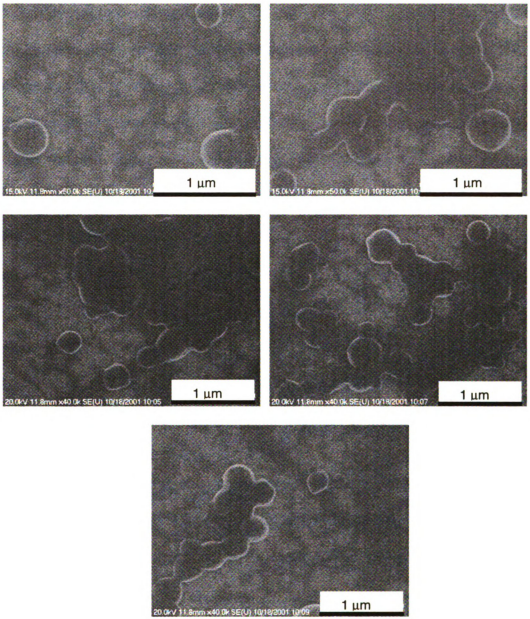

Figure 4.8. SEM photographs of poly(L-lactide)-*b*-poly(OEGMA) particles freeze-dried on a gold substrate

Preliminary results on drug loading

Lidocaine (Figure 4.9) is one the most accurately documented local anesthetics and is a widely used model compound for the encapsulation and delivery of hydrophobic drugs. The dialysis procedure described earlier was used to incorporate lidocaine in poly(L-lactide)-*b*-POEGMA nanospheres. Equal weights of lidocaine and the copolymer were loaded into a dialysis tube and dialyzed against water.

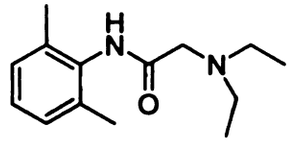

lidocaine

Figure 4.9. The chemical structure of lidocaine

The amount of lidocaine incorporated into the nanospheres must be determined to measure the drug loading efficiency in this system. The lidocaine concentration can be quantified by UV/vis spectroscopy once the molar extinction coefficient, ε, is known. Methanol solutions of lidocaine with known concentrations were prepared and the spectrum of each solution was measured. A plot of absorbance at 262 nm vs. concentration gave $\varepsilon = 210$ L mol^{-1} cm^{-1} (**Figure 4.10**). To determine the loading, a known amount of drug-loaded nanospheres were dried under vacuum to remove water. To avoid interference from the polymer, the nanospheres were extracted with methanol, a non-solvent for the polymer. NMR analysis confirmed that only lidocaine was extracted into

the solvent. The methanol solution of lidocaine was then filtered through a 0.2 μm filter to remove dust, concentrated, transferred to a 50 mL volumetric flask and then diluted to give exactly 50 mL. The UV absorbance at 262 nm was measured and the concentration determined. For 100 mg of copolymer, 100 mg of lidocaine and 50 mL of dioxane, the drug loading efficiency (wt%) (= [(amount of remaining drug in nanoparticles)/(initial feeding amount of drug)] × 100%) was 13%. Drug loading efficiency is affected by many factors such as preparation methods, block length, molecular weight of the (co)polymer, size and distribution of the nanoparticles as well as the hydrophobic/hydrophilic nature of the drug incorporated. Although the loading efficiency obtained was not superior to those obtained in literature, the advantages of having this amphiphilic block copolymer as a drug delivery matrix are obvious: the use of a stabilizer (e.g. poly(vinyl alchol)) and low boiling point halogenated solvents can be avoided by choosing the proper preparation method. Higher loading efficiencies can be expected for a more hydrophilic drug.

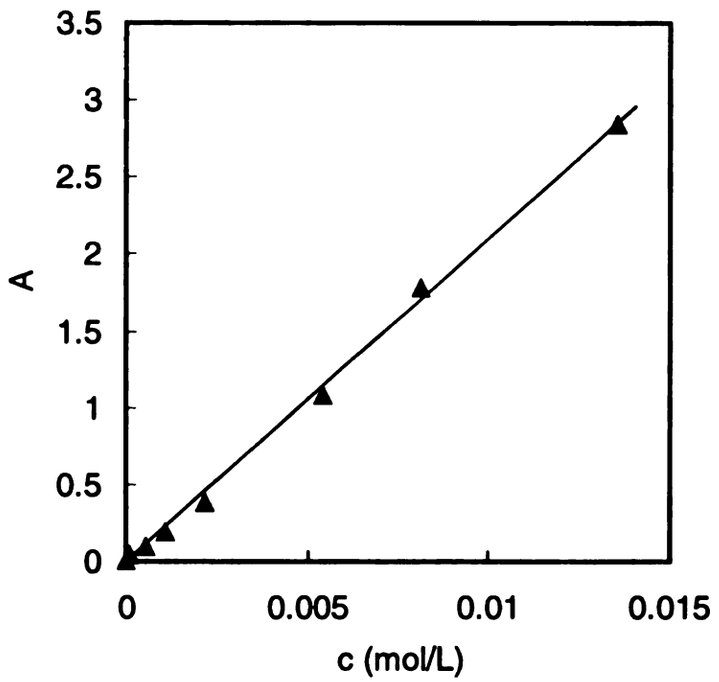

Figure 4.10. UV absorbance vs. concentration of lidocaine in methanol (λ= 262 nm)

4.4. Experimental Section

General Unless otherwise specified, ACS reagent grade starting materials were used as received from commercial suppliers. Toluene was freshly distilled from sodium benzophenone ketyl under nitrogen. Oligo(ethylene oxide) methacrylate (OEGMA) (M_n average 300 g/mol, Aldrich) was purified by passing the neat monomer through basic alumina and was stored in a freezer at –17 °C in a helium-filled drybox. Racemic and L-lactide were recrystallized three times from ethyl acetate before use. Dialysis tubing (flat width: 50 mm; vol/cm: 7.94 mL; wall thickness: 30 μm; molecular weight cutoff: 3,000 g/mol) used for the preparation of polymer nanoparticles was obtained from Fisher Scientific.

Characterization ^1H and ^{13}C NMR analyses were performed at room temperature in $CDCl_3$ on a Varian Gemini-300 spectrometer using TMS as the chemical shift standard. Reflectance FTIR spectra were obtained under nitrogen using a Nicolet Magna-560 FTIR spectrometer containing a PIKE grazing angle (80°) attachment. Typically, 256 scans were collected using a MCT detector. Polymer molecular weights were measured by gel permeation chromatography (GPC) at 35 °C in THF using a Plgel 20μ Mixed column at a flow rate of 1 mL/min. Two detectors were used, a Waters R410 Differential Refractometer and a Waters 996 Photodiode Array. The concentration of the polymer samples was 1 mg/mL, and each solution was filtered through a Whatman 0.2μm PTFE filter before injection. The molecular weights are reported relative to monodisperse polystyrene standards. Differential scanning calorimetry (DSC) data were obtained with a Perkin Elmer DSC 7 instrument calibrated with indium

and hexyl bromide standards. The samples were placed in aluminum pans, and were heated at 10 °C/min under a helium atmosphere. Liquid nitrogen was used as the coolant. Strain recovery experiments were run on a Paar-Physica UDS-200 stress-controlled rheometer equipped with a forced-air oven. A 25 mm diameter cone-and-plate fixture was used for the measurements.

Synthesis and purification of polylactide-*b*-POEGMA using CuBr catalyst Polylactide prepared from the difunctional initiator was used as the ATRP initiator. CuBr/bpy was used as the catalyst and anisole or toluene as the reaction solvent. In a helium filled drybox, the polylactide macroinitiator was dissolved in anisole or toluene at 70 °C, and then predetermined amounts of catalyst, ligand and monomer were added to start the polymerization. The conversion of monomer to polymer was monitored by NMR. The polymerization was stopped by taking the reaction flask out of the drybox and opening it to air. The polymer solution was diluted with toluene and then was washed twice with aqueous EDTA to remove residual copper catalyst. After filtration, the polymer solution was concentrated and extracted with hexanes. The purified block copolymer was dried under vacuum until it reached constant weight.

Preparation of polylactide-*b*-POEGMA nanoparticles using dialysis Poly(L-lactide)-*b*-POEGMA (20 mg, 6.4 mole % OEGMA) and 20 mL of dioxane were loaded of into a dialysis tube. The tube was immersed into a 2L water bath filled with Milli-Q water and equipped with a stir bar and a stopcock on the bottom. The Milli-Q water was replaced continuously for the first 2 hours and

every 6 hours afterwards. Within half an hour, the solution inside the dialysis tube became translucent and the dialysis was stopped after 24 hours.

Preparation of polylactide-*b*-POEGMA nanoparticles loaded with Lidocaine using dialysis The same procedure was applied with the only change being that lidocaine was added in the dialysis tube as well.

References

1. Okamoto, H.; Kano, Y.; Nakashima, S.; Kotaka, T.; Takahashi, S.; Kasemura, T.; Nozawa, Y. *J. Adhes.* **1999**, *71*, 263-278.

2. Zhang, F.; Kang, E. T.; Neoh, K. G.; Huang, W. *J. Biomater. Sci., Polym. Ed.* **2001**, *12*, 515-531.

3. Fujimoto, K.; Inoue, H.; Ikada, Y. *Cent. Biomed. Eng.* **1993**, *27*, 1559-1567.

4. Zhang, F.; Kang, E. T.; Neoh, K. G.; Wang, P.; Tan, K. L. *Biomaterials* **2001**, *22*, 1541-1548.

5. Ward, J. H.; Peppas, N. A. *J. Control. Release* **2001**, *71*, 183-192.

6. Spamacci, K.; Tondelli, L.; Laus, M. *J. Polym. Sci. Pol. Chem.* **2000**, *38*, 3347-3354.

7. Davis, K. A.; Paik, H. J.; Matyjaszewski, K. *Macromolecules* **1999**, *32*, 1767-1776.